AN INVESTIGATION OF THE ELECTRONIC STRUCTURES OF TRANSITION METAL COMPLEXES BY SINGLE CRYSTAL POLARIZED SPECTROSCOPY

Thesis by

Charles Dane Cowman, Jr.

In Partial Fulfillment of the Requirements

for the Degree of

Doctor of Philosophy

California Institute of Technology

Pasadena, California

1974

(Submitted August 14, 1973)

ACKNOWLEDGMENTS

I gratefully acknowledge my advisor, Professor Harry B. Gray, for his constant support and enthusiasm. His chemical insight has helped me to focus on problems of interest and significance. He has endowed me with a sense of self-reliance. I owe him much.

I wish to thank those people who have worked with me on various projects. Dr. Jack Thibeault was most helpful in sorting out theoretical arguments. The efforts of Dr. Ronald Ziolo and Dr. Olavi Siiman in the x-ray studies were appreciated. Dr. Phillip Stevens of U.S.C. has been helpful in the MCD studies. Greg Geoffroy has been most kind in communicating his photochemical results. Dr. George Rossman, perhaps most of all, deserves special recognition for collaboration on equipment design and maintenance.

I thank Sarah for financial and moral support during my first years of study. She has been the catalyst for my discovery of life. I thank Steven Frank, Fran Longo, Dana Powers, and Millie Clarke for their friendship. The warmth of the Beauchamp Group and their help have made the writing of this manuscript bearable.

ABSTRACT

A technique for growing thin film single crystals using tetra-n-butylammonium as a cation is detailed. The polarizations of both ligand field and charge transfer transitions were measured at 5°K for a number of transition metal monomeric and dimeric species. The polarized spectra for the d^8 square planar complexes $Ni(CN)_4^{2-}$ and $Pt(CN)_4^{2-}$ confirm the $d \rightarrow a_{2u}$ π^* CN nature of the charge transfer bands. Spin orbit coupling was found to be important. The d orbital ordering $dxy \leq dxz, dyz < dz^2 \ll dx^2-y^2$ was found. The absorption spectra of the planar chlorobridged species $Pt_2Cl_6^{2-}$ and $Pd_2Cl_6^{2-}$ were found to exhibit anomalously large intensities for the spin-forbidden bands in the in-plane direction perpendicular to the metal-metal axis. The observed splitting of the lowest spin allowed d-d transition confirms the existence of metal-metal interaction. The ligand field absorption spectra of the square pyramidal $OsNCl_4^-$ and $OsNBr_4^-$ species are dominated by the equatorial allowed $dxy \rightarrow dxz, dyz$ transition. Progressions of the totally symmetric metal-nitrogen stretch are observed on the transition. The observation of an axial polarized double progression of the metal-halogen symmetric stretch requires the inclusion of spin orbit coupling. The d orbital ordering $dxy < dxz, dyz < dx^2-y^2 < dz^2$ is identical to that in vanadyl ion. The $\delta \rightarrow \delta^*$ transition in the quadruply bonded $Re_2Cl_8^{2-}$ and $Re_2Br_8^{2-}$ species has been positively identified by the MCD and polarization data in the $Re_2X_8^{2-}$ complexes, compared to the polarization of this band

in the lower symmetry species $Re_2Cl_6[PEt_3]_2$. Progressions of the totally symmetric metal-metal stretch characterize the band envelope. The related $Mo_2Cl_8^{4-}$ and $Mo_2Cl_4[PEt_3]_4$ species also contain an analogous temperature independent band. The applicability of the molecular orbital scheme proposed by Cotton was confirmed. The polarized spectra of the $Re_2Cl_9^{2-}$ anion suggest a C_{4v} structure related to the $Re_2X_8^{2-}$ complex. The polarization of the absorption bands of $Re_2Cl_9^{-}$ were distinctly different; this species is known to have a D_{3h} confacial bioctahedral structure.

TABLE OF CONTENTS

INTRODUCTION

The technique of single crystal polarized spectroscopy has proved extremely useful in elucidating the assignments of ligand field bands.[1] For a single crystal the environment and orientation of the species of interest are constant; they may be determined precisely by x-ray crystallography. Spectral studies at low temperatures can then be interpreted using group theory to provide information concerning the electric or magnetic dipole nature of the transition, vibronic coupling, and effective geometry of the excited state.

Unfortunately single crystals sufficiently thin to permit measurements of intense absorption features are obtained only with difficulty by ordinary crystallization techniques. The small size of those crystals with acceptable thicknesses generally necessitates the use of microscopic optics.[2,3] The crystal is fastened over a pinhole apperature, smaller than the crystal, to prevent the transmission of stray light. The inherent loss of light intensity from masking the beam requires the use of both a high intensity light source and condensing optics. The convergent nature of the light incident upon the crystal face can seriously distort the true polarization ratios. Liquid helium temperature data are seldom obtained the spectral constraints imposed by the microscopic optics generally preclude the use of a helium dewar.

The alternative usually employed is the "doping" of the metal complex into an isomorphous host lacking absorption in the region

of interest.[4,5] Because the optical properties of the doped crystal are those of the host lattice, only non-isotropic hosts will yield polarization data. The orientation of non-octahedral or tetrahedral metal complexes within the lattice is seldom known with certainty, although frequently such orientation may be inferred. While "doping" allows lattitude in the choice of concentration of the "solute," intermolecular crystal lattice interactions may significantly preturb the "solute" molecule. A suitable isomorphous compound of known crystal structure may not exist.

Liquid crystal polarized spectroscopy[6,7] circumvents the problems of intermolecular interactions, previous knowledge of the crystal structure, and of achieving the "optical dilution" required to observe intense bands. The most widely used room temperature nematics, N(p-methoxy benzylidene) p-n-butyl aniline[8] (nematic 20° - 41°C) and p-(p' - ethoxybenzoxy) phenyl butyl carbonate[6,7] (nematic 56° - 87°C) possess UV cutoffs of 400 nm and 300 nm respectively. Polarization studies of bands in the UV cannot be made. Few inorganic compounds are sufficiently soluble in the organic liquid crystal to give any absorption spectra at all. The shape of the molecule is critical in determining the alignment: the long axis of the molecule is statistically aligned along the long axis of the liquid crystal molecule.[6,7] Molecules possessed of "equant" shapes lack the alignment necessary to observe polarization effects. Resolution by this technique is about equal to that of the compound in solution. Low temperature studies are not possible.

The approach adopted by this author, the use of thin film single crystals, circumvents many of the problems encountered with other techniques. The substitution of tetraalkylammonium cations for alkali or alkaline-earth cations affects the facility with which the compounds crystalize. The films formed by evaporation of organic solvents rapidly crystallized to form large, thin single crystals. Single crystals of suitable optical dilution were routinely obtained. Because the crystals were grown on a substrate, further manipulation and mounting were unnecessary. Liquid helium temperatures were easily reached without the accompanying shattering that plagues inorganic salts. The orientation of the anions was determined by various techniques: polarized IR, optical properties of the crystal, comparison with previous polarized single crystal data, polarization ratios of the bands, or x-ray crystal structure.

The following sections will detail the experimental method and equipment design. Data analysis will be discussed.

References

1. N. S. Hush and R. J. M. Hobbs, Progr. Inorg. Chem., 10, 259 (1968) and references therein.

2. P. Day, A. F. Orchard, R. J. P. Williams, J. Chem. Phys., 42, 1973 (1965).

3. R. G. Burns, Mineralogical Applications of Crystal Field Theory, Cambridge University Press, New York, N.Y. (1970).

4. D. S. McClure, Electronic Spectra of Molecules and Ions in Crystals, Academic Press, New York, N.Y. (1959).

5. C. J. Ballhausen, The Measurement and Interpretation of Transition Ion Crystal Spectra, Vol. I, ed. by C. N. R. Rao and J. R. Ferraro, Academic Press, New York, N.Y. (1970).

6. R. A. Levenson, H. B. Gray, and G. P. Caesar, J. Amer. Chem. Soc., 92, 3653 (1970).

7. G. P. Caesar and H. B. Gray, J. Amer. Chem. Soc., 91, 191 (1969).

8. H. Kelker and B. Scheurle, Angew. Chem. (Int. Ed.), 8, 884, (1969).

CHAPTER 1

Crystal Growing

Thin film crystals were grown by placing a small amount of the compound, usually < 1 mg., in the center of a clean substrate disk. About four drops of solvent were added around the compound to create a minimum of mixing as the solvent spread, covering the solid. As the compound began to dissolve, the resultant dense solution flowed outward in an even film. When all the solvent had evaporated, an even film was deposited. Within a few minutes nucleation usually began. The crystals formed at these points filled the entire film area. The thickness of the film could be controlled to some extent by varying the initial amount of solid.

A second factor which influenced the number of crystals formed, and hence the size of each, was the rate of evaporation of solvent from the film. The substrate, with solution, was covered by an inverted beaker. The smaller the beaker, the more rapidly the atmosphere within became saturated with solvent vapor, and consequently the slower the final rate of crystallization of the film. The inverted beaker also served as a dust cover to prevent dust particles from adhering to the sticky film surface, forming additional nucleation centers.

Crystals grown from aqueous solution generally tend to assume a prismatic habit; they seldom grow as thin plates. This, in part, is due to the high surface tension of water: water has a

high contact angle with the substrate. Organic solvents have much lower surface tension. Tetraalkylammonium salts rapidly crystallize from organic solvents as thin film crystals.

The substrates on which the thin film crystals are grown must be clean to minimize the contact angle and prevent formation of a doughnut-shaped film. Substrates were cleaned with "Cromerge," washed with distilled water, and laid on end to dry in air. Freshly cleaned surfaces gave best results. Optosil grade silica windows, 7/8" diameter, were generally used as substrates. Polarized far IR - visible comparisons employed aluminum oxide as a substrate.

The thin film crystals were examined under a polarizing microscope. Regions of single crystalinity were located; the surrounding area was marked off using black tape. Only regions with sharp extinctions between crossed polarizers were chosen.

Characterization of Crystals

The density may be measured either by floatation[1,2] in a liquid of equal density or by volume displacement[1,3](pycnometry). The latter technique was most useful since tetraalkylammonium salts tend to be soluble in virtually all polar organic solvents, precluding measurement by floatation. The volume displacement method gives the density ρ by

$$\rho_{sample} = \frac{(B - A)(D - A)}{(D - A - C + B)E} \qquad (1)$$

where

A = weight of empty density bottle

B = weight of density bottle + sample

C = weight of density bottle + sample, filled with liquid

D = weight of density bottle filled with liquid

E = volume of bottle

The concentration C of a solid is given by the formula

$$C = \frac{10^3 \rho}{(MW)} \tag{2}$$

where (MW) is the molecular weight and (ρ) is the density.

The thicknesses of the thin film crystals could not be determined with a micrometer. The crystals were too thin to allow accurate measurement; the variation of the substrate thickness was of the same order of magnitude as the crystal thickness. The interference colors of the crystal when viewed between crossed polarizers in a polarizing microscope permit a much more accurate determination of thickness for colorless crystals. The retardation ΔS (interference color) is proportional to the thickness d. The proportionality constant is the birefringence, Δn.[4] Birefringence is the difference of the refractive indices. Very thick sections of the thin film crystals possessed first order white, $\Delta S \cong 0.25\ \mu$, or occasionally first order orange, $\Delta S \cong 0.43\ \mu$, interference colors. Those crystals which allowed observation of charge transfer absorption bands had retardations less than $0.1\ \mu$.[5]

The refractive indices may be measured by immersion in oils of known refractive index. The high solubility of tetraalkylammonium salts makes such determinations difficult. The sign and magnitude of the birefringence is related to the stacking of anion planes within the crystal.[6] Planes parallel to one another will have a large negative birefringence with the out-of-plane direction having the lowest refractive index—fast direction. Planes parallel to a single direction but not to each other have a large positive birefringence; the planes will be parallel to the direction of highest index—slow direction.

Alternately the thickness of the crystal may be determined if interference fringes are present. Constructive interference, corresponding to an absorption minimum, will occur whenever the internally reflected ray is in phase with the transmitted ray as both exit the crystal. The thickness d in microns will be

$$d = \frac{m}{2n}\left(\frac{\lambda_1\lambda_2}{\lambda_1 - \lambda_2}\right) \times 10^{-4} \qquad \lambda_1 > \lambda_2 \tag{3}$$

where λ_1 and λ_2 are the wavelengths in Å of maxima x and x + m respectively. n, the refractive index, will depend upon the polarization direction. For the special case of a uniaxial crystal aligned such that it may be rotated by θ about its unique axis, both the refractive indices and thickness may be obtained from just the shift of the interference fringes with rotation.[7]

Description of Equipment

A Cary 17 spectrophotometer equipped with an extended cell compartment was used to obtain absorption spectra in the visible-ultraviolet region. A Cary 14 RI spectrophotometer was used in the near infrared. A matched pair of double Glan-Taylor air spaced calcite polarizing prisms[8] was used for polarization measurements. These polarizers have transmission to 2150 Å and a minimum useable symmetrical angular field of 12°. The ordinary ray is totally reflected at both limits of the useable angular field. The polarizers were mounted so that they rotated in tandem to balance absorption of light in sample and reference compartments. Incorrect alignment results in a non-linear baseline due to the small self polarization of the Cary optics. The polarizers were always positioned before the sample. The entering beam convergence of the Cary was thus further reduced. The crystal was positioned at the center of the sample compartment, with the substrate on the exit side. In all cases the polarizers were rotated while the sample was fixed. Low temperature measurements approaching liquid helium temperature were obtained for samples in an Andonian Associates liquid helium dewar.[9] This dewar is a variable temperature cold gas dewar. Temperatures were monitored by measuring the resistance of a calibrated carbon resistor. At 5°K temperatures could be determined ± .1°K. Cool down time to 5°K was about fifteen minutes. Samples could be interchanged. Once a particular sample was

positioned within the dewar, both horizontal and vertical translations were performed to maximize the transmission of light through the crystal.

Polarization spectral measurements were obtained along the previously identified extinction directions of the crystal. Baselines obtained for these same polarizer orientations, but without the sample, were subtracted from all spectra. Calibrated neutral density filters were used in the reference beam. Spectral bandwidths were generally less than 2 Å.

Infrared measurements were obtained on a Perkin-Elmer 225 spectrometer equipped with a wire grid polarizing element.

Polarized absorption data are measured with the plane of polarization along the mutually perpendicular extinction directions of the crystal. For uniaxial crystals spectral measurements obtained along the direction parallel to the unique axis are labeled $A_{\parallel}$; measurements where the plane of polarization is 90° from this direction are labeled $A_{\perp}$. The two directions may be easily distinguished by the optical properties of the crystal and no ambiguity arises. Nomenclature for biaxial crystals is not so well defined. The Orthorhombic system has three mutually perpendicular C_2 axes, any one of which may be chosen as the parallel direction. The extinction directions are constrained by crystal symmetry to lie parallel to the C_2 axes. The monoclinic system has a single C_2 axis, b. This unique axis is generally chosen as the parallel direction. The (010) face presents a special problem since the

extinction directions are not constrained by symmetry, and may rotate with wavelength. Data obtained for such faces are highly suspect. For similar reasons polarized spectra of triclinic crystals, where no symmetry constraints exist, are difficult to analyse.[10]

The raw data, $A_{\parallel}$ and $A_{\perp}$, are of little use unless such measurements can be related to the molecular symmetry elements. It is the molecular symmetry which will determine the selection rules. The absorption is equal to the sum of the squares of the direction cosines of the crystal extinction directions with the molecular orthogonal axes. Consider Figure 1 in which the extinction directions, $\parallel$ and $\perp$, lie in the plane of the crystal face. Orthogonal molecular axes x, y, and z, make angles θx, θy and θz with the $\parallel$ crystal direction and angles γx, γy, and γz with the $\perp$ crystal direction. For clarity only x and z are shown.

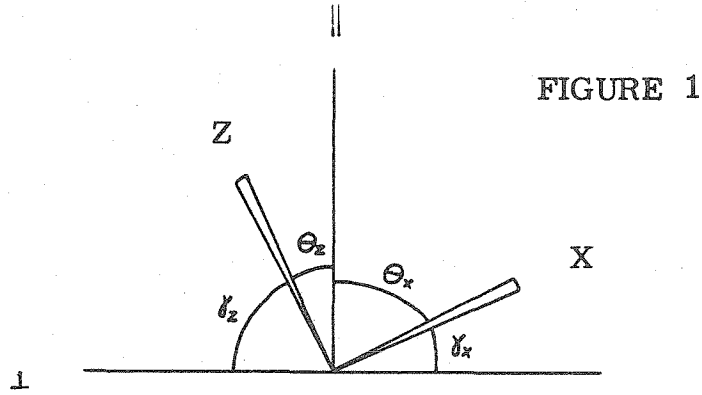

FIGURE 1

The measured absorbances will then be

$$A_{\parallel} = \cos^2 \theta z \; Az + \cos^2 \theta x \; Ax + \cos^2 \theta y \; Ay \qquad (4)$$

$$A_{\perp} = \cos^2 \gamma z \; Az + \cos^2 \gamma x \; Ax + \cos^2 \gamma y \; Ay \qquad (5)$$

where Ax, Ay, and Az are the true molecular absorbances along the orthogonal molecular axes. Since

$$\cos^2 \theta x + \cos^2 \theta y + \cos^2 \theta z = 1 \tag{6}$$

$$\cos^2 \gamma x + \cos^2 \gamma y + \cos^2 \gamma z = 1 \tag{7}$$

equations (4) and (5) may be written as

$$A_{\parallel} = \cos^2 \theta z \, Az + \cos^2 \theta x \, Ax + [1 - \cos^2 \theta z - \cos^2 \theta x] Ay \tag{8}$$

$$A_{\perp} = \cos^2 \gamma z \, Az + \cos^2 \gamma x \, Ax + [1 - \cos^2 \gamma z - \cos^2 \gamma x] Ay. \tag{9}$$

In general, equations (8) and (9) may be solved if polarization data is obtained for two faces.

The usual case in which the molecule possesses a C_3 or C_4 axis or higher considerably simplifies these equations. In such cases, Ax and Ay are indistinguishable, and only the orientation of the unique z axis is important.

$$A_{\parallel} = \cos^2 \theta z \, Az + \sin^2 \theta z \, Ax, y \tag{10}$$

$$A_{\perp} = \cos^2 \gamma z \, Az + \sin^2 \gamma z \, Ax, y \tag{11}$$

For a right spherical triangle, Figure 2,

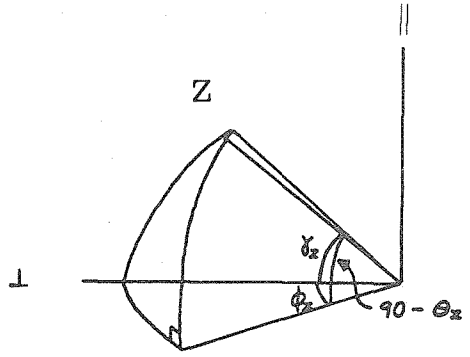

FIGURE 2

$$\cos \gamma z = \cos \phi z \cos (90 - \theta z) \tag{12}$$

$$\cos \gamma z = \sin \theta z \cos \phi z \tag{13}$$

Equation (11) may then be written in the form

$$A_{\perp} = \sin^2 \theta z \cos^2 \phi z \, Az + [1 - \sin^2 \theta z \cos^2 \phi z] Ax, y \tag{14}$$

Equations (10) and (14) are then in the form originally reported by Piper.[11] Figure 3 shows the relationship of θ and ϕ for light propagating normal to the crystal face.

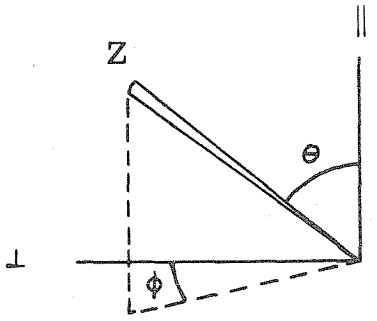

FIGURE 3

For a <u>tetragonal</u> crystal, Equation 11 may be even further simplified. Here $\bar{A}_{\perp}$ will be the <u>average</u> of the two unique orientations of the z axis.

$$A_{\perp_1} = \sin^2 \theta \cos^2 \phi \, Az + [1 - \sin^2 \theta \cos^2 \phi] Ax, y \tag{14}$$

$$A_{\perp_2} = \sin^2 \theta \cos^2 (\phi + 90) \, Az + [1 - \sin^2 \theta \cos^2 (\phi + 90)] \, Ax, y \tag{15}$$

$$\bar{A}_{\perp} = \tfrac{1}{2} \sin^2 \theta \, Az + [1 - \tfrac{1}{2} \sin^2 \theta] Ax, y \tag{16}$$

equation (16) does not depend upon ϕ.[12] In general, equations (10) and (14) must be averaged whenever non-equivalent molecules are present in the unit cell.

In many cases a crystal structure is not available to define the orientations of the molecular axes with respect to the crystal extinction directions. The polarization ratios can be used to determine θ, ϕ.[12,13] For a completely z polarized band Ax, y = 0 and equations 10 and 14 give

$$\frac{A_{\perp}}{A_{\parallel}} = \frac{\sin^2 \theta \cos^2 \phi}{\cos^2 \theta} \tag{17}$$

similarly for a completely xy polarized band Az = 0

$$\frac{A_{\perp'}}{A_{\parallel'}} = \frac{1 - \sin^2 \theta \cos^2 \phi}{\sin^2 \theta} \tag{18}$$

solving for the angles gives

$$\sin^2 \theta = \frac{1 - A_{\perp}/A_{\parallel}}{A_{\perp'}/A_{\parallel'} - A_{\perp}/A_{\parallel}} \tag{19}$$

$$\cos^2 \phi = \frac{A_{\perp'}/A_{\parallel'} - 1}{A_{\parallel}/A_{\perp} - 1} \tag{20}$$

The inverse matrix for conversion of $A_{\parallel}$, $A_{\perp}$ into absorbances parallel (π) and perpendicular (σ) to z is given by

$$\begin{bmatrix} \dfrac{1 - \sin^2\theta\cos^2\phi}{\cos^2\theta - \sin^2\theta\cos^2\phi} & \dfrac{-\sin^2\theta}{\cos^2\theta - \sin^2\theta\cos^2\phi} \\ \dfrac{-\sin^2\theta\cos^2\phi}{\cos^2\theta - \sin^2\theta\cos^2\phi} & \dfrac{\cos^2\theta}{\cos^2\theta - \sin^2\theta\cos^2\phi} \end{bmatrix} \tag{21}$$

For uniaxial crystals electric dipole transitions may be differentiated from magnetic dipole transitions by comparing the axial (isotropic) spectra with the π and σ spectra. The coincidence of σ and axial spectra proves the electric dipole origin of a transition. The π and axial spectra will be identical for magnetic dipole transitions.

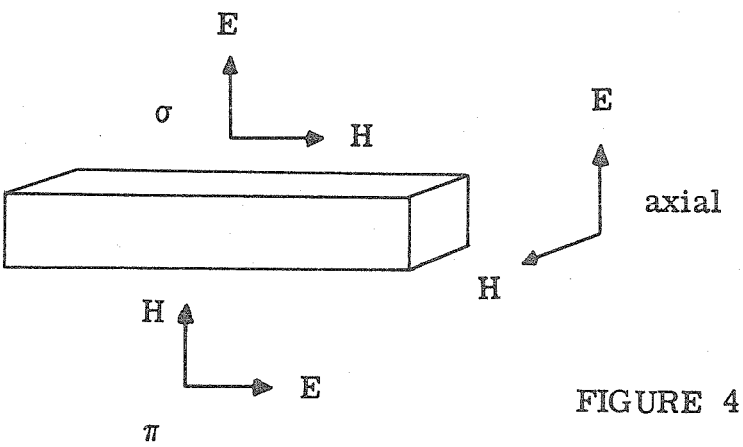

FIGURE 4

Once the spectra have been transformed into molecular absorbances, the symmetry selection rules appropriate to the molecular point group may be utilized in making a final assignment. The electric dipole moment operator transforms as the x, y, z translations; the magnetic dipole moment operator as the corresponding rotations. A transition will be fully allowed if the direct

product of the symmetries of the ground state, excited state, and dipole moment operator contain the totally symmetric representation.[14,15] Even when the direct product indicates that a transition is forbidden, coupling with an excited state vibration of appropriate symmetry may provide intensity. Such "vibronic" transitions may be differentiated from fully allowed transitions by their temperature dependence. Vibronic bands have a coth $(\frac{h\nu}{kT})$ temperature dependence,[16] exhibiting reduced intensities at lower temperatures. Spin-orbit coupling is important for the second and third row transition metals; the use of double groups is necessary. The transformation properties of the spin functions may be found in appendix A.

References

1. International Tables of X-ray Crystallography, Vol. 3, p. 18; Kynoch Press, Birmingham, England (1968).
2. P. Wulff and A. Heigl, Z. Phys. Chem. A153, 187 (1931).
3. J. Johnston and L. H. Adams, J. Amer. Chem. Soc., 34, 563 (1912).
4. P. F. Kerr, Optical Mineralogy, McGraw-Hill, New York, N.Y. (1957).
5. Ibid., numbers obtained from the enclosed Michael-Levy chart.
6. N. H. Hartshorne and A. Stuart, Crystals and the Polarizing Microscope, Edward Arnold Inc., London, England (1970).
7. D. S. Martin, R. M. Rush, R. F. Kroening and P. E. Fanwick, Inorg. Chem., 12, 301 (1973).
8. Karl Lambrecht Corp, 4318 N. Lincoln Ave, Chicago, Illinois, Catalog No. DGTYA15.
9. Andonian Associates, Inc., 26 Thayer Road, Waltham, Massachusetts catalog No. 3L/250 of the 02417m series.
10. R. F. Stewart and N. Davidson, J. Chem. Phys., 39, 255 (1963).
11. T. S. Piper, J. Chem. Phys., 35, 1240 (1961).
12. W. A. Eaton and R. M. Hochstrasser, J. Chem. Phys., 46, 2533 (1967).
13. E. W. Thulstrup and J. H. Eggers, Chem. Phys. Letters, 1, 690 (1968).

14. F. A. Cotton, Chemical Applications of Group Theory, John Wiley and Sons, Inc, New York, N.Y. (1963).

15. C. J. Ballhausen, The Measurement and Interpretation of Transition Ion Crystal Spectra, Vol. 1, Ed. by C.N.R. Rao and J. R. Ferraro, Academic Press, New York, N.Y. (1970).

16. O. G. Holmes and D. S. McClure, J. Chem. Phys., 26, 1686 (1957).

CHAPTER 2

Polarized Crystal Spectra of $Ni(CN)_4^{2-}$ and $Pt(CN)_4^{2-}$

The formulation of detailed assignments for the electronic absorption spectra of the square planar, d^8 low-spin complexes $Ni(CN)_4^{2-}$ and $Pt(CN)_4^{2-}$ has been hindered by the extremely limited band polarization data available.[1-3] The intense charge transfer features of these compounds absorb too strongly to permit such characterization using crystals of inorganic alkali or alkaline earth cations. There is strong evidence that metal-metal and intermolecular interactions in the simple inorganic salts of the tetracyanometallates complicate the interpretation of the low intensity features observed in the few existing polarized crystal spectra.[4-8]

The intense bands observed in the ultraviolet have been assigned as metal(d) → ligand (π^* CN) charge transfer since these features are shifted to higher energy in the analogous $Au(CN)_4^-$ complex.[1] It is characteristic of M → L charge transfer to shift to higher energies upon increasing the metal oxidation number.[2] The most stable ligand antibonding orbital has a_{2u} symmetry,[1] consisting of the p_z metal orbital and a combination of the four ligand π_v orbitals. This gives a stable "ring" π bonding orbital.

Previous assignments of the three observed features in the spectra of both $Ni(CN)_4^{2-}$ and $Pt(CN)_4^{2-}$ in solution have been based on intensity arguments.[1] The most intense band was assigned as the allowed transition $^1A_{1g} \rightarrow {}^1E_u$ (dxz, dyz → $a_{2u}\pi^*$). The transition

$^1A_{1g} \rightarrow {}^1A_{2u}$ ($dz^2 \rightarrow a_{2u}\ \pi^*$), also allowed, was expected to have greater intensity than the forbidden $^1A_{1g} \rightarrow {}^1B_{1u}$ ($dxy \rightarrow a_{2u}\ \pi^*$) band. These remaining spectral features were assigned accordingly. This required a different ordering of d orbitals for the nickel and platinum complexes. Additional shoulders, resolved in frozen glass spectra[2] were attributed (rather unconvincingly) to splittings of the ^1E_u state caused by lowered symmetry due to ion pairing.

The magnetic circular dichroism solution spectra of these compounds[9, 10] revealed three positive A terms in each compound. The presence of an A term in the MCD requires the presence of a degenerate excited state; in D_{4h} symmetry only E states are degenerate. These results could be explained only by considering strong mixing of spin orbit states.[10]

The confusion surrounding the virtual orbital ordering of square planar π bonded complexes can be dispelled only by an explanation of the optical spectra based upon clear identification of the states present. For this reason a polarized single crystal spectral investigation of these complexes was undertaken.

Thin film single crystals of suitable area and optical dilution for polarization work can be readily obtained using tetra-n-butylammonium as the cation. Crystals of $[(n\text{-}C_4H_9)_4N]_2[Ni(CN)_4]$ were grown from dichloromethane solution; crystals of $[(n\text{-}C_4H_9)_4N]_2[Pt(CN)_4]$ were obtained from 1, 2-dichloroethane. A typical crystal measured 3 × 5 mm^2 and was less than one micron thick. Crystals

grown on aluminum oxide substrates allowed correlation of the optical polarization data with the orientation of the anion planes. Polarized infrared spectra of the in-plane polarized E_u(C≡N stretch) fundamental at 2110 cm^{-1} for $Ni(CN)_4^{2-}$, 2120 cm^{-1} for $Pt(CN)_4^{2-}$ showed the in-plane direction to coincide with the ⊥ (i.e., σ) direction of the optical data. Polarization of the E_u mode yielded $\frac{A_{\perp}'}{A_{\parallel}'}$ ratios of 1.39 for $Ni(CN)_4^{2-}$ and 1.42 for $Pt(CN)_4^{2-}$. The virtually identical ratios suggest that the same face was examined in both compounds. Distinct striations in crystals of both complexes were observed along the ∥ direction.

It is possible to calculate the average orientation of the planar D_{4h} anions with respect to the crystal face using equations 19 and 20. The ratio $\frac{A_{\perp}'}{A_{\parallel}'}$ is closely approximated by the ratio obtained from the polarized infrared data. Similarly the strongly ∥ polarized bands at 279 and 291 nm in the $Ni(CN)_4^{2-}$ spectra yield an upper limit for $A_{\perp}/A_{\parallel}$; for the calculation these latter bands were assumed to be completely polarized. Any vibronic coupling would decrease the ratio $A_{\perp}/A_{\parallel}$ and the angle ϕ would approach 90°. The observed ratio of $A_{\perp}/A_{\parallel}$ was 0.036, yielding values of $\theta = 57°32'$ and $\phi = 83°$.

An examination of known crystal structures of $Ni(CN)_4^{2-}$ salts with inorganic cations[11-13] shows the planar anions tend to stack parallel to each other with the metal-metal chain along the c crystal axis. The z molecular axis makes an angle of 4-6° with respect to this direction. The 7° angle, the complement of ϕ, agrees well with these other structures.

Using the experimentally determined values of θ and ϕ, equations 10 and 14 become

$$A_{\parallel} = .2882\ A\pi + .7118\ A\sigma \tag{22}$$

$$A_{\perp} = .0106\ A\pi + .9894\ A\sigma \tag{23}$$

where $A\pi \equiv Az$ and $A\sigma \equiv Ax, y$ for the D_{4h} anion. The inverse matrix (21) was calculated to be

$$\begin{bmatrix} A\pi \\ A\sigma \end{bmatrix} = \begin{bmatrix} 3.564 & -2.564 \\ -.038 & 1.038 \end{bmatrix} \begin{bmatrix} A_{\parallel} \\ A_{\perp} \end{bmatrix} \tag{24}$$

This matrix was used to transform the $A_{\parallel}$ and $A_{\perp}$ spectra of both $Ni(CN)_4^{2-}$ and $Pt(CN)_4^{2-}$ although it was derived from polarization ratios of the $Ni(CN)_4^{2-}$ alone. The nearly identical $A_{\perp}'/A_{\parallel}'$ ratios of the two complexes and the lack of a π polarized band with no significant band overlap in $Pt(CN)_4^{2-}$ from which an exact value of $A_{\perp}/A_{\parallel}$ could be obtained, suggest that use of this inverse matrix will not affect any conclusions drawn from π and σ spectra.

The density of the tetracyanometallates was found by volume displacement from heptane to be 1.068 g/cm^3 for $[(n\text{-}C_4H_9)_4N]_2[Ni(CN)_4]$ and 1.188 g/cm^3 for $[(n\text{-}C_4H_9)_4N]_2[Pt(CN)_4]$. The concentrations in the crystals using equation 2 were 1.649 M and 1.515 M respectively.

Liquid helium temperature polarized spectra of $[(n\text{-}C_4H_9)_4N]_2[Ni(CN)_4]$ are presented in Figures 5-8.

FIGURE 5

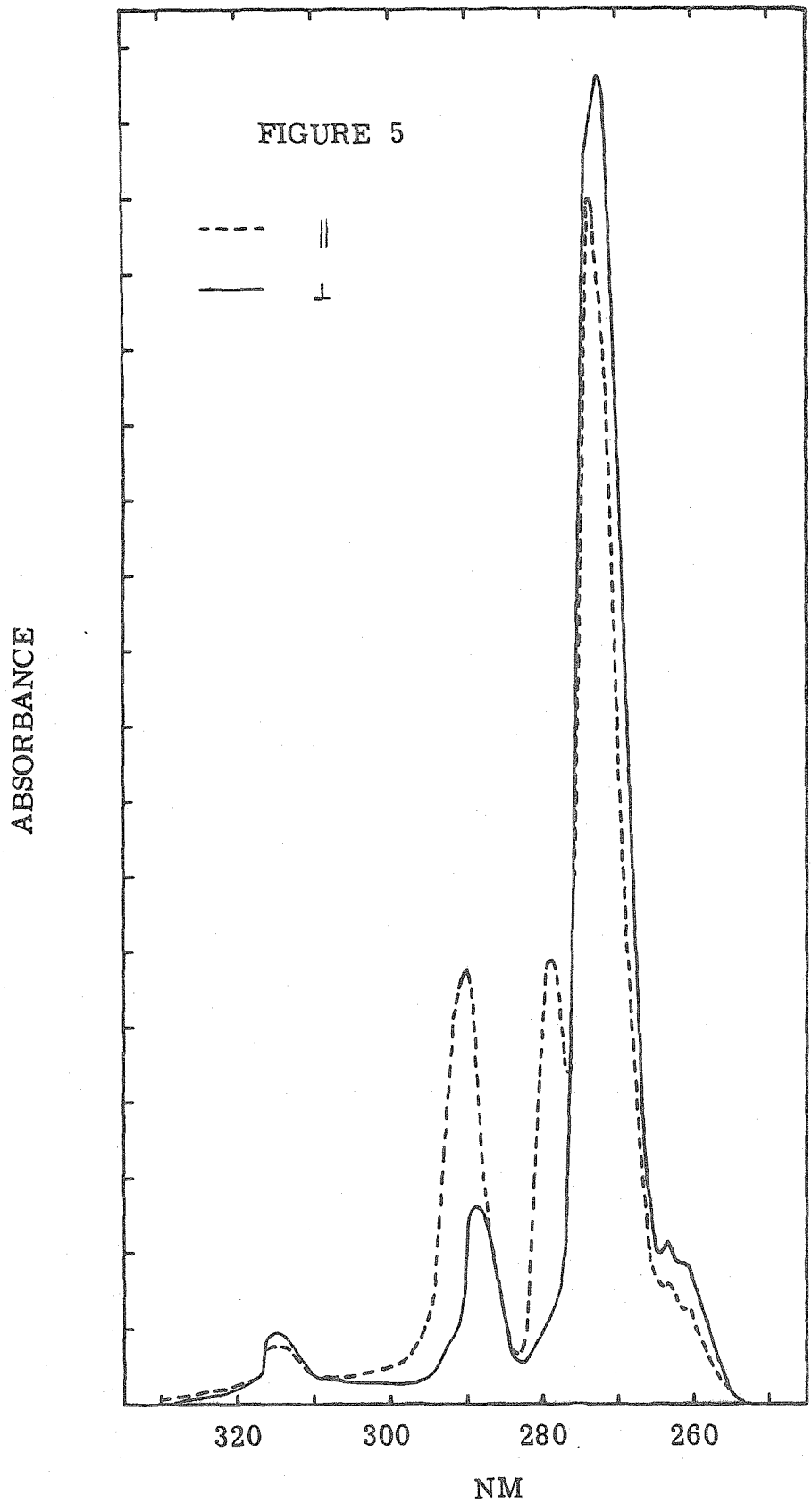

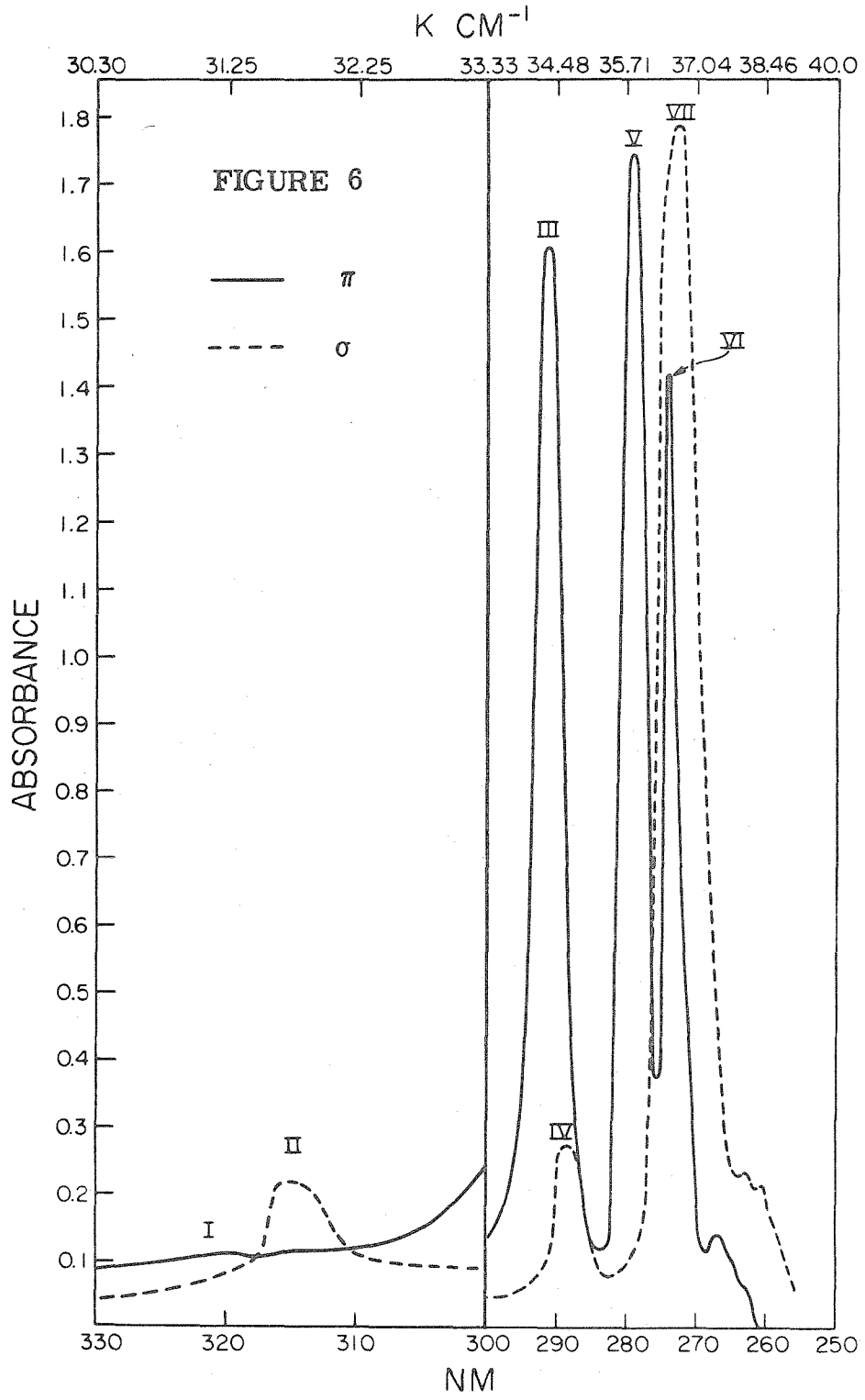
K CM⁻¹
30.30
31.25
32.25
33.33
34.48
35.71
37.04
38.46
40.0
FIGURE 6
π
σ
I
II
III
IV
V
VI
VII
ABSORBANCE
1.8
1.7
1.6
1.5
1.4
1.3
1.2
1.1
1.0
0.9
0.8
0.7
0.6
0.5
0.4
0.3
0.2
0.1
330
320
310
300
290
280
270
260
250
NM

Figure 7: Polarized crystal spectra at 4.8°K for a thick crystal of $[(n\text{-}C_4H_9)_4N]_2[Ni(CN)_4]$. No bands were observed on the low energy tail. Spectra were analyzed using equations (10) and (14).

$$\frac{A_{\perp}'}{A_{\parallel}'} = 1.210, \quad \frac{A_{\perp}}{A_{\parallel}} = .758, \quad \theta = 47°3' \qquad \phi = 35°54'$$

$$A_{\parallel} = .4646\ A\pi + .5354\ A\sigma \tag{25}$$

$$A_{\perp} = .35136\ A\pi + .64864\ A\sigma \tag{26}$$

Figure 8: σ and π spectra of the low energy region of $[(n\text{-}C_4H_9)_4N]_2[Ni(CN)_4]$ using the inverse matrix

$$\begin{bmatrix} 5.7297 & -4.7297 \\ -3.1039 & 4.1039 \end{bmatrix} \tag{27}$$

FIGURE 7

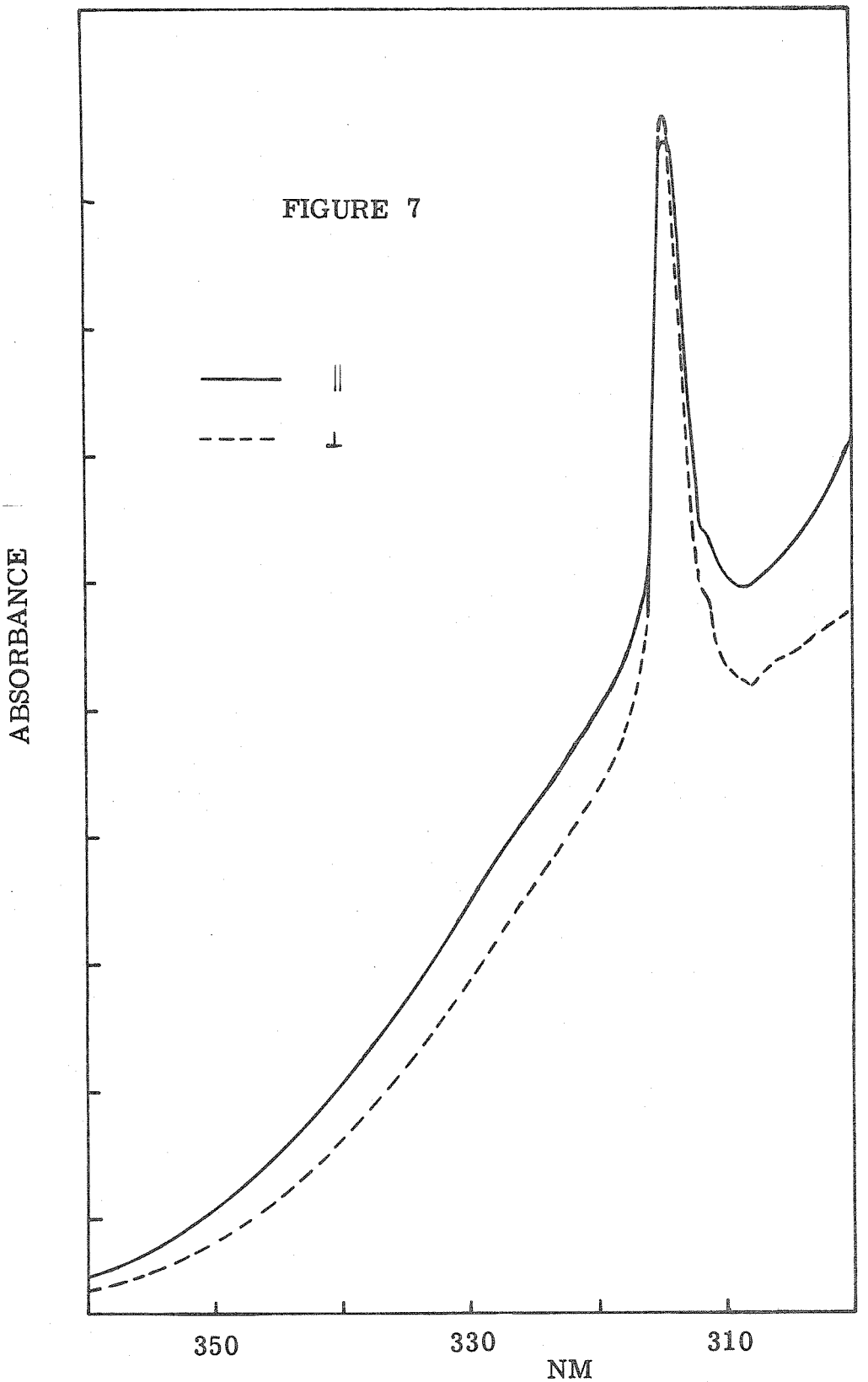

FIGURE 8

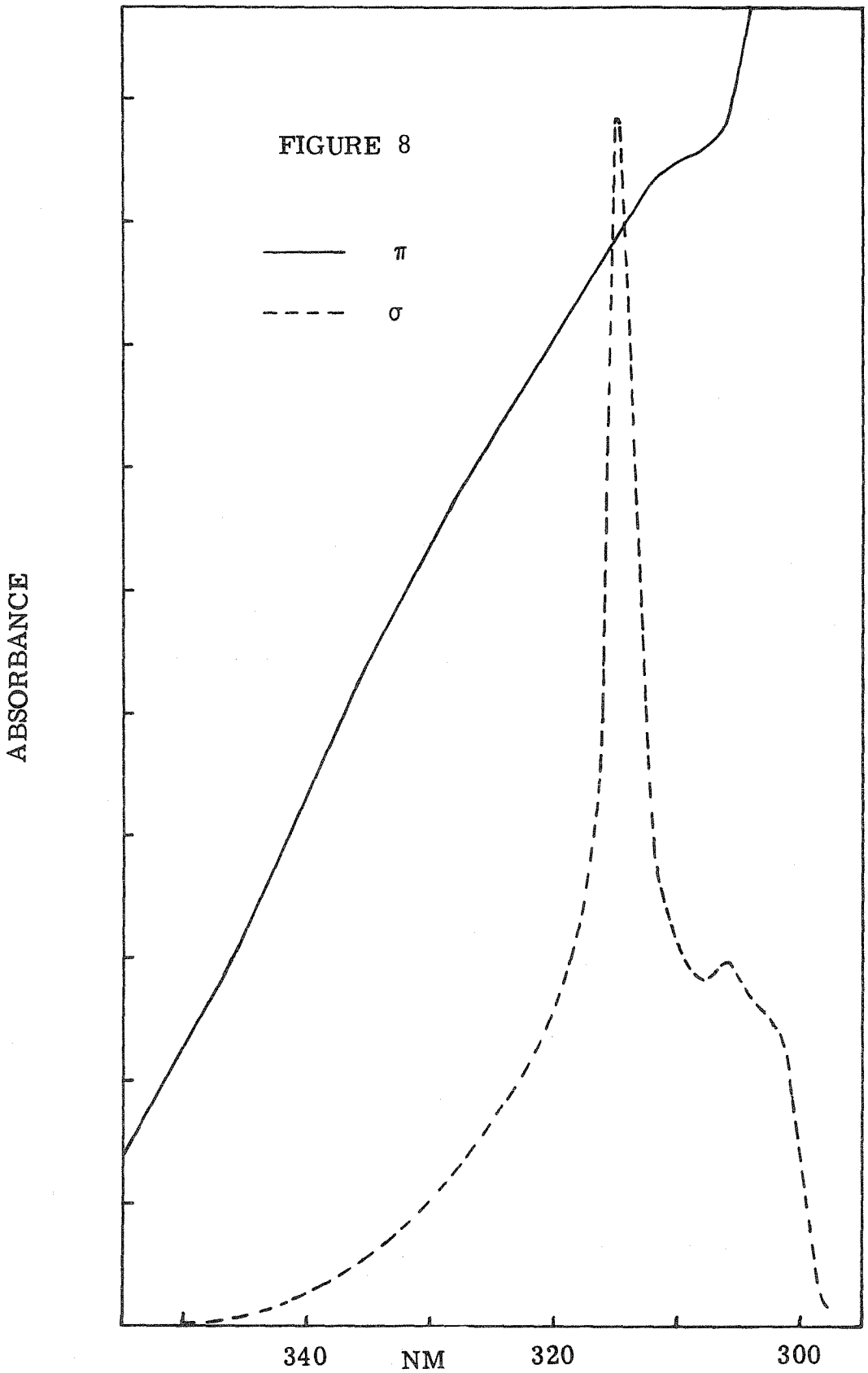

The most intense features of the 5°K single crystal spectra are in good agreement with previously reported 77°K data obtained from frozen EPA solutions.[2] The positions and assignments of the transitions are given in Table 2. Table 1 shows the symmetries of the spin orbit excited states and the accompanying selection rules for D_{4h}. These rules will be utilized in assigning the absorption spectra.

Bands III and VII have previously been assigned as the d → a_{2u} π^* charge transfer transitions $^1A_{1g} \rightarrow {}^1A_{2u}$ ($a_{1g}dz^2 \rightarrow a_{2u}\ \pi^*$) and $^1A_{1g} \rightarrow {}^1E_u$ (e_g, dxz, dyz → $a_{2u}\ \pi^*$), respectively. These assignments are fully substantiated by the polarizations observed. The strong σ polarization and observation of an MCD A term at 37,200 cm^{-1}[10] definitely establishes band VII as $^1A_{1g} \rightarrow {}^1E_u$. Most surprisingly, there are two comparably intense π polarized transitions, bands III and V, where only one is expected. This can occur only if the states of A_{2u} symmetry derived from $^1A_{2u}$ and ^3E_u are completely spin orbit mixed.[10] Band V has previously been observed as a shoulder in the frozen glass.[2] Bands III and V are assigned as $^1A_{1g} \rightarrow$ a A_{2u} ($^1A_{2u}$) and $^1A_{1g} \rightarrow$ b A_{2u} (^3E_u) respectively. Band IV, resolved in σ polarization from band III, is not a vibronic component of the latter. The presence of a weak MCD A term at 35,200 cm^{-1} [9,10] confirms the presence of an excited state of E symmetry. Band IV is assigned as the spin orbit mixed $^1A_{1g} \rightarrow E_u$ (^3E_u, $^3B_{1u}$) transition.

The sharp spike, band VI, revealed in π polarization is 2135 cm^{-1} higher than π allowed band III. This corresponds almost

Table 1

transition	excited state	symmetry	vibration required to be allowed: πA_{2u}	σE_u
$b_{2g}\, d_{xy} \rightarrow a_{2u}\, \pi^*$	$^3B_{1u}$	B_{2u}	B_{1g}	E_g
		E_u	E_g	allowed
	$^1B_{1u}$	B_{1u}	B_{2g}	E_g
$a_{1g}\, d_{z^2} \rightarrow a_{2u}\pi^*$	$^3A_{2u}$	A_{1u}	A_{2g}	E_g
		E_u	E_g	allowed
	$^1A_{2u}$	A_{2u}	allowed	E_g
$e_g\, d_{xz}\, d_{yz} \rightarrow a_{2u}\, \pi^*$	^3E_u	E_u	E_g	allowed
		A_{1u}	A_{2g}	E_g
		A_{2u}	allowed	E_g
		B_{1u}	B_{2g}	E_g
		B_{2u}	B_{1g}	E_g
	^1E_u	E_u	E_g	allowed
$b_{2g}\, d_{xy} \rightarrow b_{1g}\, d_{x^2-y^2}$	$^1A_{2g}$	A_{2g}	—	E_u
$a_{1g}\, d_{z^2} \rightarrow b_{1g}\, d_{x^2-y^2}$	$^1B_{1g}$	B_{1g}	B_{2u}	E_u
$e_g\, d_{xz}\, d_{yz} \rightarrow b_{1g}\, d_{x^2-y^2}$	^1E_g	E_g	E_u	$A_{2u} + B_{2u}$

ground state is $^1A_{1g}$ x, y axes along ligands

in D_{4h} S = 0 transforms as A_{1g}

S = 1 transforms as $A_{2g} + E_g$

Table 2

$Ni(CN)_4^{2-}$

Band	nm	cm^{-1}	Assignment $^1A_{1g} \rightarrow$	Polarization
I	321.5	31,100	$^1B_{1g}$	π
II	314.0	31,845	$^3A_{2u}$, ^1E_g	σ
	316.0	31,645	$^1A_{2g}$	σ
III	291.0	34,365	$^1A_{2u}$	π
IV	288.5	34,660	$^3B_{1u}$, ^3E_u	σ
V	279.0	35,840	^3E_u	π
VI	274.0	36,500	$^1B_{1u}$ or $^1A_{2u} + \nu_1$	π
VII	272.5	36,700	^1E_u	σ
VIII	272.0	36764.7	$^1E_u + n\nu_2$ or $^1B_{1u}$	
	268.9	37188.5		
	265.9	37608.1		
	263.0	38022.8		
	260.3	38417.2		
	257.7	38804.8		

$\nu_1 = A_{1g}$ C≡N stretch 2149 cm^{-1}

$\nu_2 = A_{1g}$ Ni-C stretch 417 cm^{-1}

exactly to the ground state A_{1g} cyanide stretch of 2149 cm^{-1}.[14] The sharp nature of the band is in agreement with this assignment. The very weak feature at 249 nm, may be due to the third component of such a progression. Alternatively band VI may be assigned as $^1A_{1g} \rightarrow {}^1B_{1u}$ (b_{2g} dxy $\rightarrow a_{2u}\ \pi^*$) allowed π by vibronic coupling with a B_{2g} vibration.

The σ polarized progression, collectively labeled VIII has vibrational spacing 424 - 387 cm^{-1}. This corresponds to the ground state A_{1g} metal-carbon stretch of 417 cm^{-1}.[14] The origin of this progression may be from either band VII, ^1E_u (e_g, dxz, dyz $\rightarrow a_{2u}\ \pi^*$), or $^1B_{1u}$ (b_{2g} dxy $\rightarrow a_{2u}\ \pi^*$). Calculations by Veillard et al.,[15] place the $^1B_{1u}$ state at higher energies than ^1E_u. The presence of a π component to this progression is consistent with either assignment.

An examination of Table 1 in view of the assignments presented above reveals that vibronic coupling of charge transfer bands by the E_g vibrational mode (an out-of-plane bend) is not an effective intensity gaining mechanism. The E_g vibration should be sterically restricted by the stacking of anion planes. The original assumption made in computing the molecular orientation was that vibronic coupling of bands III, V, and VII was negligible; the proposed assignments are self-consistent.

None of the weak transitions below 30,000 cm^{-1} reported in the polarized single crystal study of $K_2\ Ni(CN)_4$[6] were observed in even the thickest crystals of the tetra-n-butyl ammonium salt.

The predominantly axial (σ) crystal faces examined, Figure 7, would, however, make any π polarized bands weak. That none of these bands has been observed in solution either suggest that their origin is intermolecular. One band has been characterized as a magnetic dipole transition.[7] This transition red shifts with decreasing metal-metal distance. A theoretical model of coupling of in-plane dipole moments between stacked anions predicts that a closer approach should produce both a red shift and an increase in intensity as $\frac{1}{r^3}$ interaction increases. With large interionic spacings, the anions approximate the oriented gas model. The absence of such transitions in the crystal examined here agrees with the large metal-metal distance required for packing the bulky cations in the unit cell.

Based primarily upon the observation of these weak, but unexplainable π polarized bands, Ballhausen et al.,[6] postulated that the excited states of the ligand field transitions $^1A_{1g} \rightarrow {}^1B_{1g}$ (a_{1g} $dz^2 \rightarrow b_{1g}$ $dx^2 - y^2$) and $^1A_{1g} \rightarrow {}^1E_g$ (e_g, $dxz, dyz \rightarrow b_{1g}$ dx^2-y^2) were unstable with respect to D_{2d} distortion. The relevant symmetry rules would be those in common between D_{4h} and D_{2d}.[16] In the paper by Ballhausen the alternate choice of axes is made: the x, y axes are chosen 45° from those generally used to characterize D_{4h} in order to coincide with D_{2d} axes. This merely interchanges B_1 and B_2 notations. Transitions $^1A_1 \rightarrow {}^1B_2$ ($dz^2 \rightarrow dx^2$-y^2) and $^1A_1 \rightarrow {}^1E$ ($dx^2yz \rightarrow dx^2y^2$) would then be allowed, π and σ respectively. This

line of reasoning is entirely equivalent to assuming strong vibronic coupling of the B_{2u} mode, the vibration which distorts a square plane into a D_{2d} structure.

Band II is assigned as $^1A_{1g} \rightarrow {}^1E_g$ (e_g dxz, dyz $\rightarrow b_{1g}$ dx^2-y^2) on the basis of the strong σ polarization and a weak MCD A term[9,10] at ~ 32,400 cm^{-1}. $^1A_{1g} \rightarrow E_u(^3A_{2u})$ may also be present. The temperature independent behavior of band II is not in conflict with assignment as a ligand field band; the transition is fully allowed in the lower symmetry. The asymmetry of band II, which shows noticeable splitting, suggests that the transition $^1A_{1g} \rightarrow {}^1A_{2g}$ (b_{2g} dxy $\rightarrow b_{1g}$ dx^2-y^2) which is vibronically σ polarized may also be present.

The shoulder, band I, has previously been shown to be π polarized for inorganic cations.[5] This is in agreement with the broad indistinct π shoulder shown in Figure 8. The broad nature of the band is in accord with assignment as $^1A_{1g} \rightarrow {}^1B_{1g}$ (a_{1g} $dz^2 \rightarrow b_{1g}$ dx^2-y^2) which is D_{2d} distorted in the excited state.

The band shapes substantiate the interpretation offered above, and give additional insight into the nature of the charge transfer and ligand field excited states. Transitions to the a_{2u} π^* orbital should strengthen the metal-carbon bonds, while weakening the C≡N ones. The vibrational progressions observed demonstrate this clearly. The charge transfer excited state should be rigorously planar, as illustrated by the sharpness of the bands.

The spectra of $Pt(CN)_4^{2-}$ presented in Figures 9 and 10, may be analyzed by analogy to the $Ni(CN)_4^{2-}$ spectra. Band II, which exhibits strong π polarization, has previously been resolved in frozen EPA solution at 77 °K.[2] It is assigned as $^1A_{1g} \rightarrow a\,A_{2u}(^1A_{2u})(a_{1g}\,dz^2 \rightarrow a_{2u}\,\pi^*)$. As in $Ni(CN)_4^{2-}$, a second intense π polarized feature is resolved, band VII. The latter is assigned as $^1A_{1g} \rightarrow b\,A_{2u}(^3E_u)$. These states are spin-orbit mixed. The most intense σ polarized band, band VIII, has intensity comparable to the π allowed transitions. It is assigned as $^1A_{1g} \rightarrow {}^1E_u$ (e_g dxz, dyz $\rightarrow a_{2u}\,\pi^*$). The MCD shows a clear A term at 46,100 cm^{-1},[10] in accord with assignment as a transition to a degenerate excited state. These three bands are analogous to bands III, V, and VII, respectively in $Ni(CN)_4^{2-}$.

The σ polarized transition in $Pt(CN)_4^{2-}$, band III, also has an MCD A term (at 39,200 cm^{-1})[10] associated with it. This band is $^1A_{1g} \rightarrow E_u(^3E_u)$. The larger spin orbit coupling for platinum allows greater intensity stealing than in nickel; band IV in $Ni(CN)_4^{2-}$ has a much lower relative intensity.

Spin orbit states which were very weak or not observed in the nickel complex are easily recognized in the $Pt(CN)_4^{2-}$ spectra. Band I is assigned as $^1A_{1g} \rightarrow E_u\ (^3A_{2u})$ in accord with the observed σ polarization and the MCD A term at 35,800 cm^{-1}.[10] The π polarized peak labeled band IV is assigned as the $^1A_{1g} \rightarrow A_{1u}$, B_{1u}, B_{2u} (^3E_u) states which become allowed by vibronic coupling of in-plane bending and stretching vibrational modes. Band V appears in both polarizations. The MCD effect for this band is too small to assign either an A or B term unequivocally to this region. The proposed assignment, $^1A_{1g} \rightarrow E_u$, B_{2u} ($^3B_{1u}$) would allow intensity in both polarizations.

FIGURE 9

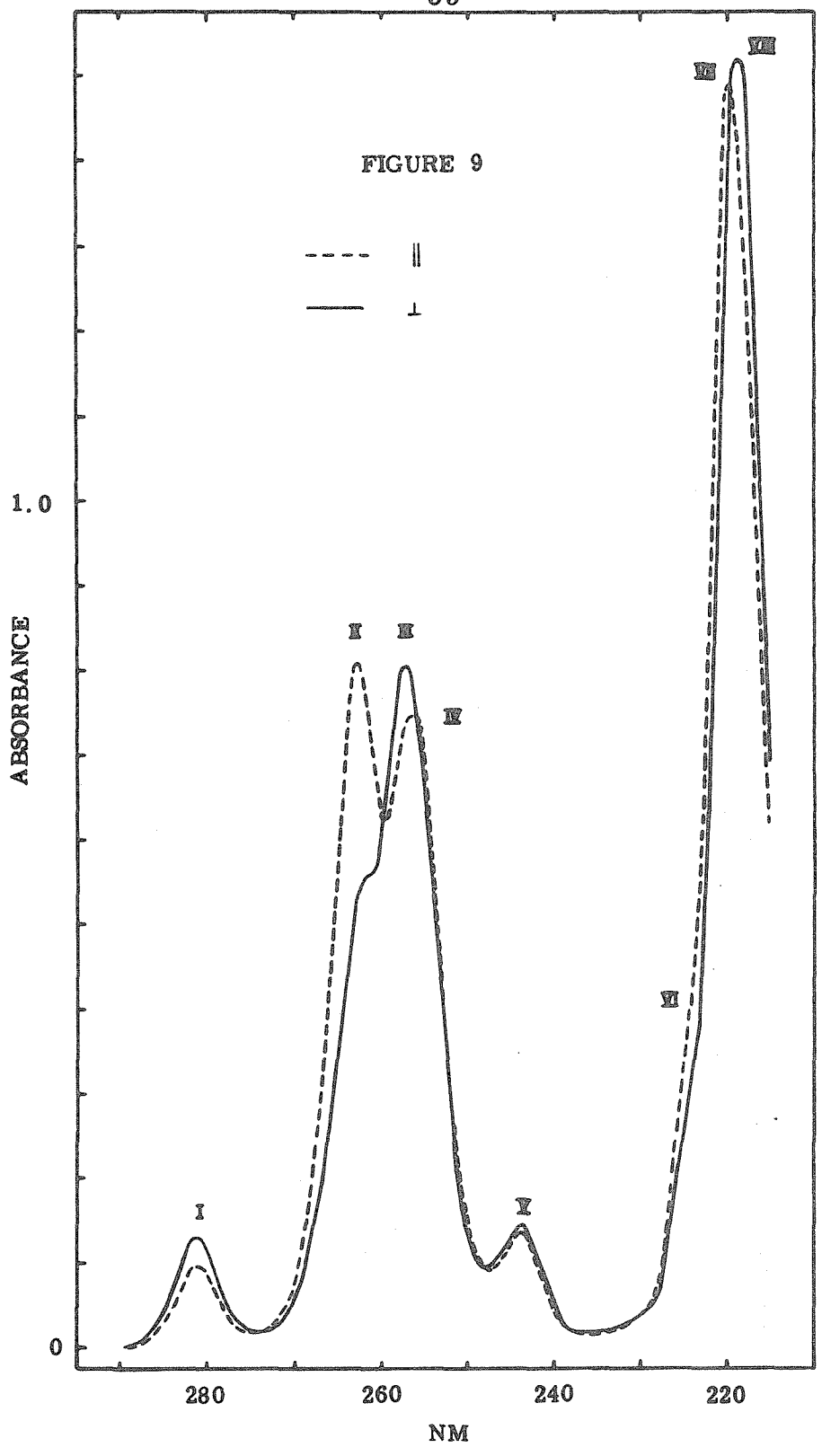

FIGURE 10

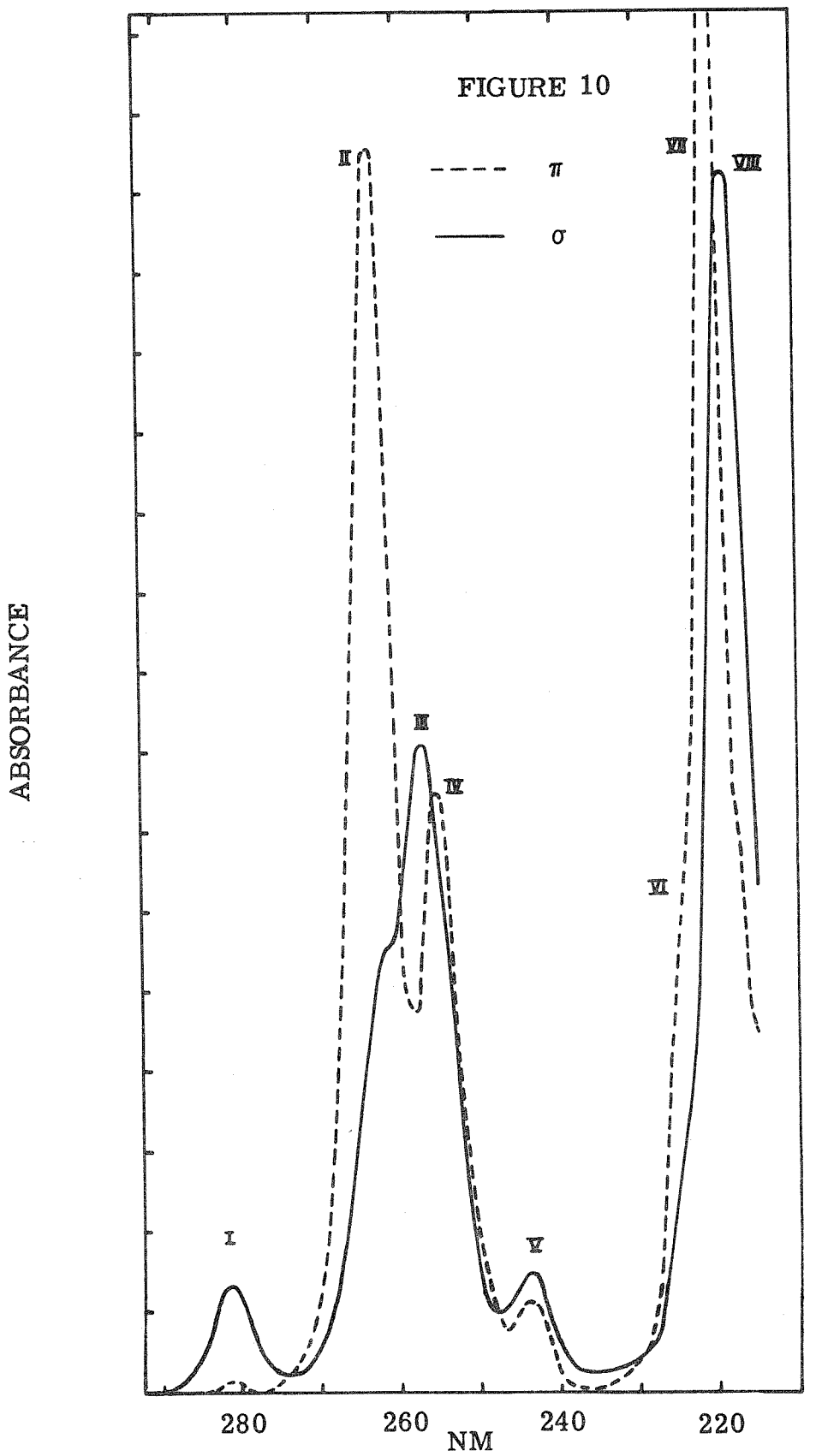

Table 3

$Pt(CN)_4^{2-}$

Band	nm	cm^{-1}	Assignment $^1A_{1g} \rightarrow$	Polarization
I	281.5	35,524	$^3A_{2u}$	σ
II	263.0	38,023	$^1A_{2u}$	π
III	257.2	38,880	^3E_u	σ
IV	255.5	39,139	^3E_u	π
V	243.5	41,068	$^3B_{1u}$	σ, π
VI	225.5	44,346	$^1B_{1u}$ or $^1B_{1g}$	π
VII	220.8	45,290	^3E_u	π
VIII	218.8	45,704	^1E_u	σ

As in $Ni(CN)_4^{2-}$, vibronic coupling of E_g out-of-plane bends appears to be relatively ineffective as an intensity gaining mechanism. The small σ shoulder on the low energy side of band III apparently originates from vibronic coupling of band II, $^1A_{1g} \rightarrow {}^1A_{2u}$. This indicates that coupling of E_g, though very weak, is not totally absent in $Pt(CN)_4^{2-}$.

A weak shoulder can be distinguished in the low energy side of band VII, probably π polarized. This band, band VI, may be either $^1A_{1g} \rightarrow {}^1B_{1u}$ (b_{2g} dxy $\rightarrow a_{2u}\ \pi^*$) or the first ligand field band $^1A_{1g} \rightarrow {}^1B_{1g}$ (a_{1g} $dz^2 \rightarrow b_{1g}$ $dx^2\text{-}y^2$).

An alternate assignment in which bands I - IV are d $\rightarrow a_{2u}\ \pi^*$ and the higher energy bands are charge transfer transitions to a higher ligand antibonding orbital seems unlikely. The relative intensity of $^1A_{1g} \rightarrow {}^1E_u$ (band III in this alternate assignment) is only half the intensity of $^1A_{1g} \rightarrow {}^1A_{2u}$ (band II). This is in contradiction to the expected relative intensities.[1]

The ordering of virtual orbitals obtained for both $Ni(CN)_4^{2-}$ and $Pt(CN)_4^{2-}$ is dxy ~ dxz, dyz < $dz^2 \ll a_{2u}^*$, $dx^2\text{-}y^2$. This ordering is surprising because square planar d orbital orderings invariably place the dz^2 orbital lowest. The anomalous destabilization of the dz^2 orbital can be simply understood. The dz^2 orbital is σ antibonding. The strong back bonding of the metal with the cyanide ligands strengthens the σ bonds and destabilizes dz^2.

References

1. H. B. Gray and C. J. Ballhausen, J. Amer. Chem. Soc., 85, 260 (1963).

2. W. R. Mason and H. B. Gray, J. Amer. Chem. Soc., 90, 5721 (1968).

3. A. I. Ryskin, A. M. Tkachuk, and N. A. Tolstoi, Opt. Spectrosk., 17, 304 (1964).

4. C. Moncuit and H. Poulet, J. Phys. Radium., 23, 353 (1962).

5. M. L. Colin, Bull. Soc. Royal Sci. Liege, 34, 130 (1965).

6. C. J. Ballhausen, N. Bjerrum, R. Dingle, K. Ericks and C. R. Hare, Inorganic Chem., 4, 514 (1965).

7. J. P. Dahl, R. Dingle, and M. T. Vala, Acta Chem. Scand, 23, 47 (1969).

8. C. Moncuit, Chim. Phys., 64, 494 (1967).

9. P. J. Stephens, A. J. McCaffery and P. N. Schatz, Inorg. Chem., 7, 1923 (1968).

10. S. B. Piepho, P. N. Schatz, and A. J. McCaffery, J. Amer. Chem. Soc., 91, 5994 (1969).

11. E. M. Holt and K. J. Watson, Acta. Chem. Scand., 23, 14 (1969).

12. F. K. Larsen, R. Hazell, and S. E. Rasmussen, ibid., 23, 61, (1969).

13. N. G. Vannerberg, ibid., 18, 2385 (1964).

14. D. Jones, I. J. Hyams, and E. R. Lippincott, Spectrochim. Acta, 24A, 973 (1968).

15. J. Demuynck and A. Veillard, Theoret. Chim. Acta, 28, 241 (1973).

16. C. K. Ingold and G. W. King, J. Chem. Soc., 2708 (1953).

CHAPTER 3

Polarized Crystal Spectra of $Pt_2Cl_6^{2-}$ and $Pd_2Cl_6^{2-}$

An attempt by a worker in our laboratory to prepare the π-cyclopropenyl analogue of zeise's salt, $K[Pt(C_2H_4)Cl_3]$, produced a compound of the expected stoichiometry.[1] A subsequent x-ray structural investigation[2] showed that the complex formed was actually the cyclopropenium salt of $Pt_2Cl_6^{2-}$, tetrachloro -μ, μ'-dichloro-diplatinate (II). Although the $(C_6H_5)_4As^+$ [3] and $(C_3H_7)_3POH^+$ cations[4] are also known to precipitate the $Pt_2Cl_6^{2-}$ anion from solutions of tetrachloroplatinate (II), $Pt_2Cl_6^{2-}$ salts are rare. All the other anions $M_2X_6^{2-}$ (M = Pt, Pd) (X = Cl, Br, I) can be easily isolated.[5,6]

The only existing related x-ray structure is for the compound $[(C_2H_5)_4N]_2[Pt_2Br_6]$.[5,7] The structure of the $Pt_2Cl_6^{2-}$ anion is shown in Figure 11 and the packing within the unit cell in Figure 12. The Cl_1 - Pt_1 - Cl_2 angle[2] is 84.9° compared to the Br_1 - Pt_1 - Br_2 angle[7] of 86.19°. The Pt - Pt distance in the chloride[2] is 3.418 Å; the bromide metal-metal distance is 3.55 Å.[7] No metal-metal attractive interaction is apparent structurally in these compounds.

The similarity between the spectra of the d^8 square planar D_{4h} monomers and the D_{2h} bridged dimers[8] also suggests that metal-metal interactions are small. That the extinction coefficients of the dimer are more than twice those of the monomer has been interpreted as due to the lower C_{2v} symmetry of the metal ion in the

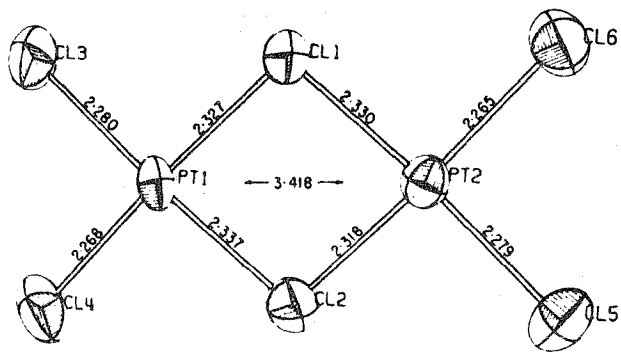
CL3
CL1
CL6
2.280
2.327
2.330
2.365
PT1
3.418
PT2
2.268
2.337
2.318
2.279
CL4
CL2
CL5

FIGURE 11

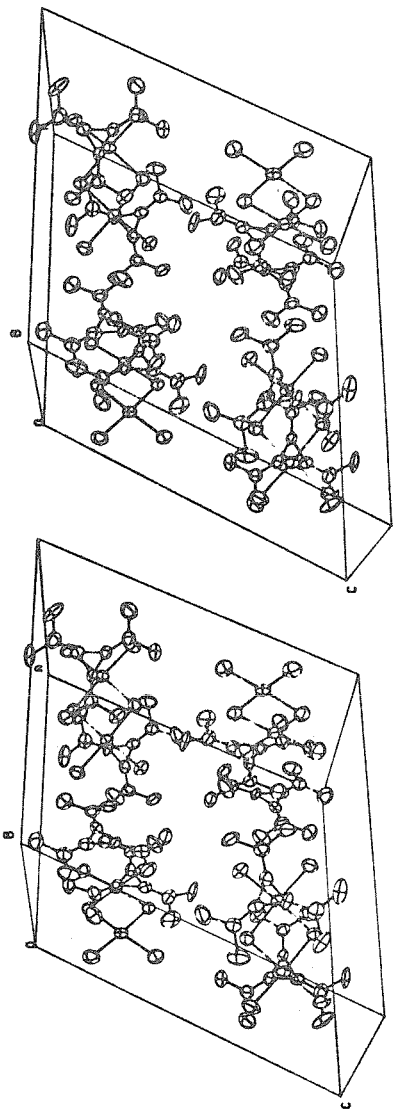

FIGURE 12

dimer.[8] The assignment of the dimer spectra should then be directly related to that of the monomer.

A number of polarized single crystal spectra have been obtained for K_2 $PtCl_4$.[9-11] These measurements are in accord with a doped crystal study of $PtCl_4^{2-}$.[12] The 15°K polarized single crystal spectra of K_2 $PtCl_4$ from reference 11 are shown in Figure 13. The x, y polarized band at 26,300 cm^{-1} is universally assigned as $^1A_{1g} \rightarrow {}^1A_{2g}$ (b_{1g} $dx^2-y^2 \rightarrow b_{2g}$ dxy); no vibronic coupling is possible in z polarization and no z component is observed. The z polarized band at 29,800 cm^{-1} (x, y component at 29,200 cm^{-1}) is assigned as $^1A_{1g} \rightarrow {}^1E_g$ (e_g dxz, dyz $\rightarrow b_{2g}$ dxy) on the basis of both solution and liquid helium temperature single crystal MCD measurements[13,14] which show a definite A term near 30,000 cm^{-1}. The third spin-allowed ligand field band is found at 36,500 cm^{-1} in the reflectance spectra[15] and 37,500 cm^{-1} in the thin film crystal. This band has xy polarization, opposite to that observed for the $^1A_{1g} \rightarrow {}^1E_g$ band, which is in agreement with the expected vibronic mechanism $E_u > B_{1u}$. The out-of-plane B_{1u} vibrational mode is restricted by the anion stacking. This transition is assigned as $^1A_{1g} \rightarrow {}^1B_{2g}$ (a_{1g} $dz^2 \rightarrow b_{2g}$ dxy). This orbital ordering $dz^2 < dxz, dyz < dx^2-y^2 \ll$ dxy is also supported by MO calculations.[12,16,17] The assignments of the three triplet transitions at 18,000 cm^{-1}, 20,600 cm^{-1}, and 24,000 cm^{-1} are $^1A_{1g} \rightarrow {}^3E_g$, $^1A_{1g} \rightarrow {}^3A_{2g}$, and $^1A_{1g} \rightarrow {}^3B_{2g}$ respectively.[12] The assignments of the lowest two triplet bands have been reversed by some authors.[9,18]

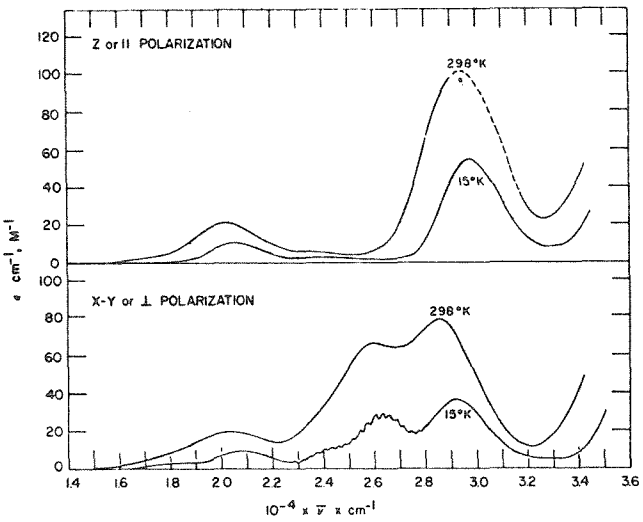

Absorption spectra of a K_2PtCl_4 crystal with polarized light; crystal thickness 46.5 μ.

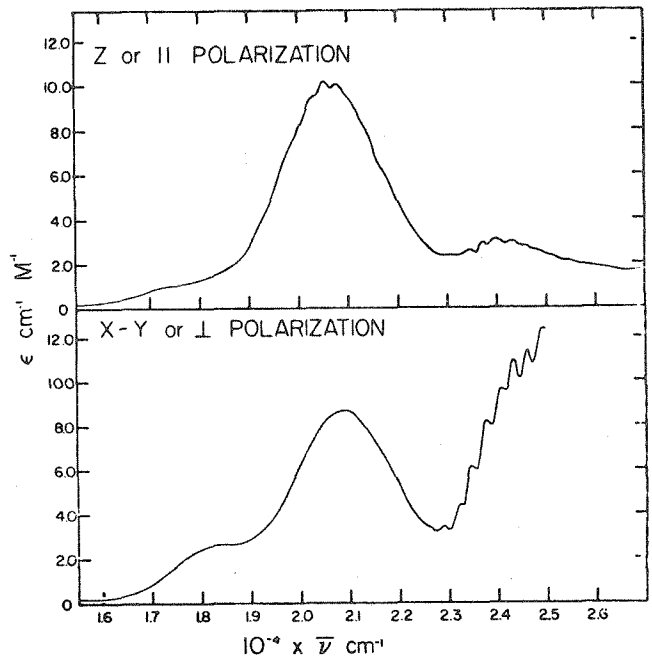

Absorption spectra of a K_2PtCl_4 crystal with polarized light at 15°K.; crystal thickness 113 μ.

FIGURE 13

Table 4

$Pt\ Cl_4^{2-}$ Ligand Field Bands

Transition	Excited State	Symmetry	Vibration Required to be allowed $\pi\ A_{2u}$	$\sigma\ E_u$
$b_{1g}\ dx^2y^2 \rightarrow b_{2g}dxy$	$^3A_{2g}$	A_{1g}	A_{2u}	E_u
		E_g	E_u	$A_{2u} + B_{1u}$
	$^1A_{2g}$	A_{2g}	---	E_u
$e_g\ dxz, dyz \rightarrow b_{2g}\ dxy$	^3E_g	E_g	E_u	$A_{2u} + B_{1u}$
		A_{1g}	A_{2u}	E_u
		A_{2g}	---	E_u
		B_{1g}	---	E_u
		B_{2g}	B_{1u}	E_u
	^1E_g	E_g	E_u	$A_{2u} + B_{1u}$
$a_{1g}\ dz^2 \rightarrow b_{2g}\ dxy$	$^3B_{2g}$	B_{1g}	---	E_u
		E_g	E_u	$A_{2u} + B_{1u}$
	$^1B_{2g}$	B_{2g}	B_{1u}	E_u

ground state is $^1A_{1g}$ x, y axes are between ligands in D_{4h}

S = 0 transforms as A_{1g}

S = 1 transforms as $A_{2g} + E_g$

The dimer has D_{2h} symmetry. The x axis is chosen to lie along the metal-metal direction, y is perpendicular to this direction and in-plane, and z is normal to the anion plane. Weak interaction of the metal ions is assumed. The d orbitals will interact as shown in Figure 14. The dz^2 orbitals have essentially no overlap and should be considered as one center orbitals. Similarly the dyz orbitals can only interact via superexchange through bridging chlorine d orbitals.

For an electron excited from a localized (one-center) orbital, dz^2 or dyz, into an orbital, dxy ± dxy, delocalized appreciably over both centers, the selection rules governing the transition will be those appropriate to the point group composed of elements in common between the C_{2v} monomer and the D_{2h} dimer. This point group is C_{2v}. In the lower symmetry both dxy ± dxy orbitals transform as b_1. The selection rules for these transitions are given in Table 5.

When both the excited electron and the hole are delocalized over both centers D_{2h} symmetry rigorously applies. The selection rules for these transitions are shown in Table 6. In Table 6 all of the possible singlet d-d transitions are shown, but only those triplets with ungerade orbital symmetry were considered. All triplets with gerade symmetry will be forbidden. There are two triplets of each symmetry listed, corresponding to the two singlets. The dyz orbitals were also considered in the delocalized case because of the possibility of superexchange. Both cases predict identical polarizations.

Figure 14

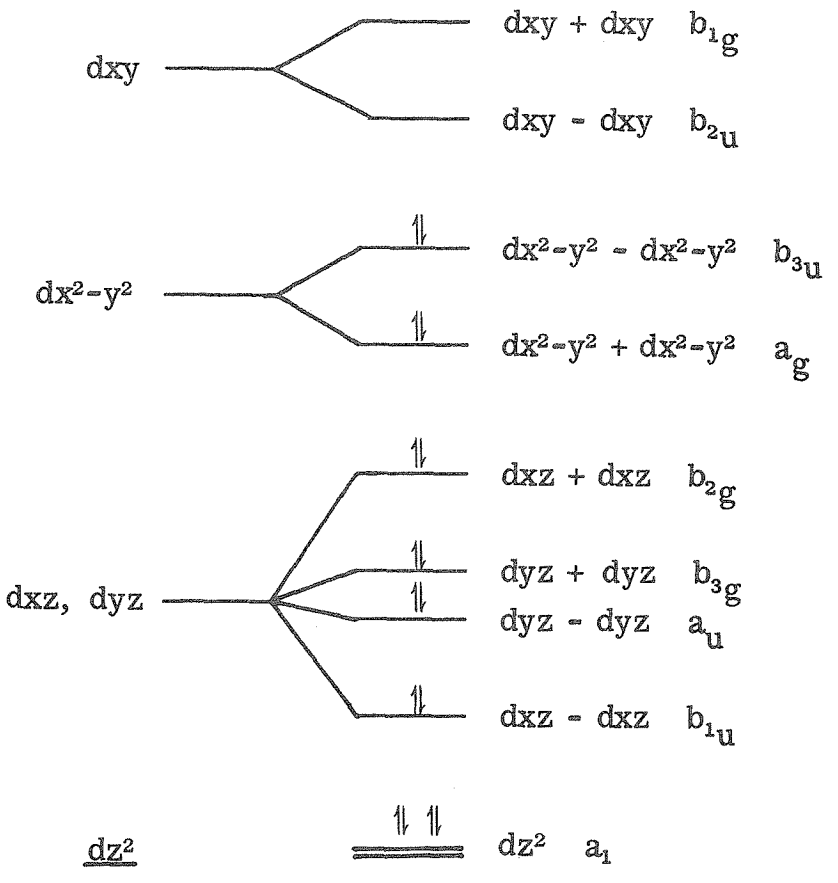
dxy
dxy + dxy b1g
dxy - dxy b2u
dx²-y²
dx²-y² - dx²-y² b3u
dx²-y² + dx²-y² ag
dxz, dyz
dxz + dxz b2g
dyz + dyz b3g
dyz - dyz au
dxz - dxz b1u
dz²
dz² a1

Table 5

Selection Rules for One Center → Two Center Transitions in C_{2v} Symmetry

		Excited State Symmetry	Polarization
a_2 dyz → b_1 dxy ± dxy	$^1A_1 \rightarrow {}^1B_2$	B_2	z
	$^1A_1 \rightarrow {}^3B_2$	A_1	x
		A_2	
		B_1	y
a_1 dz^2 → b_1 dxy ± dxy	$^1A_1 \rightarrow {}^1B_1$	B_1	y
	$^1A_1 \rightarrow {}^3B_1$	A_1	x
		A_2	
		B_2	z

the d orbitals transform in C_{2v} as

dxy	b_1	x	a_1
dx^2-y^2	a_1	y	b_1
dxz	b_2	z	b_2
dyz	a_2		
dz^2	a_1		

S = 0 transforms as a_1

S = 1 transforms as $a_2 + b_1 + b_2$

Table 6

Selection Rules for Delocalized Transitions in D_{2h} Symmetry

		Excited State Symmetry	Polarization
$dx^2-y^2 \rightarrow dxy$	$^1A_g \rightarrow {}^1B_{1g}$	B_{1g}	
	$^1A_g \rightarrow {}^1B_{2u}$	B_{2u}	y
	$^1A_g \rightarrow {}^1B_{2u}$	B_{2u}	y
	$^1A_g \rightarrow {}^1B_{1g}$	B_{2u}	
	$^1A_g \rightarrow {}^3B_{2u}$	B_{3u}	x
		A_u	
		B_{1u}	z
$dxz \rightarrow dxy$	$^1A_g \rightarrow {}^1B_{3g}$	B_{3g}	
	$^1A_g \rightarrow {}^1A_u$	A_u	
	$^1A_g \rightarrow {}^1A_u$	A_u	
	$^1A_g \rightarrow {}^1B_{3g}$	B_{3g}	
	$^1A_g \rightarrow {}^3A_u$	B_{1u}	z
		B_{2u}	y
		B_{3u}	x
$dyz \rightarrow dxy$	$^1A_g \rightarrow {}^1B_{1u}$	B_{1u}	z
	$^1A_g \rightarrow {}^1B_{2g}$	B_{2g}	
	$^1A_g \rightarrow {}^1B_{2g}$	B_{2g}	
	$^1A_g \rightarrow {}^1B_{1u}$	B_{1u}	z

Table 6 (Cont'd)

	Excited State Symmetry	Polarization
$^1A_g \rightarrow {}^3B_{1u}$	A_u	
	B_{3u}	x
	B_{2u}	y

$S = 0$ transforms as A_g

$S = 1$ transforms as $B_{1g} + B_{2g} + B_{3g}$

x	b_{3u}
y	b_{2u}
z	b_{1u}

The dimeric D_{2h} model differs from the C_{2v} perturbed monomer model only for transitions between orbitals delocalized over both centers. Four bands are predicted by the dimer model for each of these transitions. While the C_{2v} model predicts that $dx^2-y^2 \rightarrow dxy$ will be allowed and y polarized, the D_{2h} model predicts <u>two</u> such $^1A_g \rightarrow {}^1B_{2u}$ allowed y polarized transitions. Only for $dx^2-y^2 \rightarrow dxy$ can the two models be distinguished.[8] The $dyz \rightarrow dxy$ transitions are probably best characterized in the monomeric model, and there are no allowed singlet $dxz \rightarrow dxy$ transitions. Polarized single crystal spectra at 5°K were measured to resolve this point.

Large single crystals of $\{[(CH_3)_2N]_3C_3\}_2\{Pt_2Cl_6\}$ were provided by Daniel Harris. The crystals were imbedded in parafin and solvent ground using acetonitrile-hexane. The diamond-shaped (100) face was dichroic - red along c and pink along the b axis; the square (111) face was dichroic pink to yellow. Crystals were mounted with epoxy over pinholes cut in lead foil. Single crystal polarized spectra at 5°K are presented in Figures 15 - 17.

The crystals are monoclinic, space group $P2_1/c$, with four formula units per unit cell. The density, as determined by volume displacement from carbon tetrachloride, is 2.23 g/cm^3. The calculated density is 2.09 g/cm^3. The lattice constants were found to be a = 17.383 Å, b = 11.234 Å, c = 17.192 Å, and β = 117.46°.[2] The least squares plane of the anion[2] is

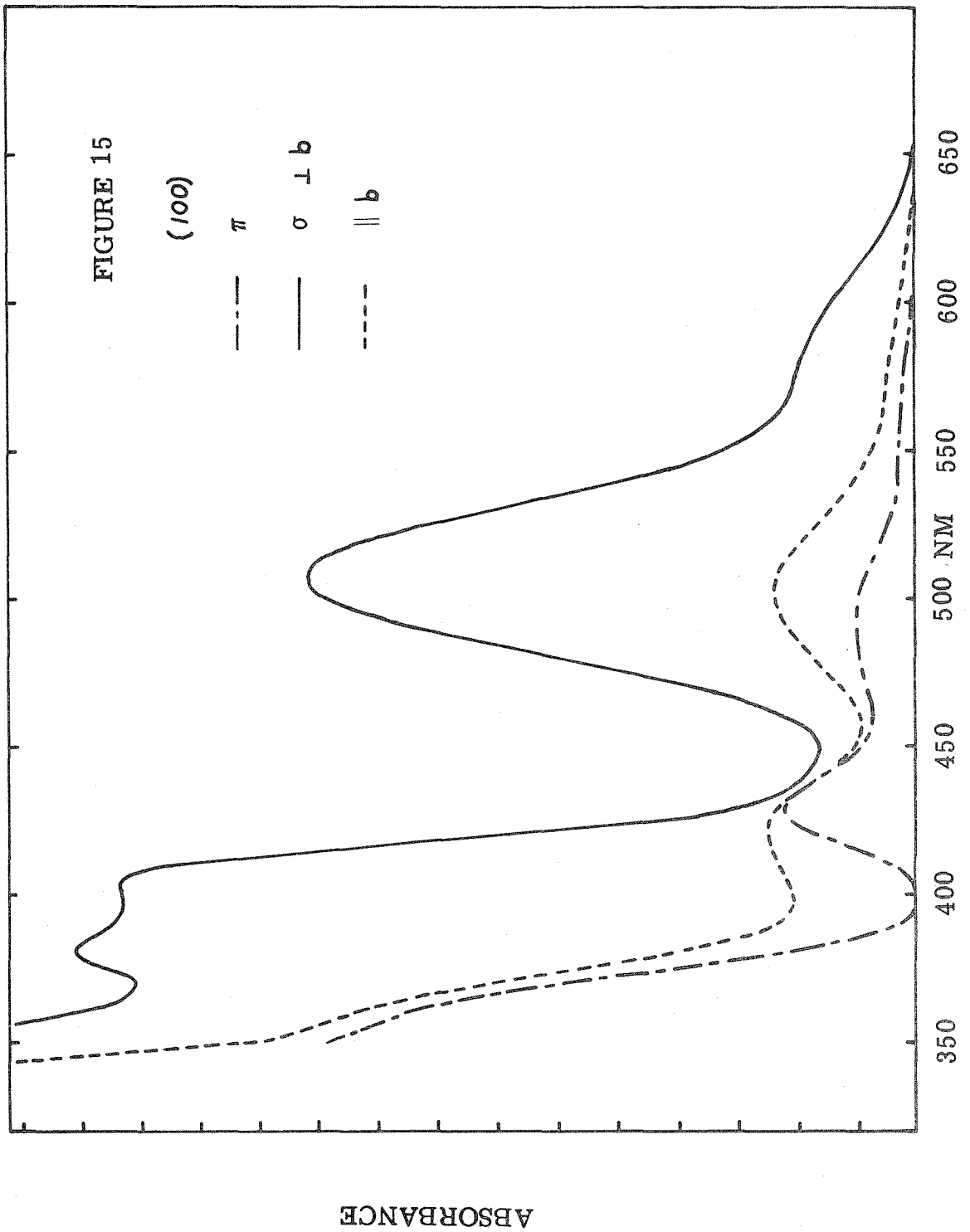
FIGURE 15
(100)
π
σ ⊥ b
σ ∥ b
ABSORBANCE
350
400
450
500 NM
550
600
650

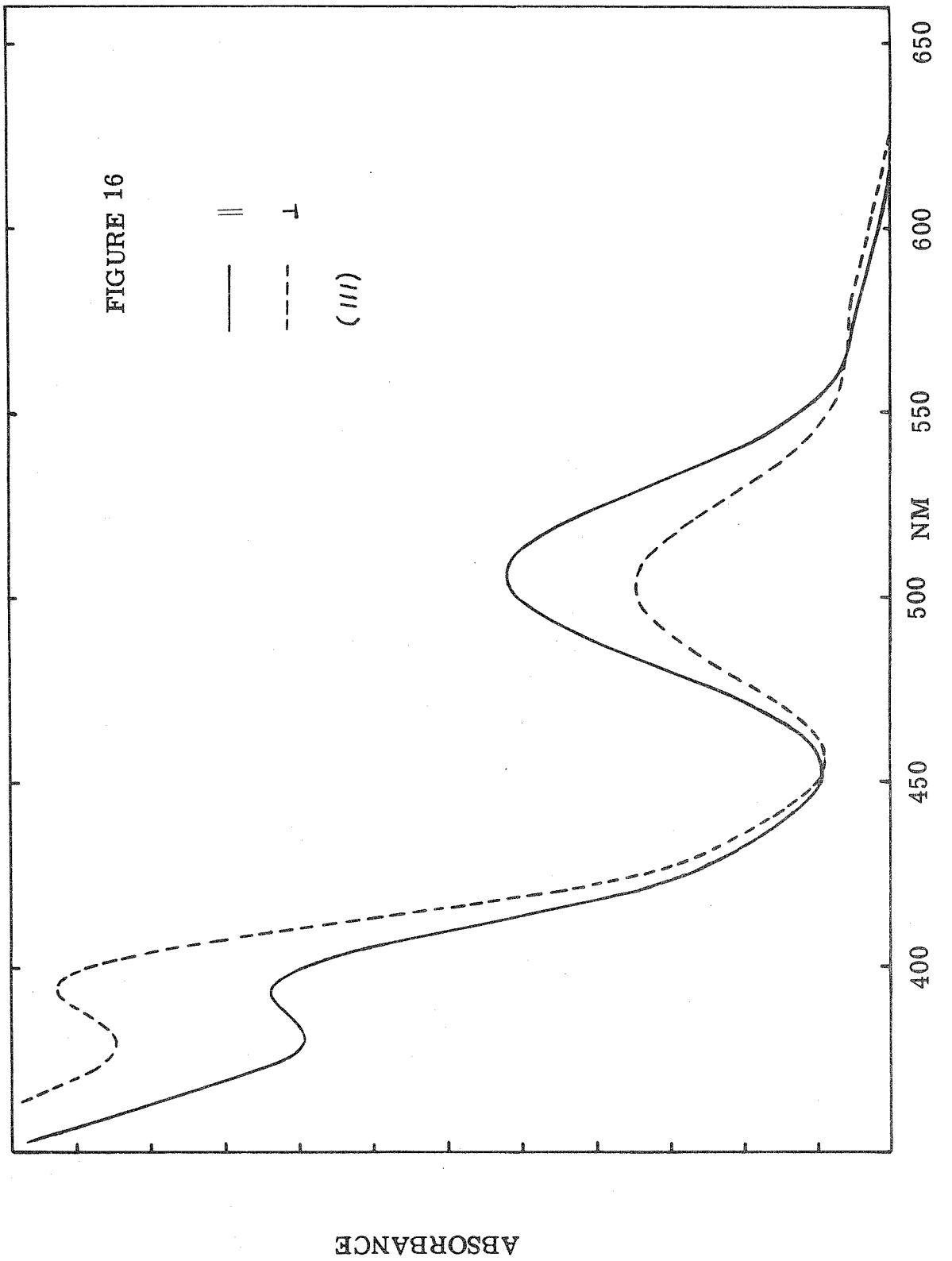
FIGURE 16
(111)
∥
⊥
ABSORBANCE
400
450
500
550
600
650
NM

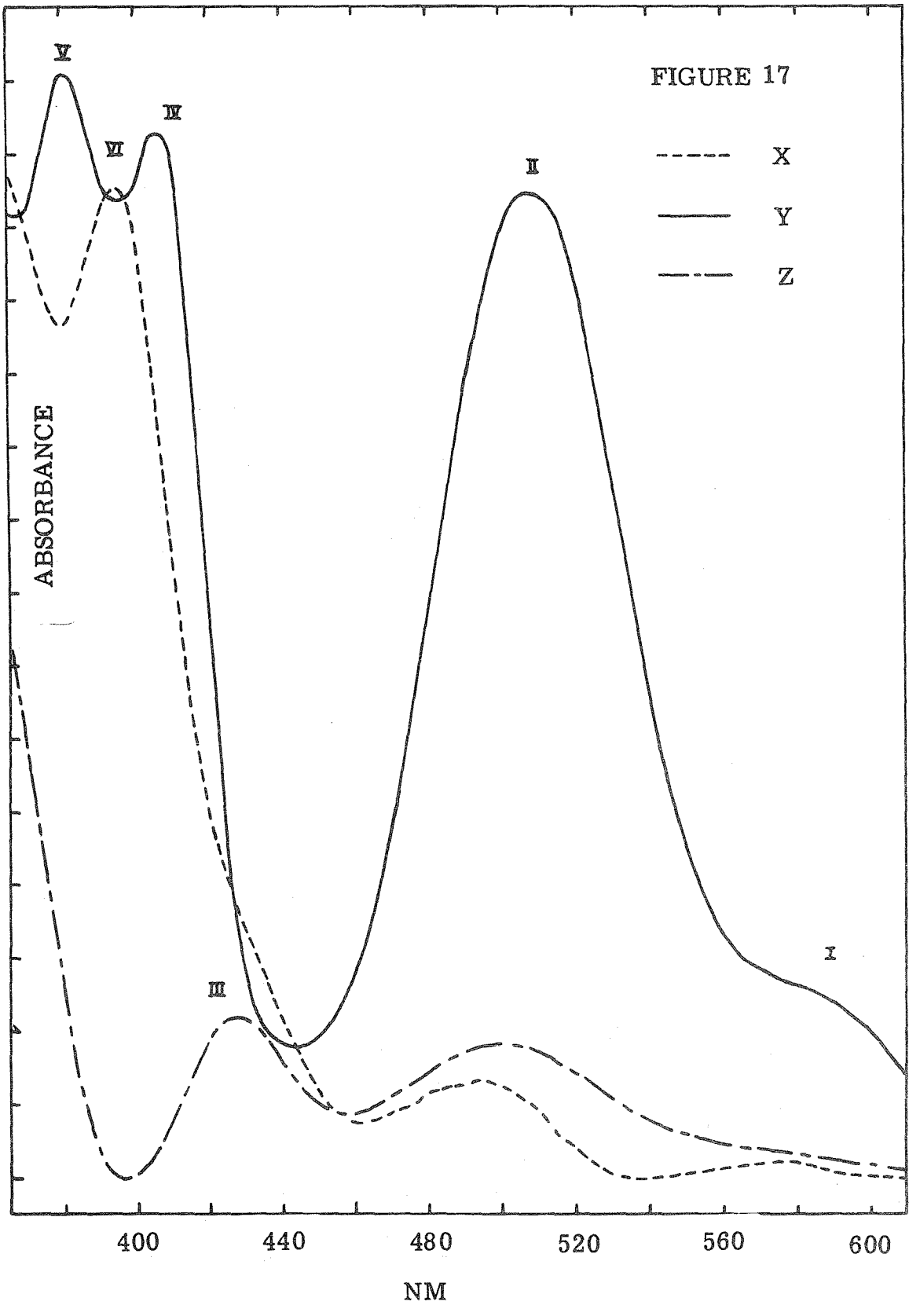
FIGURE 17
X
Y
Z
V
VI
IV
II
III
I
ABSORBANCE
400
440
480
520
560
600
NM

$$.339\,x' + .940\,y' + .047\,z' - .883 = 0 \qquad (28)$$

where x′, y′, z′ are coordinates of the atoms in Å units along the $\bar{a}$, $\bar{b}$, $\bar{c}^*$ monoclinic cell directions, respectively. The normal $\bar{z}$ to the least squares plane in the alternate orthogonal coordinate system $\bar{a}^*$, $\bar{b}$, $\bar{c}$ is

$$\bar{z} = .3225\,\bar{a}^* + .9400\,\bar{b} - .1146\,\bar{c} \qquad (29)$$

the extinction directions for the (100) face are simply $\bar{b}$ and $\bar{c}$.

The molecular axis $\bar{x}$ corresponds to the projection of the metal-metal direction in the least squares plane.

$$\bar{x} = -.7917\,\bar{a}^* + .3339\,\bar{b} + .5116\,\bar{c} \qquad (30)$$

The squares of the direction cosines of the direction cosines of the $\bar{x}$, $\bar{y}$, $\bar{z}$ molecular axes relative to the extinction directions give the absorbances $\parallel$ and $\perp$ to b using equations 4 and 5.

$$A_{\parallel} = .8836\,A_z + .1115\,A_x + .0055\,A_y \qquad (31)$$

$$A_{\perp} = .0131\,A_z + .2617\,A_x + .7247\,A_y \qquad (32)$$

The two distinct anion orientations are equivalent for the (100) face. The calculated values of $\theta = 19.95°$ and $\phi = 70.44°$ allow the preliminary resolution of $A_{\parallel}$ and $A_{\perp}$ into $A\pi$ and $A\sigma$ by the matrix (21)

$$\begin{bmatrix} A\pi \\ A\sigma \end{bmatrix} = \begin{bmatrix} 1.1337 & -.1337 \\ -.0150 & 1.0150 \end{bmatrix} \begin{bmatrix} A_{\parallel} \\ A_{\perp} \end{bmatrix} \qquad (33)$$

This approximation is strictly valid only for chromophore centers of three fold symmetry or higher. Day et al.[8] have performed a similar resolution on polarized spectra of $[(C_2H_5)_4N]_2[Pt_2Br_6]$ with virtually identical results.

The square face was identified as (111) from x-ray photographs. The normal to the face makes an angle of 51°24′ with the b crystallographic axis. For this face the extinction directions are

$$\| = -.5321\ \bar{a}^* + .7813\ \bar{b} - .3254\ \bar{c} \tag{34}$$

$$\perp = -.5217\ \bar{a}^* + .8530\ \bar{c} \tag{35}$$

For the anion with molecular axes defined above in equations (29) and (30),

$$A_{\|} = .3601\ Az + .2659\ Ax + .3740\ Ay \tag{36}$$

$$A_{\perp} = .0708\ Az + .7215\ Ax + .2077\ Ay \tag{37}$$

This anion makes angles $\theta = 53.12°$ and $\phi = 70.57°$ with the extinction directions.

The other anion has the related molecular axis

$$z = -.3225\ \bar{a}^* + .9400\ \bar{b} + .1146\ \bar{c} \tag{38}$$

$$x = .7917\ \bar{a}^* + .3339\ \bar{b} - .5116\ \bar{c} \tag{39}$$

which gives

$$A_{\|} = .8687\ Az + .0000\ Ax + .1313\ Ay \tag{40}$$

$$A_{\perp} = .0708\ Az + .7215\ Ax + .2077\ Ay \tag{41}$$

for angles of $\theta = 26.69°$ and $\phi = 53.67°$ with the extinction directions. These two anion orientations must be averaged.

$$\bar{A}_{\parallel} = .6144\ Az + .1330\ Ax + .2527\ Ay \quad (42)$$

$$\bar{A}_{\perp} = .0708\ Az + .7215\ Ax + .2077\ Ay \quad (43)$$

The polarized data for these two faces will allow resolution of the spectra along the molecular axes. The known values of $A_{\parallel}$, $A_{\perp}$, $\bar{A}_{\parallel}$, $\bar{A}_{\perp}$ (equations 31, 32, 42, 43) are four equations in four unknowns B, Ax, Ay, Az. B is the ratio by which equations 42, 43 must be multiplied to compensate for the differing thicknesses of the two faces. B has a value of 1.14.

The molecular absorbances

$$A_z = -.2214\ \bar{A}_{\perp} + 1.1466\ A_{\parallel} + .0470\ A_{\perp} \quad (44)$$

$$A_x = 1.7863\ \bar{A}_{\perp} - .1189\ A_{\parallel} - .4482\ A_{\perp} \quad (45)$$

$$A_y = -.6411\ \bar{A}_{\perp} + .0222\ A_{\parallel} + 1.5409 A_{\perp} \quad (46)$$

are plotted in Figure 17.

The proposed assignments of the resolved molecular spectra are presented in Table 7. The two allowed y polarized bands - IV, V- $^1A_g \rightarrow {}^1B_{2u}$ ($dx^2-y^2 \rightarrow dxy$) confirm the existence of a small but significant metal-metal interaction within the halogen bridged dimer. The most remarkable difference between the monomer and dimer spectra is the intensification of the y polarized triplet, band II, in the dimer. This band has an intensity nearly equal to that of the

Table 7

$Pt_2Cl_6^{2-}$

Band	nm	cm^{-1}	Assignment $^1A_g \rightarrow$	Polarization
I	590	16,950	$^3B_{1u}$	y
II	509	19,650	$^3A_u + {}^3B_{2u}$	y
III	428	23,320	$^3B_1$	z
IV	407	24,600	$^1B_{2u}$	y
VI	395	25,300	$^3B_1$	x
V	381	26,250	$^1B_{2u}$	y

lowest allowed singlets. The fact that the triplet and lowest singlets have the same polarization strongly suggests intensity borrowing via spin orbit coupling.

The observed spectra are assigned analogously to the tetrachloroplatinate (II) monomer. Band I, with y > x polarization is assigned as $^1A_g \rightarrow {}^3B_{1u}$ (dyz → dxy). No z component is allowed for this transition. Band II is similarly assigned as $^1A_g \rightarrow {}^3A_u$ (dxz → dxy). All polarizations are allowed; the y polarization intensity being the result of strong spin orbit mixing. Possibly also present under the band envelope is the $^1A_g \rightarrow {}^3B_{2u}$ (dx^2-y^2 → dxy) transition. Band III, which is z polarized, and band VI, with x polarization, are assigned as $^1A_1 \rightarrow {}^3B_1$ (dz^2 → dxy). The slight x shoulder at the same energy as band III may alternately be the x component. Band VI would then be assigned as a vibronic component of $^1A_g \rightarrow {}^1B_{1g}$ (dx^2-y^2 → dxy).

The single crystal polarized spectra of the $Pd_2Cl_6^{2-}$ dimer, tetrachloro -μ, μ'-dichloro-dipalladate (II), should be similarly amenable to assignment by analogy to the spectra of the related monomer, K_2 $PdCl_4$. The polarized single crystal spectra of K_2 $PdCl_4$ is shown in Figure 18. For this d^8 square planar complex, the spectra are expected to be almost identical to the isomorphous platinum compound. The xy polarized shoulder at 20,000 cm^{-1} is generally assigned as $^1A_{1g} \rightarrow {}^1A_{2g}$ (dx^2-y^2 → dxy) because of the apparent absence of any z component. This transition is observed

FIGURE 18

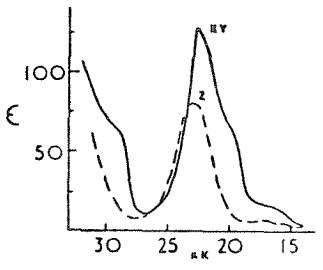

Polarized transmission spectrum of a crystal of K_2PdCl_4. The notation *z* denotes absorption with the electric vector perpendicular to the ionic planes (i.e., along the *c* axis), while *xy* refers to the in-plane absorption. The units of the abscissas are 1000 cm^{-1} and of the ordinates are liters per mole-centimeter.

at 26,000 cm^{-1} in $PtCl_4^{2-}$, as expected for the larger value of 10 Dq of the third row metal. The xy polarized feature at 22,600 cm^{-1} (z maxima at 23,000 cm^{-1}) is assigned as $^1A_{1g} \rightarrow {}^1E_g$ (dxz, dyz → dxy). This assignment is highly unsatisfactory since this transition is $PtCl_4^{2-}$ is z polarized. A number of other arguments concerning the expected ordering and relative energy separation between the xy and z components also reveal discrepancies in this assignment.[15] The remaining xy polarized shoulder at 29,500 cm^{-1} is assigned as $^1A_{1g} \rightarrow {}^1B_{2g}$ ($dz^2 \rightarrow$ dxy).

The availability of the low temperature polarized spectra of the related platinum dimer, $Pt_2Cl_6^{2-}$ provides an additional basis for assignments. Any proposed assignment of the spectra of $Pd_2Cl_6^{2-}$ should be consistent with both the platinum dimer and the $PdCl_4^{2-}$ monomer. The single crystal polarized spectra of two faces of $[(n\text{-}C_4H_9)_4N]_2[Pd_2Cl_6]$ at 5°K are shown in Figures 19, 20. The compound was prepared by the method of Mason and Gray.[6]

Thin single crystals of $[(n\text{-}C_4H_9)_4N]_2[Pd_2Cl_6]$ were grown from dichloromethane. The crystals were dichroic red to pale yellow-orange. The predominant face obtained, labeled (100) is shown in Figure 19. No x-ray data exist for this compound. The similar species $[(C_2H_5)_4N]_2[Pd_2Br_6]$ is probably ismorphous to the compound $[(C_2H_5)_4N]_2[Pt_2Br_6]$.[7] The well developed face of the latter complex is (100); the anions are stacked with their x molecular axes parallel to one crystal axis.[7] An examination of the selection rules presented in Tables 5 and 6 reveals that no allowed x polarized

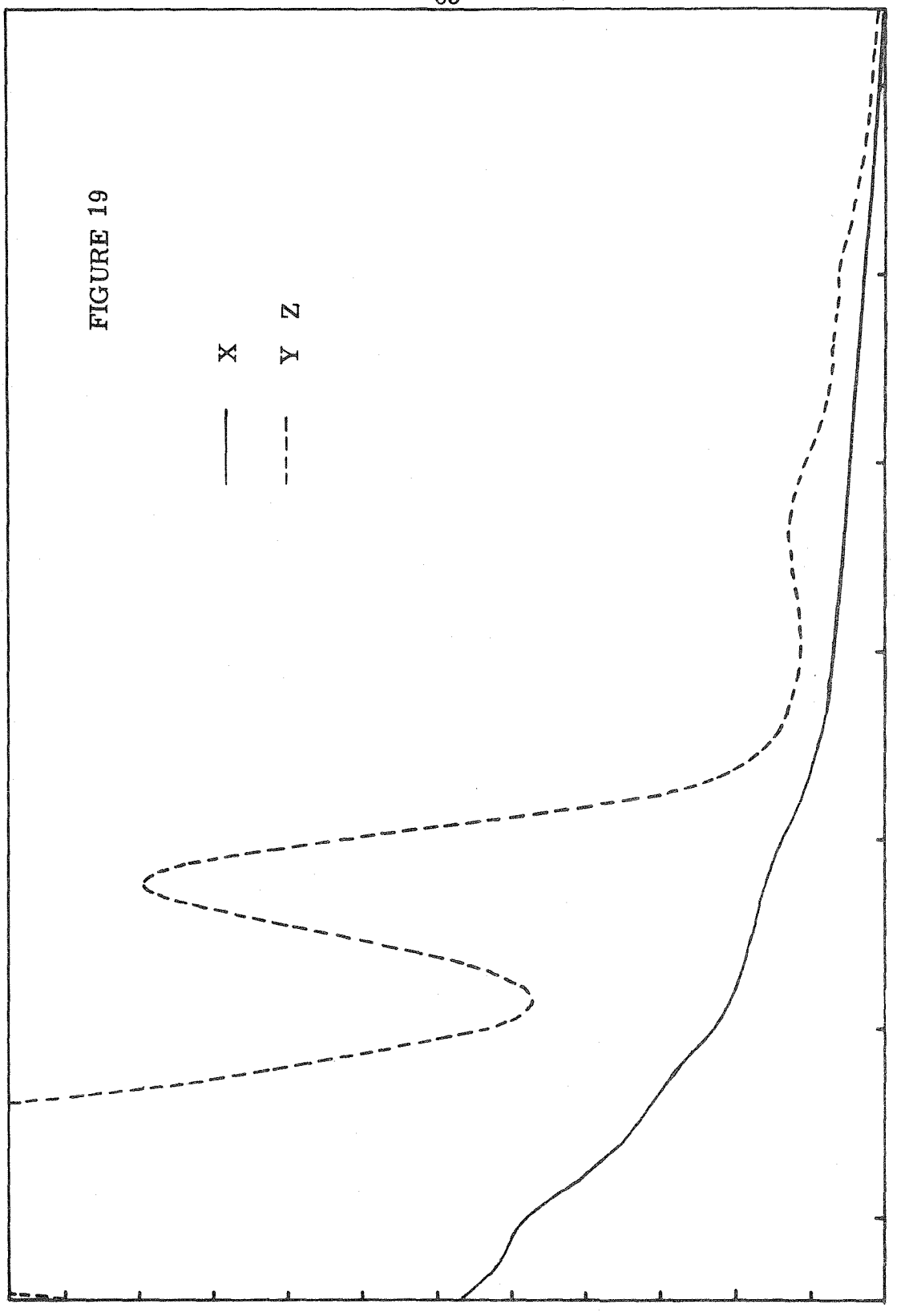
FIGURE 19
X
Y Z
250
300
350
400
450
500
550
NM
ABSORBANCE

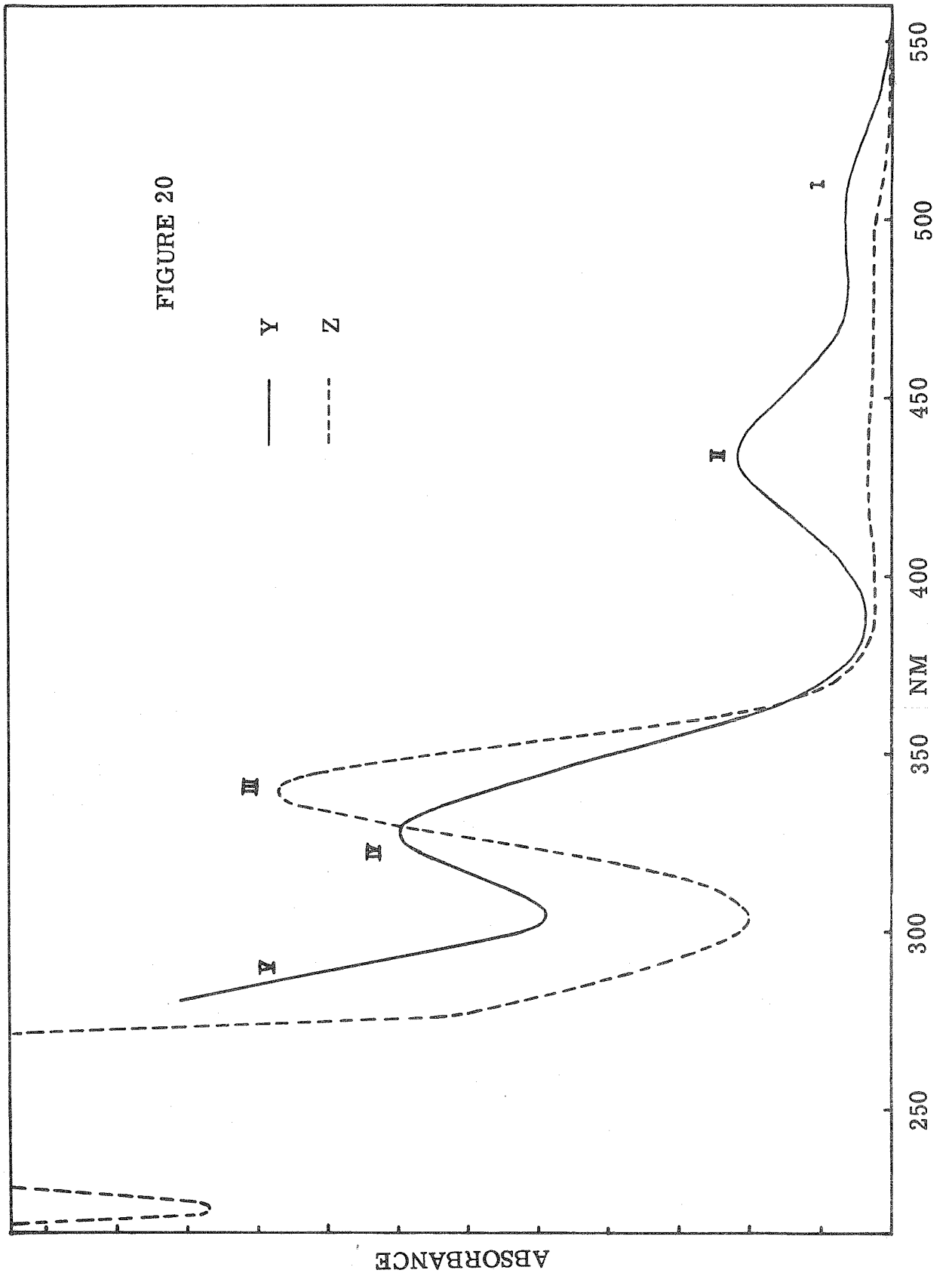

FIGURE 20

transitions exist. One polarization direction in Figure 19 contains no absorptions. This direction is designated as x. The other direction will contain some combination of y and z molecular absorbances.

Interference fringes have been measured along the two extinction directions of this face. The birefringence was calculated from equation (3) to be (.0536) n_x where $n_{y,z} > n_x$. The lowest refractive index was found to be $n \cong 1.50$ by immersion in benzene. Solubility problems limited a more accurate determination. The birefringence, .0804, and the retardation (.050 -.0 66 μ) allow the approximate thickness of this face to be determined: .6 - .8 μ. The density was determined by volume displacement from cyclohexane to be 1.387 g/cm^3.

In the second crystal face, Figure 20, the polarization direction with the strong low energy absorptions is assigned as y. The analogous low energy features of the $Pt_2Cl_6^{2-}$ spectra were previously shown to be strongly y polarized. This direction has the highest refractive index. The other polarization orientation contains x and z. Since the x direction has no absorptions, the z absorptions are resolved. The molecular orientations are extremely fortuitous!

There are two possible assignments of the $^1A_g \rightarrow {}^1B_{2u}$ ($dx^2-y^2 \rightarrow dxy$) band in the dimer, bands I or II. Both bands have the predicted y polarization. Following the accepted monomer

assignment of the band at 20,000 cm^{-1} as $^1A_{1g} \rightarrow {}^1A_{2g}$ ($dx^2-y^2 \rightarrow dxy$)[15] the y polarized band at 23,000 cm^{-1} in the dimer must be $^1A_1 \rightarrow {}^1B_1$ ($dz^2 \rightarrow dxy$). The intense z polarized feature at 29,450 cm^{-1} is assigned as $^1A_{1g} \rightarrow {}^1B_{1u}$ ($dyz \rightarrow dxy$). This assignment suggests an unusual ordering of the $PdCl_4^{2-}$ monomer d orbitals, $dxz \;\; dyz < dz^2 < dx^2-y^2 \ll dxy$ which differs significantly from the firmly established ordering in $PtCl_4^{2-}$, $dz^2 < dxz \; dyz < dx^2-dy^2 \ll dxy$. The intensified triplet state found in $Pt_2Cl_6^{2-}$ to have comparable intensity to the singlets is absent in this assignment of the $Pd_2Cl_6^{2-}$ spectra.

If credence is given to these objections, an alternate assignment is desirable. The y polarized band II at 23,000 cm^{-1} is assigned as $^1A_g \rightarrow {}^1B_{2u}$ ($dx^2-y^2 \rightarrow dxy$). Band I, also y polarized, contains the intensified triplet ^3A_u, $^3B_{1u}$ states found in $Pt_2Cl_6^{2-}$. Band III remains $^1A_g \rightarrow {}^1B_{1u}$ ($dyz \rightarrow dxy$) and band IV becomes the vibronically allowed $dxz \rightarrow dxy$ component. The y polarized shoulder at 34,750 cm^{-1}, band V, is $^1A_1 \rightarrow {}^1B_1$ ($dz^2 \rightarrow dxy$). This assignment gives the d orbital ordering $dz^2 < dxz$, $dyz < dx^2-y^2 \ll dxy$.

Acceptance of this alternative depends upon a successful correlation to the $PdCl_4^{2-}$ monomer spectra. The xy polarized band at 22,600 cm^{-1} in $PdCl_4^{2-}$ would become $^1A_{1g} \rightarrow {}^1A_{2g}$ ($dx^2-y^2 \rightarrow dxy$). The z polarized maxima at 23,000 cm^{-1} would not be a vibronic component of this band, which is impossible, but rather the missing z polarized triplet, $^3A_{2g}$, observed in $PtCl_4^{2-}$ at 20,600 cm^{-1}.

The xy shoulder at 20,000 cm^{-1} in $PdCl_4^{2-}$ would then be less intense than the z peak, as observed in $PtCl_4^{2-}$.

The $dx^2-y^2 \rightarrow dxy$ transition ($\Delta E = 10\,Dq$) is placed at 22,600 cm^{-1}; the value of 10 Dq for platinum is 26,000 cm^{-1}. The dxz, yz $\rightarrow$ dxy energies are 29,500 cm^{-1} and 29,800 cm^{-1} respectively.

The band intensities of the palladium dimer are considerably higher than those of the platinum species.[6, 8] This may indicate a stronger metal-metal interaction in $Pd_2Cl_6^{2-}$. Alternately the presence of a low lying L $\rightarrow$ M charge transfer may make intensity stealing important.

Table 8

$Pd_2Cl_6^{2-}$

Band	nm	cm^{-1}	Assignment $^1A_g \rightarrow$	Polarization
I	507.5	19,700	^3A_u, $^3B_{1u}$	y
II	434	23,040	$^1B_{2u}$	y
III	339.5	29,450	$^1B_{1u}$	z
IV	328	30,500	^1A_u, $^1B_{3g}$	y
V	~ 288	34,750	$^1B_1$	y

References

1. Daniel C. Harris, Ph.D. Thesis, California Institute of Technology, 1973.

2. Jack C. Thibeault, Ph.D. Thesis, California Institute of Technology, 1973.

3. D. M. Adams, P. J. Chandler, and R. G. Churchill, J. Chem. Soc., 1272 (1967).

4. J. Chatt, J. Chem. Soc., 2301 (1950).

5. C. M. Harris, S. E. Livingstone and N. C. Stephenson, J. Chem. Soc., 3697 (1958).

6. W. R. Mason and H. B. Gray, J. Amer. Chem. Soc., 90, 5721 (1968).

7. N. C. Stephenson, Acta Cryst., 17, 589 (1964).

8. P. Day, M. J. Smith, and R. J. P. Williams, J. Chem. Soc., 668 (1968).

9. O. S. Mortensen, Acta Chem. Scand., 19, 1500 (1965).

10. D. S. Martin and C. A. Lenhardt, Inorg. Chem., 3, 1368 (1964).

11. D. S. Martin, M. A. Tucker, and A. J. Kassman, Inorg. Chem., 4, 1682 (1965).

12. H. H. Patterson, J. J. Godfrey, and S. M. Khan, Inorg. Chem., 11, 2872 (1972).

13. D. S. Martin, J. G. Foss, M. E. McCarville, M. A. Tucker, and A. J. Kassman, Inorg. Chem., 5, 491 (1966).

14. A. J. McCaffery, P. N. Schatz, and P. J. Stephens, J. Amer. Chem. Soc., 90, 5730 (1968).

15. P. Day, A. F. Orchard, A. J. Thomson, and R. J. P. Williams, J. Chem. Phys., 42, 1973 (1965).

16. H. Basch and H. B. Gray, Inorg. Chem., 6, 256 (1967).

17. F. A. Cotton and C. B. Harris, Inorg. Chem., 6, 369 (1967).

18. J. Chatt, G. A. Gamlen, and L. E. Orgel, J. Chem. Soc., 486 (1958).

CHAPTER 4

Polarized Spectra of $OsNCl_4^-$

The nitrido tetrachloroosmate(VI) anion is representative of a type of compound containing a square planar arrangement of halogen atoms and a multiply bonded axial heteroatom. While the electronic structure of this species has never previously been characterized, the related vanadyl group has been extensively studied. A close parallel will be demonstrated between these species which will further elucidate the nature of metal-nitrogen multiple bonding.

The structural similarities between the vanadyl and nitridoosmate species are summarized in Table 9. The bond distance for the ligand trans to the metal-heteroatom multiple band is significantly longer than the bond distances of the cis ligands. This has been rationalized by steric arguments.[7] For fixed metal-nitrogen and cis metal-chlorine bond distances, the N-Os-Cl angle is forced to open in order to relieve nitrogen chlorine repulsion. This forces the trans chlorine away from the metal.

The species $OsNBr_5^{2-}$ and $OsNBr_4(H_2O)^-$ have been well characterized.[12] Attempts by Russian workers to crystallize K_2OsNCl_5 produced instead the related $K\ OsNCl_4(H_2O) \cdot H_2O$;[9] the trans chloride is labile[7] as suggested by the long bond distance. That both $OsNCl_4^-$ and $OsNCl_5^{2-}$ exist in equilibrium in concentrated hydrochloric acid is demonstrated by the selective precipitation of the former with tetrabutylammonium cation and the latter with potassium.[13]

Table 9

Structural Comparison of VO^{2+} and OsN^{3+}

Compound	V = O Å	V - Xeq Å	V - Yax Å	Space Group	Reference
$VO(H_2O)_4OSO_3 \cdot H_2O$	1.591	2.048 1.983	2.223	$P2_1/c$	1
$VO(acac)_2$	1.571	1.983 1.955	---	$P\bar{1}$	2
$VO(\phi acac)_2$	1.605	1.984 1.949	---	$P2_1/c$	3
$[(C_2H_5)_4N]_2VOCl_4$ as isomorphous $TiOCl_4^{2-}$ species	1.79	2.34 2.32	---	$P4_2nm$	4
	Os≡N	Os-Xeq	Os-Yax		
$KOsNO_3$	1.62	---	---		5
	1.75	---	---		6
K_2OsNCl_5	1.614	2.359 2.367	2.605	Pnma	7
	1.75	2.37 2.32	2.60	Pnma	8
$KOsNCl_4(H_2O) \cdot H_2O$	1.74	2.35 2.34	2.50	Cmc	9, 10
$KOsNBr(H_2O) \cdot H_2O$		species is isomorphous			
$[(n\text{-}C_4H_9)_4N]OsNCl_4$		2.264		P4/n	11a
	1.478 1.472	2.422 2.197		P4/n	11b

The d orbital ordering for d^2 $OsNCl_4^-$ is shown in Figure 21. The complex is characterized in C_{4v} symmetry.

Figure 21

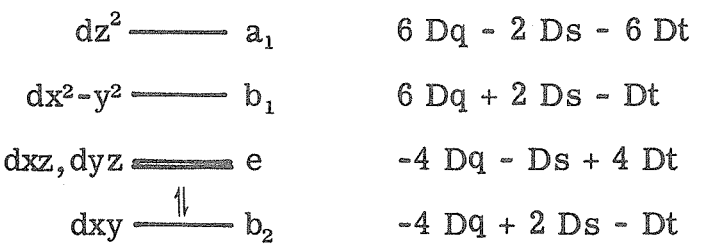

Both $OsNCl_5^{2-}$ and $OsNCl_4^-$ are diamagnetic,[14] which precludes an $(e)^2$ ground state. The b_2 dxy orbital is clearly lowest. A similar conclusion, based on MO calculations, was reached for the vanadyl complexes.[15,16] Calculations in which the $O = V - O_{eq}$ angle could be varied suggested than an angle of ~100° provided maximum stability and that the orbital ordering did not change with angle.[17] For axial compression, the crystal field model predicts that both Ds and Dt are negative quantities.[18] Negative values of Ds and Dt correspond to large σ and π bonding in the molecular orbital treatment. All the d orbitals are antibonding.

The electronic selection rules are given in Tables 10 and 11. The selection rules in Tables 10 and 11b for spin allowed transitions are identical. The greater spin orbit coupling of the osmium should also give considerable intensity to the triplet transitions. Although the direct product symmetries in Tables 10 and 11a are the same, the number of excited states is very different. The similar selection rules for $VOCl_4^{2-}$ and $OsNCl_4^-$ will be utilized in making analogous

Table 10

Selection Rules for $OsNCl_4^-$ in C_{4v} Symmetry

Transition	Excited State	Symmetry of Excited State	Vibration Required to be Allowed $\pi(A_1)$	$\sigma(E)$
b_2 dxy → e dxz, dyz	^3E	A_1	allowed	E
		A_2	---	E
		B_1	B_1	E
		B_2	B_2	E
		E	E	allowed
	^1E	E	E	allowed
b_2 dxy → b_1 dx^2-y^2	$^3A_2$	A_1	allowed	E
		E	E	allowed
	$^1A_2$	A_2	---	E
b_2 dxy → a_1 dz^2	$^3B_2$	B_1	B_1	E
		E	E	allowed
	$^1B_2$	B_2	B_2	E

ground state is $^1A_1$ x, y axes along the ligands

S = 0 transforms as A_1

S = 1 transforms as A_2 + E

Table 11

Selection Rules $VOCl_4^{2-}$ in C_{4v} Symmetry

a) Including Spin Orbit Coupling

Transition	Excited State	Symmetry of Direct Product	Vibration Required to be Allowed π (A_1)	σ (E)
b_2 dxy → e dxz, dyz	Γ_7	$A_1 + A_2 + E$	allowed	allowed
	Γ_6	$B_1 + B_2 + E$	$B_1 + B_2 + E$	allowed
b_2 dxy → b_1 dx^2-y^2	Γ_7	$A_1 + A_2 + E$	allowed	allowed
b_2 dxy → a_1 dz^2	Γ_6	$B_1 + B_2 + E$	$B_1 + B_2 + E$	allowed

$S = \frac{1}{2}$ transforms as Γ_6 ground state is $^2B_2 \equiv \Gamma_7$

b) Without Spin Orbit Coupling

b_2 dxy → e dxz, dyz	E	E	E	allowed
b_2 dxy → b_1 dx^2-y^2	B_1	A_2	---	E
b_2 dxy → a_1 dz^2	A_1	B_2	B_2	E

assignments of the electronic spectra; a number of polarized single crystal studies have been performed on the vanadyl species.[1,18,19] Other low temperature crystal and mull data is also available[20,21] for comparison.

K $OsNO_3$ was prepared by the literature method.[22] Addition of this salt to 6 N hydrochloric acid gave an immediate red color. Tetrabutylammonium chloride was added, producing an immediate pink precipitate of $[(n\text{-}C_4H_9)_4N]OsNCl_4$. The compound was washed in boiling hydrochloric acid and distilled water, filtered, and dried in a vacuum oven. Similarly, the tetrapropylammonium and tetraethylammonium salts were prepared as violet salts. The tetrapropylammonium salt turned cherry red upon drying in the vacuum oven, but returned to the original purple hydrate after several days in air. The tetraethylammonium salt is strongly birefringent, exhibiting purple to pink dichroism.

The analogous $OsNBr_4^-$ anion was prepared by the action of hydrobromic acid on $KOsNO_3$. The tetrabutylammonium and tetrapropylammonium salts were prepared as above. An initial orange precipitate appears to contain coordinated HBr. Recrystallization gave the expected cherry red products.

Large square plates of $[(n\text{-}C_4H_9)_4N]OsNCl_4$ were grown from dichloromethane-hexane. The density was found to be 1.6156 g/cm^3 by floatation in CCl_4 - CH_2I_2 and 1.6540 g/cm^3 by displacement from CCl_4. The experimental density suggests that water is not present in the unit cell. The lattice parameters are a = b = 11.7569 Å

C = 8.7890 Å.[11] The osmium-nitrogen axis coincides with the crystallographic four fold axis. Only crystals of the (001) face formed.

The infrared Os-N A_1 axial stretch and Os-Cl E in-plane stretching frequencies obtained for KBr pellets are given in Table 12.

Table 12

Compound	A_1Os-N stretch cm^{-1}	E Os-Cl stretch cm^{-1}	Coordinated water cm^{-1}
$(n\text{-}C_4H_9)_4N\ OsNCl_4$	1126	354	----
$(n\text{-}C_3H_7)_4N\ OsNCl_4$	1125	355	----
$(n\text{-}C_3H_7)_4N\ OsNCl_4(H_2O)$	1112	350, 334	3460, 1602 (sharp)
$(C_2H_5)_4N\ OsNCl_4(H_2O)$	1116	328	3480, 1610 (sharp)
$K_2\ OsNCl_5$	1073[22] - 1081[23]	336, 328[23]	----

The tetraethylammonium and tetrapropylammonium salts definitely contain coordinated water. With the exception of $[(n\text{-}C_4H_9)_4N]OsNCl_4$ which formed crystals from dichloromethane, all other compounds were crystallized from acetonitrile. The liquid helium temperature spectra of these complexes are presented in Figures 22 - 26; polarized spectra were recorded for those faces which exhibited significant anisotropy.

The most intense feature in the ligand field spectra of the $OsNCl_4^-$ species is the broad band at 630 - 450 nm. A definite splitting can be observed in the spectra of $(n\text{-}C_4H_9)_4N\ OsNCl_4$ and $(n\text{-}C_4H_9)_4N\ OsN\ Br_4$. The higher energy component is more intense and shows vibrational fine structure. This suggests the presence of an E excited

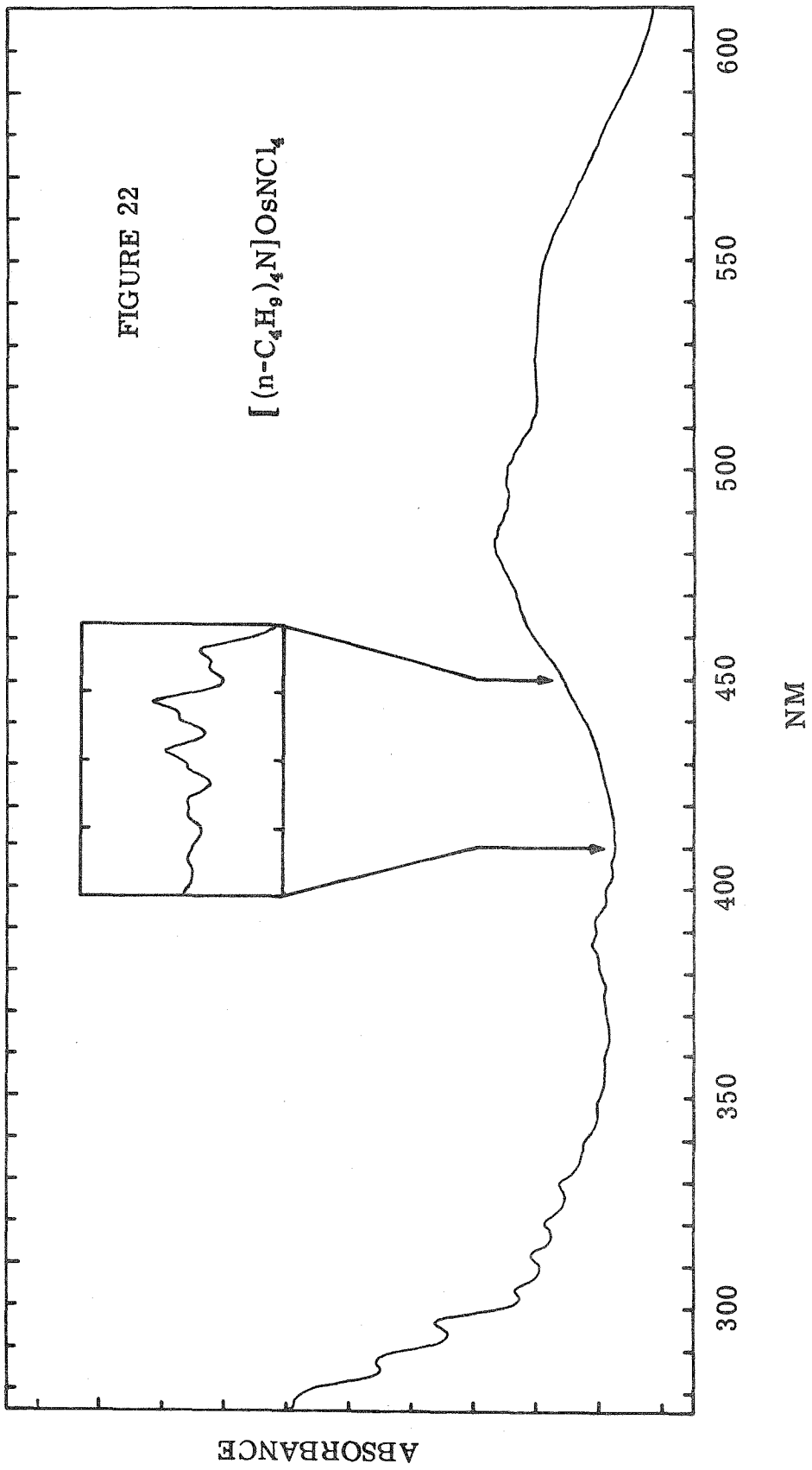
FIGURE 22
[(n-C4H9)4N]OsNCl4
ABSORBANCE
300
350
400
450
500
550
600
NM

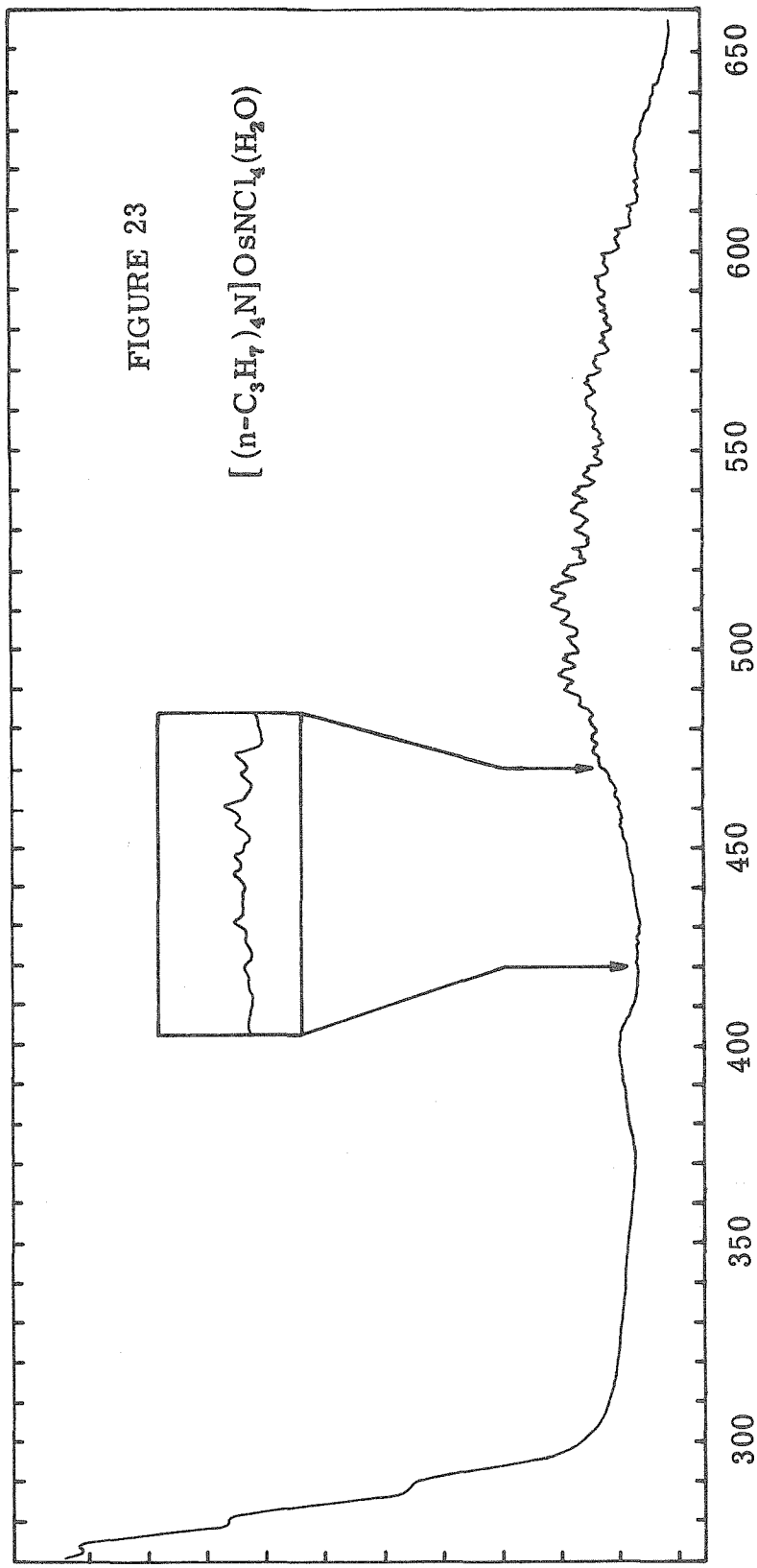
FIGURE 23
[(n-C3H7)4N]OsNCl4(H2O)
ABSORBANCE
300
350
400
450
500
550
600
650
NM

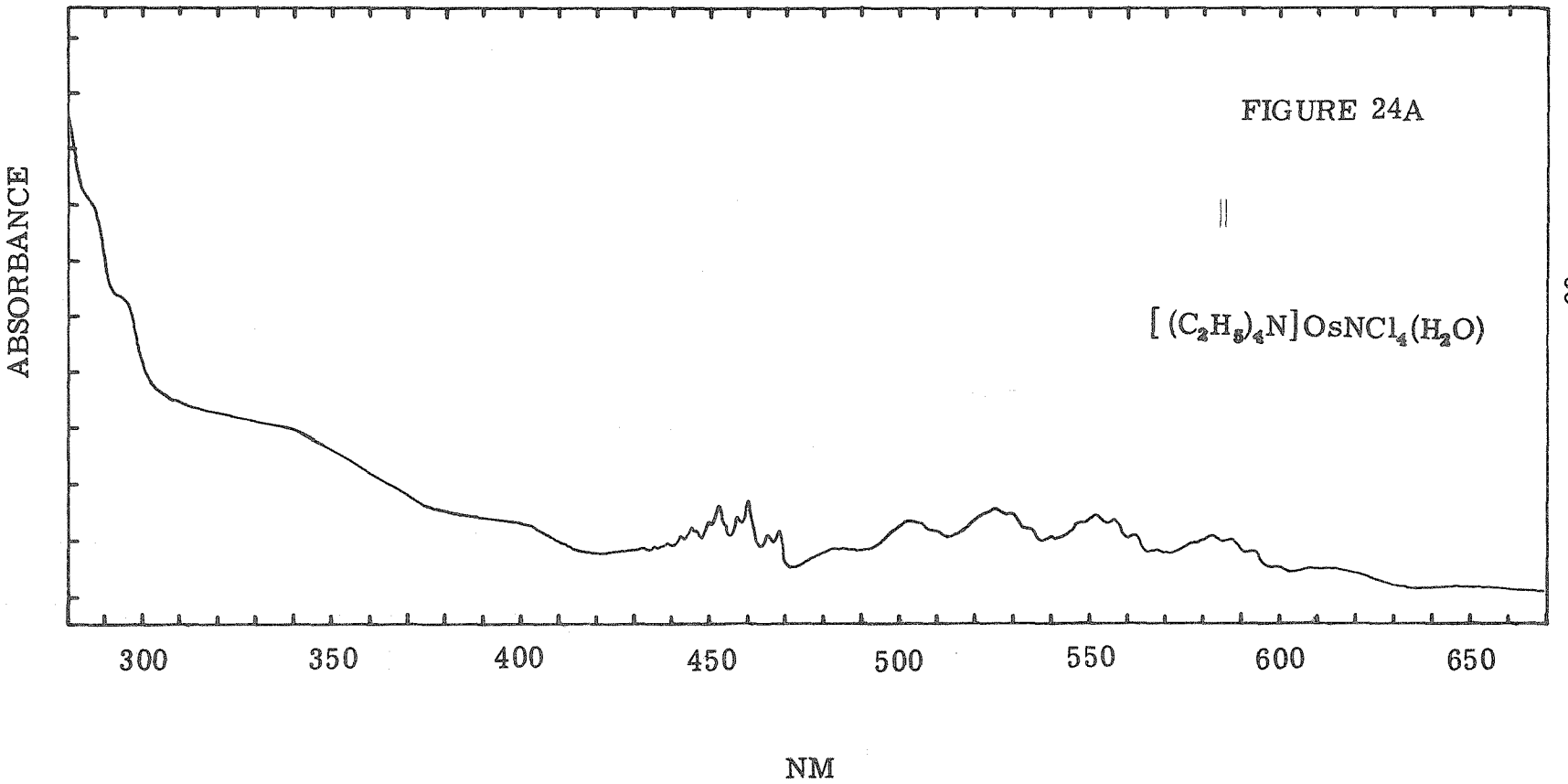
ABSORBANCE
300
350
400
450
500
550
600
650
NM
FIGURE 24A
[(C2H5)4N]OsNCl4(H2O)

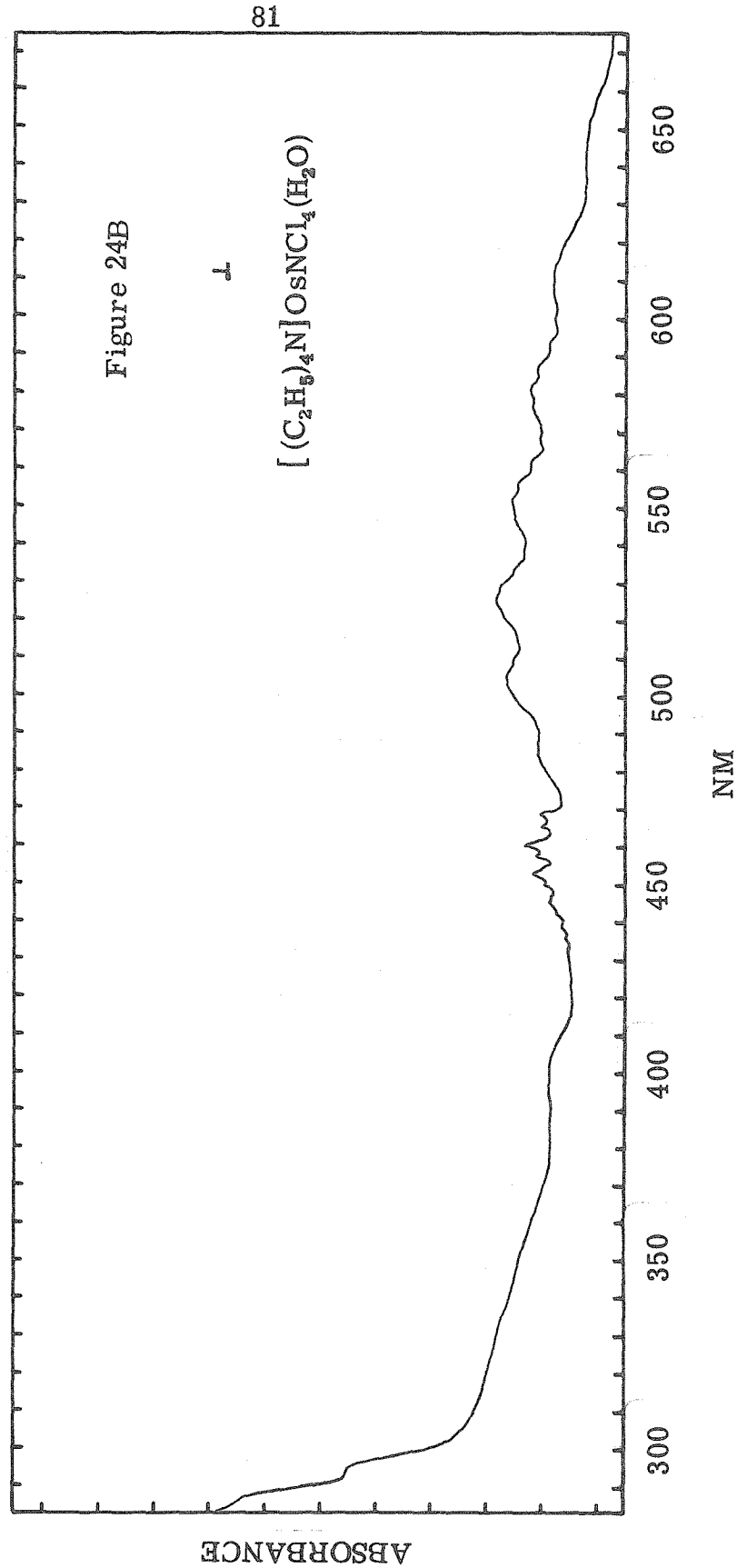

Figure 24B

$[(C_2H_5)_4N]OsNCl_4(H_2O)$

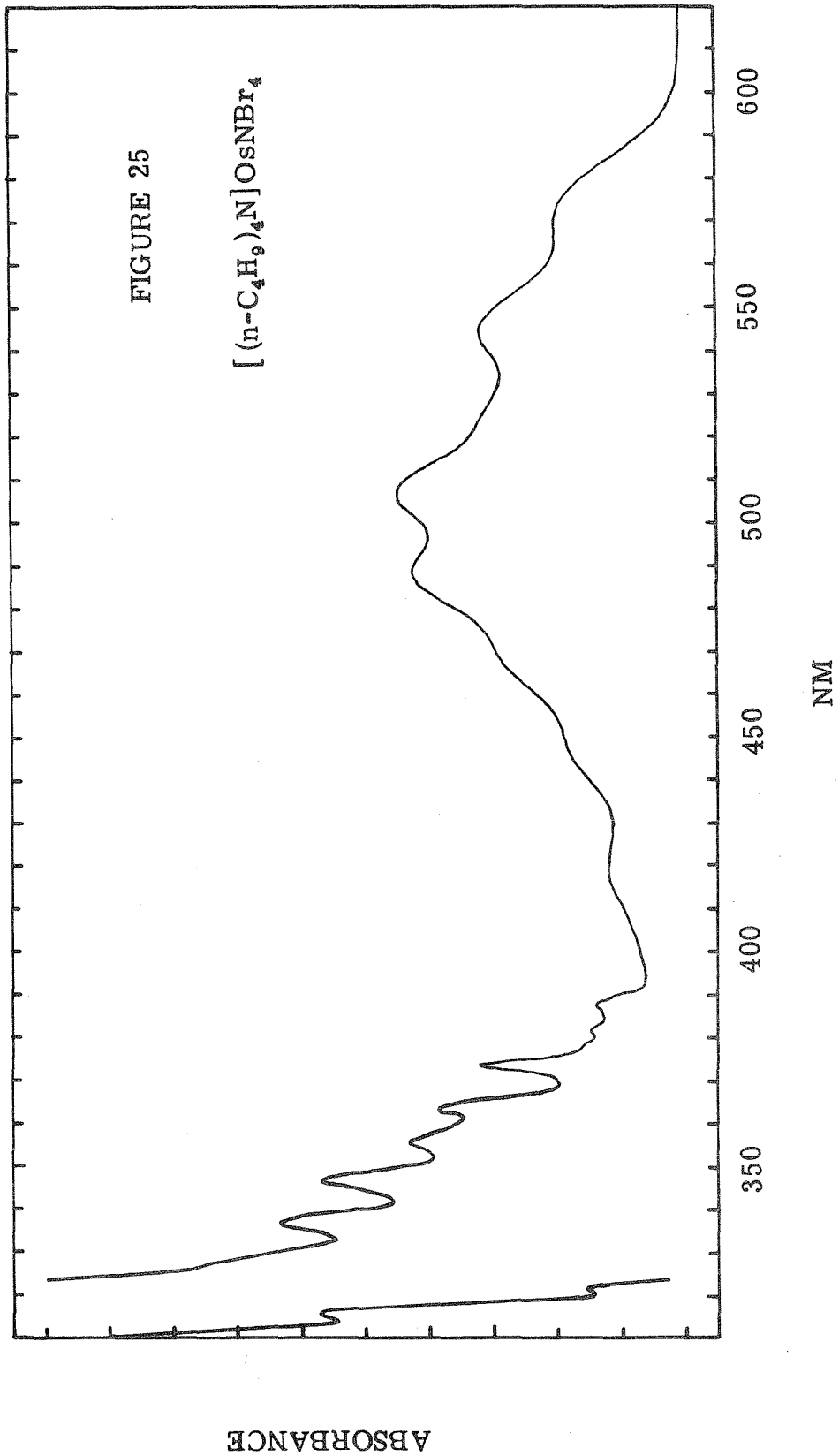
FIGURE 25
[(n-C4H9)4N]OsNBr4
ABSORBANCE
350
400
450
500
550
600
NM

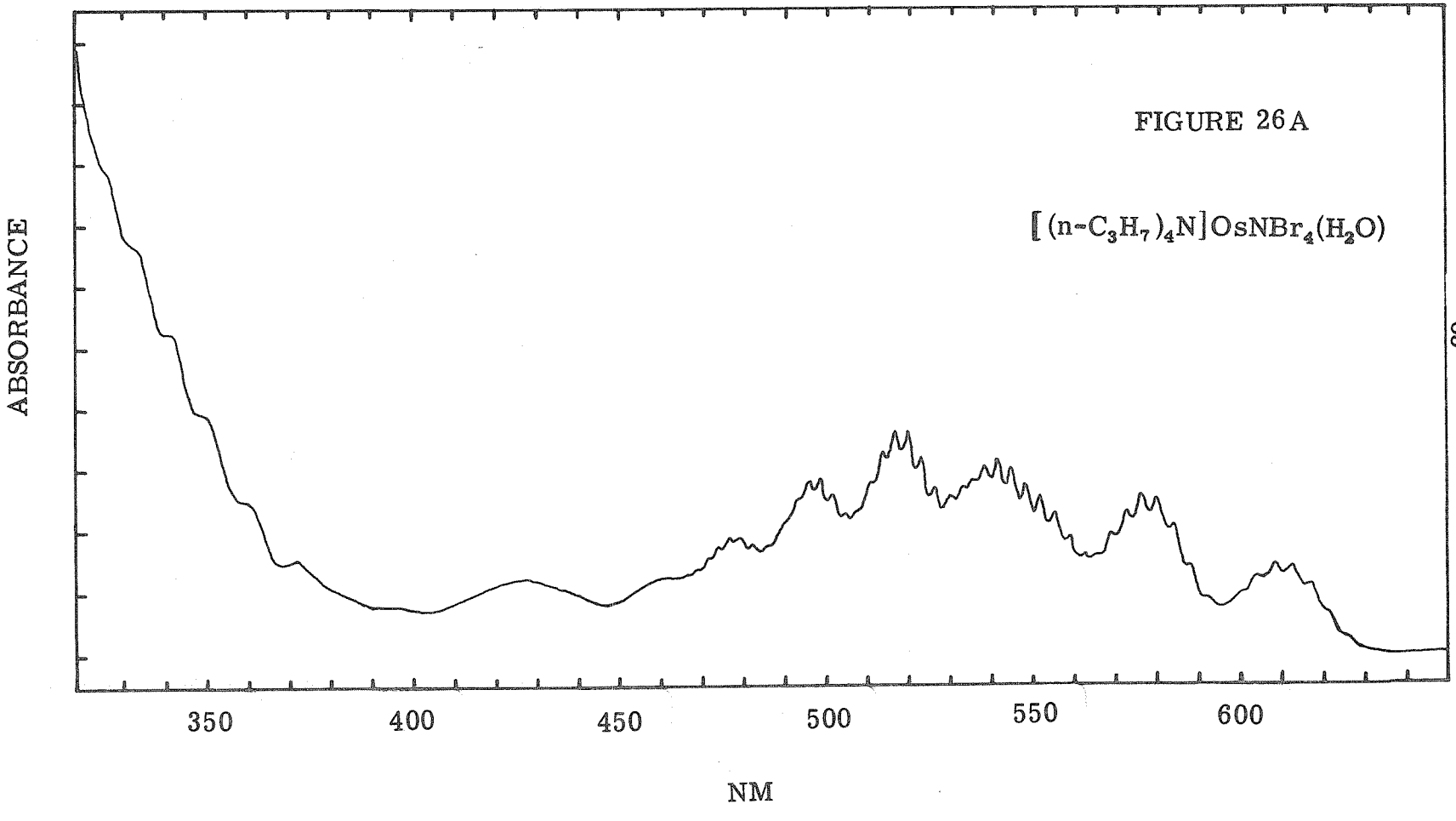

FIGURE 26A

$[(n\text{-}C_3H_7)_4N]OsNBr_4(H_2O)$

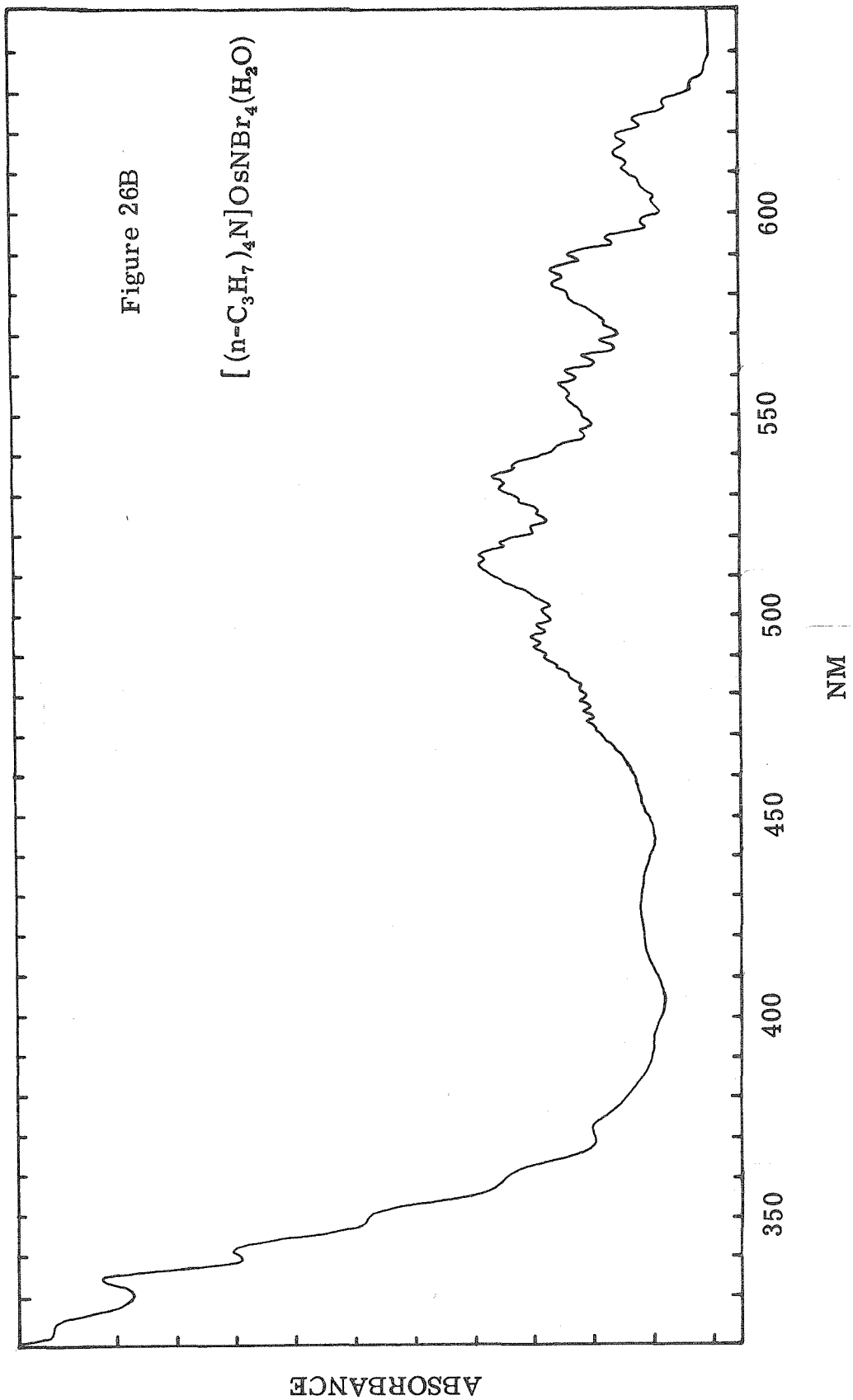

Figure 26B

$[(n\text{-}C_3H_7)_4N]OsNBr_4(H_2O)$

state in which distortion has removed the degeneracy. The species containing an axial water molecule are characterized by a more symmetrical band envelope.

The vibrational structure observed in both chloride and bromide species is identical; seven peaks of spacing ~ 900 cm^{-1} are observed. This spacing corresponds to the A_1 Os-N stretching frequency (see Table 12), weakened in the excited state. A similar band occurs at ~13,200 cm^{-1} in the VO^{2+} species, exhibiting three vibrational components of spacing 600-900 cm^{-1}.[1,18-21,24,25] This band has strong σ polarization in the VO^{2+} species.[1,18,19] The presence of the band in the axial (001) spectra of $[(n\text{-}C_4H_9)_4N]OsNCl_4$ clearly demonstrates σ polarization. This band demonstrates temperature independent allowed intensity behavior as does the vanadyl analogue.

The tetrapropyl ammonium and tetraethylammonium salts also possess a second progression on each Os-N A_1 component, 178 cm^{-1} for $OsNCl_4(H_2O)^-$ and 128 cm^{-1} for $OsNBr_4(H_2O)^-$. These complexes have been shown by their infrared spectra to possess coordinated water in the axial position. The low frequencies and frequency dependence upon the halide supports assignment of this mode as an A_1 Os-X (X = Cl, Br) umbrella deformation. The bonding of an axial ligand reduces the N≡Os-X angle, facilitating the deformation mode. The Os-Cl deformation in $OsCl_6^{2-}$ occurs at 177 cm^{-1}.[26]

Coordination of an axial ligand trans to the nitrido produces a red shift of the band envelope. The observed ordering $Bu_4N^+ > Pr_4N^+ > Et_4N^+ > K^+$ is consistent with increasing coordination in the

trans position. Such coordination would reduce the π bonding between Os $\equiv$ N. The decrease of infrared osmium-nitrogen stretching frequencies supports this. The d orbitals with π^* character are dxz, dyz of E symmetry. Reduced π bonding would stabilize the E orbitals, producing a red shift.

This transition is assigned as $^1A_1 \rightarrow {}^1E$ (b_2 dxy $\rightarrow$ e dxz, dyz), the only fully allowed ligand field transition. The band has the expected σ polarization and temperature independent intensity. Population of the π^* antibonding dxz, dyz orbitals should result in a weakened Os-N bond and a lower stretching frequency in the excited state. The related allowed triplet states are probably at much lower energy. For a large energy separation, the spin orbit mixing, and thus the intensity, are greatly reduced. However, the presence of these states under the broad $^1A_1 \rightarrow {}^1E$ envelope cannot be rejected using the available experimental data; a pure π spectra by which the $^1A_1 \rightarrow A_1(^3E)$ could be detected was not obtainable from the (001) crystal face.

Emission spectra were obtained on the Cary 81 spectrometer using the 632.8 nm excitation line of the He-Ne laser.[27] For $[(n\text{-}C_4H_9)_4N]OsNCl_4$ the peak maxima was observed at 690 nm (14,500 cm^{-1}); the 0-0 transition occurs at energies $\geq$ 15,500 cm^{-1}. The spectra of $(C_2H_5)_4N^+$ salt show a maxima at 719 nm (13,900 cm^{-1}) with emission to 15,600 cm^{-1}. Definite overlap occurs with the lowest observed absorption. The corresponding $[(n\text{-}C_4H_9)_4N]OsNBr_4$ complex has a maxima at 680 nm (14,700 cm^{-1}); the 0-0 transition lies $\geq$

15,500 cm^{-1}. The lifetime of the emission has not been measured. A long lifetime would indicate the presence of the ^3E states under the broad band envelope.

The sharp double progression at ~ 21,300 cm^{-1} in $[(C_2H_5)_4N]OsNCl_4(H_2O)$, Figure 24, is not observed in the (001) face of the tetrabutylammonium salt. This progression was observed in the KBr pellet spectra of all chloride species. The definite π polarization of this band cannot be rationalized without spin orbit coupling. The temperature independent intensity and sharp band shape are not in accord with vibronic coupling. Only the $^1A_1 \rightarrow {}^1B_2$ ($dxy \rightarrow dz^2$) transition is allowed vibronically π polarized; such an assignment would require a different d orbital ordering than MO and crystal field arguments predict. The absence of a similar peak in the vanadyl spectra strongly suggests that the transition is spin forbidden.

The position of the band is approximately constant for all chloro species; the related band in the bromides probably is buried under the $^1A_1 \rightarrow {}^1E$ band envelope. In all cases the progression spacing is identical, 380 cm^{-1}. This vibrational mode must be the osmium-chloride A_1 stretch. The corresponding E mode is observed in the infrared from 355 - 328 cm^{-1}, Table 12. The A_1 mode was not observed in the IR, although symmetry allowed, because it does not produce a change of the anion dipole moment. The double progression results from coupling of the A_1 deformation with the A_1 stretch. The value of the deformation mode was determined here to be 146 - 154 cm^{-1}, slightly weaker than the 176 cm^{-1} vibration observed coupled onto the

$^1A_1 \rightarrow {}^1E$ transition. In the latter case electron density remains localized in π^* antibonding orbitals. A transition which placed an electron in a σ^* antibonding orbital would considerably weaken the metal-halogen σ bond, while strengthening the π bonding. A lower excited state deformation frequency would be expected.

The transition is assigned as $^1A_1 \rightarrow A_1(^3A_2)$ (b_2 dxy $\rightarrow b_1$ dx^2-y^2). The related $^1A_1 \rightarrow E(^3A_2)$ is mixed with the $^1A_1 \rightarrow {}^1E$ transition and placed under the band envelope of the latter. The total absence of any σ component of $^1A_1 \rightarrow A_1(^3A_2)$ demonstrates that E vibrational modes are not important in a vibronic intensity mechanism. This conclusion is supported by the absence of π absorption for the $^1A_1 \rightarrow {}^1E$ transition in $VOCl_5^{3-}$ [18] and $VO(H_2O)_4OSO_3 \cdot H_2O$. [1]

The weak broad feature at 24,600 cm^{-1} in the σ spectra of $[(n\text{-}C_4H_9)_4N]OsNCl_4$ is assigned as the σ vibronically allowed transition $^1A_1 \rightarrow {}^1A_2$ (b_2 dxy $\rightarrow b_1$ dx^2-y^2). The blue shift of this band with temperature clearly indicates a vibronic mechanism. The weak nature of the progression, spacing ~ 469 cm^{-1}, suggests that this separation actually represents an E^2 rather than an A_1 mode. The frequency of such a mode would be 234 cm^{-1} which is reasonable for an E in-plane bend. An in-plane vibration would be expected to have the greatest effect upon an electronic transition localized in the equatorial plane.

The energy of the $^1A_1 \rightarrow {}^1A_2$ transition is 10 Dq. The value observed here, 24,600 cm^{-1}, is in good agreement with the value of 26,300 cm^{-1} observed in $PtCl_4^{2-}$. The corresponding band in $OsNBr_4^-$ is observed at lower energies, in accord with the weaker crystal field splitting of bromide.

The weak progression at 27,900 cm^{-1} in $(n\text{-}C_4H_9)_4NOsNCl_4$ is assigned as $^1A_1 \rightarrow B_1\ (^3B_2)\ (b_2\ dxy \rightarrow a_1\ dz^2)$. The progression spacing, 878 cm^{-1}, is the Os ≡ N A_1 stretch; this separation suggests a weakening as the osmium-nitrogen band. The transition is apparently blue shifted in those complexes containing an axial ligand. The more intense σ allowed progression at 32,000 cm^{-1} with the same spacing is assigned $^1A_1 \rightarrow E\ (^3B_2)\ (b_2\ dxy \rightarrow a_1\ dz^2)$.

Further assignments of features at higher energies should not be attempted without band polarization data of the charge transfer region. While no experimental difficulties are to be expected, the emphasis of present study was upon assignment of the ligand field transitions.

The assignments presented here are summarized in Tables 13 - 18.

Table 13

$[(n\text{-}C_4H_9)_4N]OsNCl_4$ -Figure 22

Å	cm^{-1}	Spacing cm^{-1}	Assignment
5012[a]	19953		^1E, $^3A_2(E)$
		773	
4825[a]	20726		
		866	
4631[a]	21592		
4459.4	22424		$^3A_2(A_1)$
		379	119
4435.9	22543		
			392
4385.3	22804		
		383	
4360.0	22936		
			384
4312.9	23186		
		396	
4288.2	23320		
			377
4240.6	23582		
4220.0	23697		
			400

4150.0	24096		
4065.4	24598		
		419	
3997.3	25017		
		470	
3923.7	25486		
		396	
3863.6	25882		
		372	
3808.9	26254		

Table 13 (Cont'd)

Å	cm^{-1}	Spacing cm^{-1}	Assignment
3589.1	27863		$^3B_3(B_1)$
		789	
3490.2	28651		
		809	
3394.4	29460		
		878	
3296.2	30338		
		877	
3203.6	31215		
3126.6	31983		$^3B_2(E)$
		851	
3045.6	32835		
		848	
2968.9	33682		
2880.8	34713		
		1001	
2800.0	35714		

a) Broad peak allowed only maxima to be determined.

Table 14

$[(n\text{-}C_3H_7)_4N]OsNCl_4(H_2O)$ -Figure 23

Å	cm^{-1}	Spacing cm^{-1}		Assignment
6178.2	16186			^1E, $^3A_2(E)$
		162		
6117.1	16348			
		164		
6056.5	16511			
		165		
5996.5	16676			
		164		
5938.2	16840			
		162		
5881.8	17002			
5851.8	17089		903	
		165		
5795.9	17254			
		164		
5741.2	17418			
		164		
5687.7	17582			
		165		
5634.7	17747			
		161		
5584.1	17908			
5558.8	17989		901	
		165		
5508.2	18155			
		162		
5459.4	18317			
		159		
5412.4	18476			
		162		
5365.3	18638			
5300.0	18868		879	
		158		
5255.9	19026			
		161		
5211.8	19187			
		162		
5168.2	19349			

Table 14 (Cont'd)

Å	cm^{-1}	Spacing cm^{-1}			Assignment
5070.6	19722			853	
		162			
5029.4	19883				
		159			
4989.4	20042				
		155			
4951.2	20197				
		155			
4913.5	20352				
4862.4	20566			845	
4635.3	21574		146		
		383		377 + 2 × 146	$^3A_2(A_1)$
4604.1	21720				
			383		
4554.4	21957				
		382			
4524.4	22102				
			379		
4495.9	22243				
				385	
4476.5	22339				
		364			
4448.2	22481				
			378		
4419.4	22627				
				374	
4404.7	22703				
			388		
4374.7	22859				
4347.7	23001				
4301.8	23246				
3980[a]	25100				$^1A_2$

Table 14 (Cont'd)

Å	cm^{-1}	Spacing cm^{-1}
2903.5	34441	
		1086
2814.7	35528	
		836
2750	36364	

a) Broad band peak maxima

Table 15

$[(C_2H_5)_4N]OsNCl_4(H_2O)$ Figure 24

Å	cm^{-1}	Spacing cm^{-1}	Assignment
6531[a]	15313		$^1E_1, {}^3A_2(E)$
6147[a]	16268	955	
6000.0	16667		
		168	
5940.0	16835		
		170	
5880.6	17005		
		179	
5819.4	17184		
		163	
5764.7	17347		
5678.8	17609	943	
		158	
5628.2	17766		
		176	
5572.9	17944		
		172	
5520.0	18116		
		162	
5471.2	18278		
5398.8	18523	913	
		165	
5351.2	18687		
		166	
5304.1	18853		
		173	
5255.9	19026		
5012[a]	19951		
4809[a]	20795	844	

Table 15 (Cont'd)

Å	cm^{-1}	Spacing cm^{-1}			Assignment
4686.5	21338				$^3A_2(A_1)$
4652.9	21492	376	154		
4605.3	21714		370	358+2×154	
4574.1	21862				
4544.7	22004	380	369		
4528.2	22084			374	
4498.2	22231	370			
4468.8	22377		375		
4453.5	22454				
4423.5	22606				
4000[a]	25000				$^1A_2$
2961.8	33764	1008			
2876.9	34772	1070			
2790.0	35842				

a) Broad band peak maxima.

Table 16

$K_2 OsNCl_5$ KBr pellet

Å	cm^{-1}		Spacing cm^{-1}	Assignment
4460.0	22422			$^3A_2(A_1)$
			149	
4430.6	22570	397		
			390	
4382.4	22819	380		
			385	
4355.3	22961			
4310.6	23199			
4283.5	23345			

Table 17

$[(n\text{-}C_4H_9)_4N]OsNBr_4$ Figure 25

Å	cm^{-1}	Spacing cm^{-1}	Assignment
5753[a]	17382	915	^1E, $^3A_2(E)$
5465[a]	18297		
5080[a]	19685	854	
4869[a]	20539	910	
4662[a]	21448	1038	
4447[a]	22487		
4162[a]	24025		$^3A_2(A_1)$
3901.8	25629	1121 / 789 / 541 / 140	
3880.6	25769		
3821.2	26170		
3785.3	26418		
3738.2	26751	1127 / 713 / 540	
3641.2	27464		
3587.1	27878		
3558.2	28104		
3470.6	28814	834	
3372.9	29648	835	
3280.6	30482	568	
3220.6	31050	554	
3164.1	31604		

a) Broad band peak maxima

Table 18

$[(n\text{-}C_3H_7)_4N]OsNBr_4(H_2O)$ Figure 26

Å	cm^{-1}	Spacing cm^{-1}		Assignment
6267.7	15955			^1E, $^3A_2(E)$
		127		
6218.2	16082			
		127		
6169.4	16209			
		118		
6124.7	16327			
		122		
6079.4	16449			
		119		
6035.9	16568			
		117		
5993.5	16685			
5928.8	16867		912	
		121		
5886.5	16988			
		118		
5845.9	17106			
		123		
5804.1	17229			
		123		
5762.9	17352			
		118		
5724.1	17470			
		116		
5686.5	17586			
5626.5	17773		906	
		114		
5590.6	17887			
		112		
5555.9	17999			
		123		
5518.2	18122			
		121		
5481.8	18242			
		112		
5448.2	18355			
		114		

Table 18 (Cont'd)

Å	cm^{-1}	Spacing cm^{-1}	
5414.7	18468		
		105	
5384.1	18573		
		104	
5354.1	18677		
5328.2	18768		995
		126	
5264.7	18994		
		118	
5232.4	19112		
		119	
5200.0	19231		
		125	
5166.5	19356		
		122	
5134.1	19478		
		121	
5102.4	19599		
		120	
5071.2	19719		
5075.9	19701		933
		115	
5046.5	19816		
		116	
5017.1	19932		
		129	
4984.7	20061		
		117	
4955.9	20178		
		121	
4926.5	20299		

Table 18 (Cont'd)

Å	cm^{-1}	Spacing cm^{-1}		
4850.0	20619		918	
		128		
4820.0	20747			
		127		
4790.6	20874			
		124		
4762.4	20998			
		120		
4735.3	21118			
		116		
4709.4	21234			
4268[a]	23400			$^1A_2$
3727.7	26827			
		834		
3615.3	27660			
		854		
3507.1	28514			
		706		
3422.4	29220			
		731		
3338.8	29951			
		680		
3264.7	30631			

a) Broad band peak maxima.

References

1. C. J. Ballhausen, B. F. Djurinskij, and K. J. Watson, J. Amer. Chem. Soc., 90, 3305 (1968).
2. R. P. Dodge, D. H. Templeton, and A. Zalkin, J. Chem. Phys., 35, 55 (1961).
3. P. K. Hon, R. L. Belford, and C. E. Pfluger, J. Chem. Phys., 43, 1323, 3111 (1965).
4. W. Haase and H. Hoppe, Acta Cryst., 24, 282 (1968).
5. F. M. Jaeger, and J. E. Zanstra, Rec. Trav. Chim., 51, 1013 (1932).
6. O. A. Dyachenko, V. M. Golyshev, and L. O. Atovmyan, Zh. Strukt. Khim., 9, 335 (1968).
7. D. Bright and J. A. Ibers, Inorg. Chem., 8, 709 (1969).
8. L. O. Atovmyan and V. V. Tkachev, Zh. Strukt. Khim., 9, 708 (1968).
9. L. O. Atovmyan and V. V. Tkachev, ibid., 9, 933 (1968).
10. L. O. Atovmyan and G. B. Bokii, ibid., 1, 501 (1960).
11a. Crystallographic data obtained by C. K. Poon was refined by Dr. O. Siiman, with the assistance of Dr. R. Marsh.
11b. Dr. Robert Bau, U. Southern California, private communication. The structure is disordered 64.5% - 36.5% by inversion of the $OsNCl_4^-$ square pyramid. N ≡ Os-Cl angle is 106.5°, 107.3°.
12. A.Werner and K. Dinklage, Ber. 39, 499 (1906).
13. C. K. Poon, private communication. W. P. Griffith and D. Pawson, JCS Chem. Comm., 418, (1973).

14. G. Rossman, private communication.
J. Lewis and G. Wilkinson, J. Inorg. Nuc. Chem., 6, 12 (1953).

15. C. J. Ballhausen and H. B. Gray, Inorg. Chem., 1, 111 (1962).

16. J. E. Drake, J. E. Vekris and J. S. Wood, J. Chem. Soc., A, 345 (1969).

17. L. G. Vanquickenborne and S. P. McGlynn, Theor. Chim. Acta, 9, 390 (1968).

18. R. A. Wentworth and T. S. Piper, J. Chem. Phys., 41, 3884 (1964).

19. A. Feltz and H. Langbein, J. Inorg. Nuc. Chem., 32, 2951, (1970).

20. O. Piovesana and J. Selbin, ibid., 31, 433 (1969).

21. G. Basu, W. Yeranos, and R. L. Belford, Inorg. Chem., 3, 929 (1964).

22. A. F. Clifford and C. S. Koboyashi, Inorg. Synth., 6, 204 (1960).

23. W. P. Griffith, J. Chem. Soc., 3694 (1965).

24. J. Selbin, T. Ortolano, and F. J. Smith, Inorg. Chem., 2, 1315 (1963).

25. T. Ortolano, J. Selbin, S. P. McGlynn, J. Chem. Phys., 41, 262 (1964).

26. F. A. Cotton and L. T. Reynolds, J. Amer. Chem. Soc., 80, 269 (1958).

27. G. Geoffroy, private communication.

CHAPTER 5

Polarized Spectra of $[(n\text{-}C_4H_9)_4N]Re_2Cl_9$

The hexachloro-μ-trichloro dirhenate(IV) anion has been shown by an x-ray investigation to possess a "confacial bioctahedral" structure.[1] This structure can be considered as two octahedra sharing a face. Each rhenium (IV) center has a d^3 configuration. Other d^3 complexes of the type $M_2X_9^{3-}$ (M = Cr, Mo, W) (X= Cl, Br) are also known to adopt the confacial bioctahedral structure.[6]

These compounds exhibit a range of metal-metal interaction. In $Cr_2Cl_9^{3-}$ the chromium ions do not lie at the centers of the octahedra, but are clearly displaced away from each other: a net repulsion appears to exist. The magnetic moment of 3.82 B.M. per chromium[3] indicates three unpaired electrons. The spectroscopic properties of the monomer and dimer are essentially identical[7] and may be interpreted in terms of an octahedral crystal field about Cr^{3+}. In contrast, the tungsten analogue demonstrates distinct metal-metal bonding; the metal atoms are displaced toward each other. The W-W distance is smaller than the Cr-Cr distance despite the reverse order of the metallic radii. The $W_2Cl_9^{3-}$ species has a temperature independent paramagnetism of .43 BM.[8] The metal-metal bonding of this complex can be considered as a σ bond between the trigonally directed dz^2 orbitals of the adjacent tungstens and 2π bonds.[6] Alternately, bonding may be considered to occur by the overlap of the t_{2g} orbitals to give three bonding interactions.[5]

Table 19

		$Cr_2Cl_9^{3-}$	$Mo_2Cl_9^{3-}$	$W_2Cl_9^{3-}$	$Re_2Cl_9^{-}$
M-Cl-M angle		76°	64°	58°	68.5°
M-M	Å	3.12	2.68	2.41	2.703
M-M (pure metal)	Å	2.50	2.725	2.74	2.75
M-Cl bridging	Å	2.52	2.52	2.48	2.41
M-Cl terminal	Å	2.34	2.39	2.40	2.29
reference		2	4,5	3	1

The metal-metal interaction of $Mo_2Cl_9^{3-}$ is intermediate between the chromium and tungsten end members and in many ways similar to the $Re_2Cl_9^-$ dimer.

The magnetic moment of $Mo_2Cl_9^{3-}$ is .6 BM and completely temperature independent. Attractive interaction between molybdenum ions is shown by the metal-chlorine-metal angle of 64°; the corresponding angle for a completely undistorted confacial bioctahedral structure is 70.5°. The polarized single crystal spectra of $Cs_3Mo_2Cl_9$ reveal two low energy bands polarized perpendicular to the C_3 axis of the anion, Figure 27.[9] These transitions have been assigned as spin-forbidden transitions within the molecular orbitals formed by overlap of the t_{2g} orbitals.[7] A similar intensification of the $^4A_2 \rightarrow {}^2E$ transition was observed in $Cr_2Cl_9^{3-}$ single crystals.[8]

The $Re_2Cl_9^-$ anion has an almost undistorted confacial bioctahedral structure: the Re-Cl-Re angle is 68.5°.[1] The magnetic moment of 1.506 BM shows antiferromagnetic coupling of the rhenium ions, consistent with a spin-paired ground state.[1] At 80°K the magnetic moment is .413 BM.

The compound $[(n\text{-}C_4H_9)_4N]Re_2Cl_9$ was prepared by the chlorine oxidation of the $Re_2Cl_8^{2-}$ salt.[10] Thin film crystals were grown from acetonitrile. The rectangular crystals are dichroic blue to yellow. On page 36 of reference 1 the crystals are reported to be blue for light polarized along the b axis and yellow perpendicular to this direction. Reference 1 mistakenly assigns this latter direction to the c axis. The C_3 axis (i.e., the Re-Re vector) is perpendicular to b,

FIGURE 27

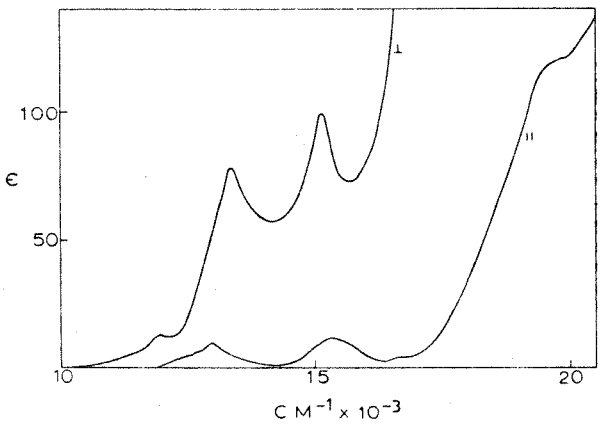

Crystal spectra of $Cs_3Mo_2Cl_9$ with incident light on a 110 face of the hexagonal crystal and polarized parallel and perpendicular to the threefold axis of the anion. The molar extinction coefficients were computed from the crystal thickness and the calculated crystal density.

being located on the mirror plane in the space group P $2_1/m$. The (100) face presents an approximately axial projection, Figure 28. Calculation of the molecular projection on (100) gives

$$A_{\|b} = Ax, y \tag{47}$$

$$A_{\perp b} = .0731\ Az + .9269\ Ax, y \tag{48}$$

where $Az \equiv C_3$. Little anisotropy should be observed for the xy polarized transitions, a prediction contrary to the observed intense dichroism. If the more reasonable choice - the (001) face - is assumed, the absorbances become

$$A_{\|b} = Ax, y \tag{49}$$

$$A_{\perp b} = .9916\ Az + .0084\ Axy. \tag{50}$$

The molecular projection is shown in Figure 29. The polarized spectra of $[(n\text{-}C_4H_9)_4N]Re_2Cl_9$ presented in Figure 30 agree with the calculated projections on (001). The low energy features are polarized perpendicular to the C_3 axis ($\|b$), a result which was previously found for $Mo_2Cl_9^{3-}$ and $Pt_2Cl_6^{2-}$. Polarization perpendicular to the metal-metal axis for spin forbidden transitions is apparently a general phenomena in chloro bridged dimers.

Interpretation of the observed spectral features does not appear to be possible without employing a dimeric metal-metal interaction model, although the spin coupling in $Re_2Cl_9^-$ is not complete. Using d orbitals orthogonalized along the C_3 axis,[11] linear combinations may be constructed for both the t_{2g} and e_g orbitals. The molecular

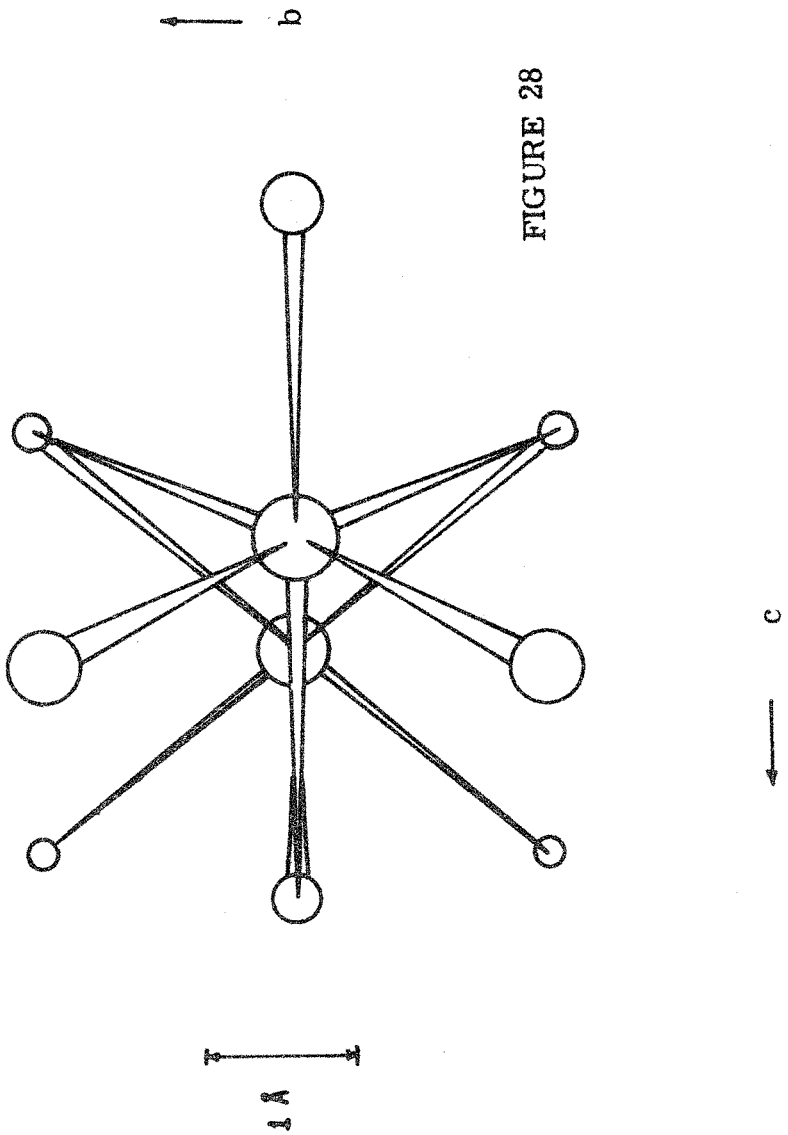

FIGURE 28

FIGURE 29

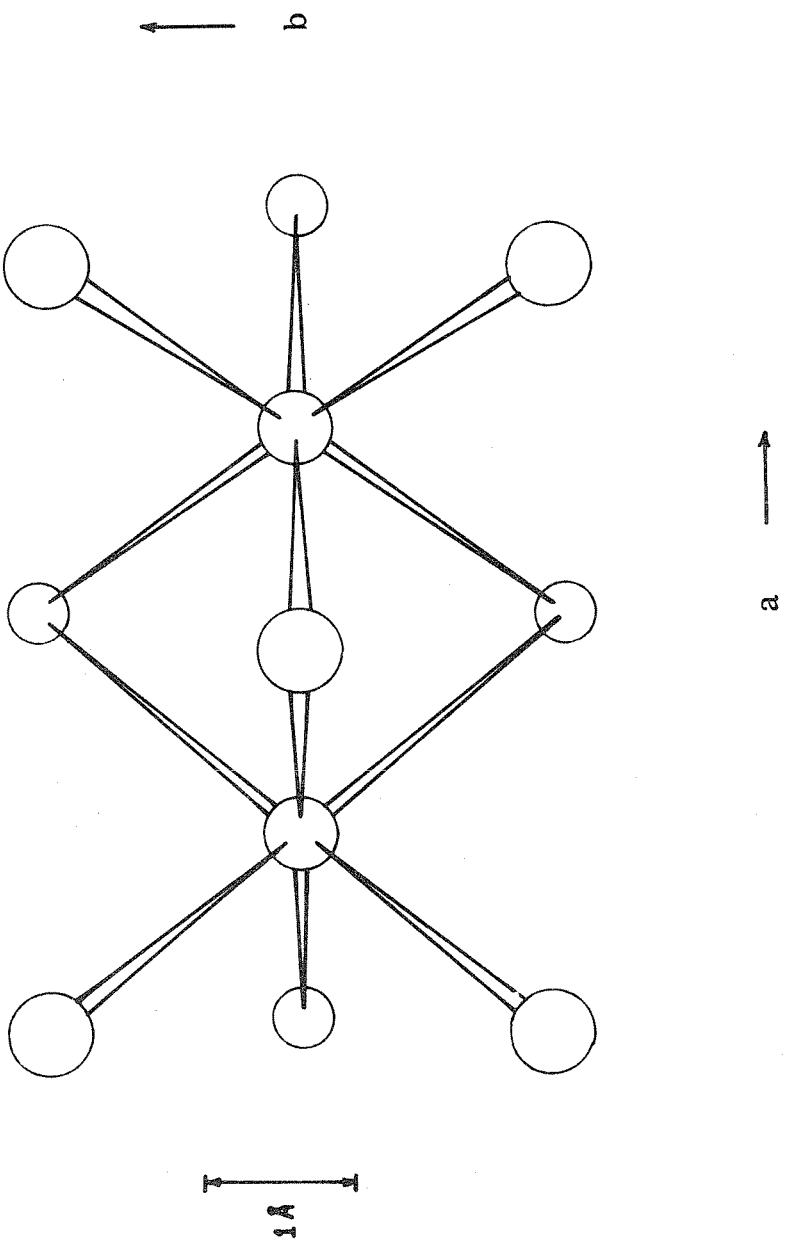

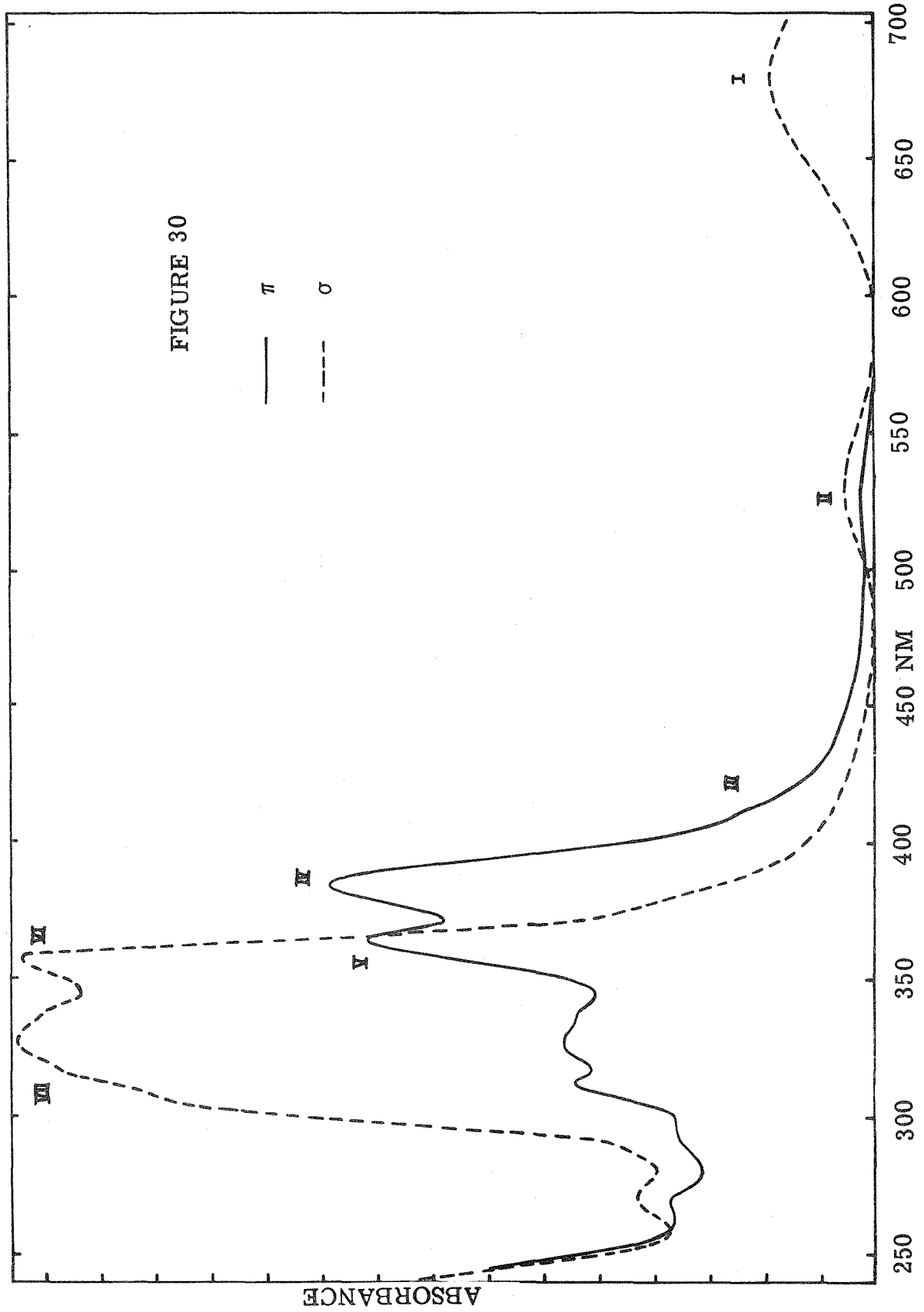
FIGURE 30
π
σ
I
II
III
IV
V
VI
VII
250
300
350
400
450 NM
500
550
600
650
700
ABSORBANCE

orbitals constructed from the e_g orbitals should be about 33,000 cm^{-2} [12] higher than those derived from the t_{2g} orbitals. The σ bonding combinations have A_1' and A_2'' symmetry; the π bonding ones have E' and E'' representations in D_{3h}, as shown in Figure 31.

The intense features in the polarized spectra, Figure 30, must be spin allowed transitions. Table 20 predicts only four allowed polarized transitions; the group of four bands above 25,000 cm^{-1} must be derivative from these. The xy polarized features at 18,900 cm^{-1} (530 nm) and 14700 cm^{-1} (680 nm) cannot be spin allowed transitions. If these bands are triplets related to the lowest intense singlet features (the two z polarized bands) they would correspond to spin forbidden transitions within the t_{2g} manifold. Peaks at 14180 cm^{-1} and 15,385 cm^{-1} in $ReCl_6^{2-}$ have been assigned as $^4A_{2g}(\Gamma_8) \rightarrow {}^2T_{2g}(\Gamma_7)$ and $^4A_{2g}(\Gamma_8) \rightarrow {}^2T_{2g}(\Gamma_8)$ respectively.[7, 12, 13] These monomer peaks are spin pairing transitions within the t_{2g} orbitals.

The polarizations of bands I and II are slightly different: the higher energy feature has a small z component, while band I is completely xy polarized. Using Table 21, assignments consistent with the experimental polarization ratios can be made. Band I is assigned as $^1A_1' \rightarrow {}^3E''$ in which the states resulting from $a_1' \rightarrow e_b''$ and $e_b' \rightarrow e_b''$ are mixed. Only xy polarization is expected. Band II is composed of the $^1A_1' \rightarrow {}^3A_2''$ states ($a_1' \rightarrow a_2''$ and $e_b' \rightarrow e_b''$) and $^1A_1' \rightarrow {}^3A_1''$ ($e_b' \rightarrow e_b''$). The xy polarization is predicted to be more intense than the z.

Bands IV and V are assigned as $^1A_1' \rightarrow {}^1A_2''$ ($e_b' \rightarrow e_b''$) and $^1A_1' \rightarrow {}^1A_2''$ ($a_1' \rightarrow a_2''$) respectively. Both are completely z polarized.

Figure 31

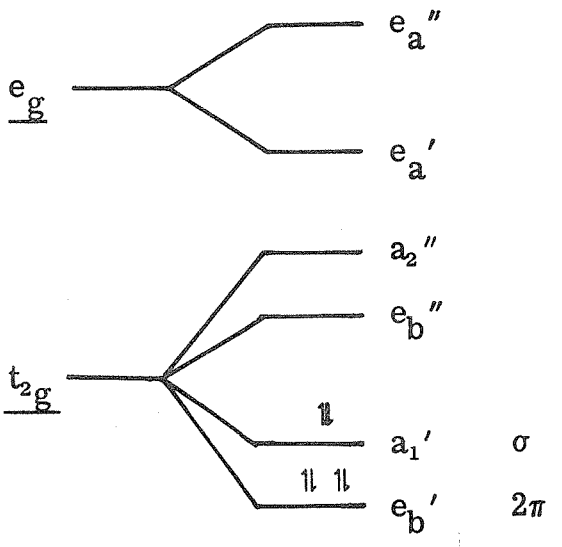

$$a_1' = t_{2g}^{\circ} + t_{2g}^{\circ}$$
$$a_2'' = t_{2g}^{\circ} - t_{2g}^{\circ}$$
$$e_b' = t_{2g}^{\pm} + t_{2g}^{\pm}$$
$$e_b'' = t_{2g}^{\pm} - t_{2g}^{\pm}$$
$$e_a' = e_g^{\pm} + e_g^{\pm}$$
$$e_a'' = e_g^{\pm} - e_g^{\pm}$$

Table 20

Predicted Spin Allowed Transitions

transition	Assignment	Polarization
	$^1A_1' \rightarrow$	
$a_1' \rightarrow e_b''$	$^1E''$	
$a_1' \rightarrow a_2''$	$^1A_2''$	z
$e_b' \rightarrow e_b''$	$^1A_1''$	
	$^1A_2''$	z
	$^1E''$	
$e_b' \rightarrow a_2''$	$^1E''$	
$a_1' \rightarrow e_a'$	$^1E'$	xy
$e_b' \rightarrow e_a'$	$^1A_1'$	
	$^1A_2'$	xy
	$^1E'$	

The direction parallel to the C_3 axis is z and xy is perpendicular.

z transforms as A_2''

xy transforms as E'

Table 21

Predicted Spin Forbidden Transitions

Transition	Assignment $^1A_1' \rightarrow$	Symmetry	Polarization
$a_1' \rightarrow e_b''$	$^3E''$	E''	xy
		$A_1' + A_2' + E'$	
$a_1' \rightarrow a_2''$	$^3A_2''$	A_1''	
		E'	xy
$e_b' \rightarrow e_b''$	$^3A_1''$	A_2''	z
		E'	xy
	$^3A_2''$	A_1''	
		E'	xy
	$^3E''$	E''	
		$A_1' + A_2' + E'$	xy
$e_b' \rightarrow a_2''$	$^3E''$	E''	
		$A_1' + A_2' + E'$	xy
$a_1' \rightarrow e_a'$	$^3E'$	E'	xy
		$A_1'' + A_2'' + E''$	z
$e_b' \rightarrow e_a'$	$^3A_1'$	A_2'	
		E''	
	$^3A_2'$	A_1'	
		E''	
	$^3E'$	E'	xy
		$A_1'' + A_2'' + E''$	z

S = 0 transforms as A_1'

S = 1 transforms as $A_2' + E''$

The former is broadened because several states lie within the manifold. The weak shoulder, band III, is assigned as the laporte-forbidden $^1A_1' \rightarrow {}^1E''$ ($a_1' \rightarrow e_b''$).

Band VI is the $^1A_1' \rightarrow {}^1E'$ ($a_1' \rightarrow e_a'$) xy polarized transition and Band VII contains the $^1A_1' \rightarrow {}^1E'$ ($e_b' \rightarrow e_a'$) manifold. The latter apparently contains a number of states. Bands VI and VII are $(t_{2g})^3 \rightarrow (t_{2g})^2(e_g)$ in nature, in accord with accepted monomer assignments.[12,13]

Ligand to metal charge transfer bands may also lie in this energy region. The observed red shift of the xy polarized bands in the complex $Re_2Br_9^-$ amounts to ~ 5500 cm^{-1}. Although such a large shift would appear to unequivocally support assignment of the intense spectral features as L → M charge transfer, the increase in metal-metal bond distance required by steric considerations in going from the chloride to the bromide could significantly decrease the metal-metal interaction. A large red shift would be expected. The increase metal-metal distance between $Mo_2Cl_9^{3-}$ and $Mo_2Br_9^{3-}$ amounts to .16 Å.[5]

The interaction model and assignments presented here are intended primarily as a basis for discussion of the $Re_2Cl_9^{2-}$ spectra, and cannot, with the available information, be considered completely rigorous.

Table 22

$Re_2Cl_8^-$

Band	Energy cm^{-1}	Assignment	Observed Polarization	Calculated Polarization
I	14700	$^1A_1' \rightarrow {}^3E''$	xy	
		$(a_1' \rightarrow e_b'')$		xy
		$(e_b' \rightarrow e_b'')$		xy
II	18900	$^1A_1' \rightarrow {}^3A_2''$	xy > z	
		$(a_1' \rightarrow a_2'')$		xy
		$(e_b \rightarrow e_b'')$		xy
		$^1A_1' \rightarrow {}^3A_1''$		
		$(e_b' \rightarrow e_b'')$		xy, z
III	24400	$^1A_1' \rightarrow {}^1E''$		
		$(a_1' \rightarrow e_b'')$		
IV	26000	$^1A_1 \rightarrow {}^1A_1''$, $^1A_2''$, $^1E''$	z	z
		$(e_b' \rightarrow e_b'')$		
V	27400	$^1A_1' \rightarrow {}^1A_2''$	z	z
		$(a_1' \rightarrow a_2'')$		
VI	27940	$^1A_1 \rightarrow {}^1E'$	xy	xy
		$(a_1' \rightarrow e_a')$		
		$^1A_1' \rightarrow {}^1A_2''$		
		$(e_b'' \rightarrow a_2'')$		

Table 22 (Cont'd)

Band	Energy cm^{-1}	Assignment	Observed Polarization	Calculated Polarization
VII	30,500	$^1A_1' \rightarrow {}^1A_1'$ $^1A_2'$ $^1E'$ $(e_b' \rightarrow e_a')$	xy	xy

References

1. P. F. Stokely, Ph.D. Thesis, Massachusetts Institute of Technology (1969).
2. G. J. Wessel and D. J. W. Ijdo, Acta. Cryst., 10, 466 (1957).
3. W. H. Watson and J. Waser, ibid., 11, 689 (1958).
4. M. J. Bennett, J. V. Brencic, and F. A. Cotton, Inorg. Chem., 8, 1060, (1960).
5. R. Saillant, R. B. Jackson, W. E. Streib, K. Folting, and R. A. D. Wentworth, Inorg. Chem., 10, 1453 (1971).
6. F. A. Cotton and D. A. Vcko, Inorg. Chim. Acta., 6, 161, (1972).
7. P. W. Smith, and A. G. Wedd, J. Chem. Soc. A, 2447 (1970).
8. R. Saillant and R. A. D. Wentworth, Inorg. Chem., 7, 1606 (1968).
9. R. Saillant and R. A. D. Wentworth, ibid., 8, 1226 (1969).
10. F. Bonati and F. A. Cotton, ibid., 6, 1353 (1967).
11. C. J. Ballhausen, Introduction to Ligand Field Theory, McGraw-Hill Co., New York, (1962) p. 68.
12. J. C. Eisenstein, J. Chem. Phys., 34, 1628 (1961).
13. P. B. Dorain and R. G. Wheeler, J. Chem. Phys., 45, 1172 (1966).

CHAPTER 6

Polarized Spectra of Quadruply Bonded Species, $Re_2Cl_8^{2-}$ and $Re_2Br_8^{2-}$

Among the most unusual examples of bonding in inorganic chemistry are the quadruply metal-metal bonded species. The tendency to form metal-metal bonds is dependent upon the degree of d orbital overlap: metal-metal interactions are greatest in the second and third row transition elements where the d orbitals extend further into space. The orbital contraction produced by the higher oxidation states reduces the possible orbital overlap. The high positive charge is stabilized by the presence of many ligands, sterically restricting the formation of metal-metal bonds. The strongest metal-metal bonding interactions will occur in those metals where the number of available bonding electrons is balanced with the resulting orbital overlap.

These factors are maximized in the d^4 Re(III) species. The eight bonding d electrons in the Re(III) dimer can form a σ, two π, and a δ bond for a total bond order of four. While the axially symmetric σ and π bonds are common and require no further description, the δ bond is unusual and some discussion is appropriate. The δ bond is the consequence of overlap between the in-plane dxy orbitals. An eclipsed conformation of ligands is required for such bonding; the more sterically favorable staggered conformation produces no net overlap. The energy stabilization achieved by the δ bond must be

larger than the rotational barrier between conformations. The quadruply bonded species with known crystal structures are listed in Table 23. The existing criteria for describing the bonding in terms of a quadruple bond are the presence of an unusually short metal-metal distance, an eclipsed structure, and diamagnetism.[15] No correlation has previously been demonstrated between the electronic spectra[15] of these species and the quadruple bond.[16] Single crystal polarized spectra of the compounds $[(n\text{-}C_4H_9)_4N]_2[Re_2X_8]$ (X = Cl, Br) and $Re_2Cl_6[PEt_3]_2$ confirm the applicability of the proposed MO model[16,17] with only minor changes and demonstrate such a spectral correlation.

$[(n\text{-}C_4H_9)_4N]_2[Re_2Cl_8]$ was prepared by the hypophosphorous acid reduction of potassium perrhenate,[18,15] although the synthetic method with the highest yield involves the fusion of Re_3Cl_9 with diethylammonium chloride.[19] The compound was crystallized as prisms from acetonitrile. Crystals could also be obtained from acetone, methanol, and nitromethane. The (100) diamond shaped crystals were dichroic - dark blue along b and pale blue parallel to c. An x-ray examination showed the compound crystallizes in the space group $P\ 2_1/c$ with a = 10.91 Å, b = 15.34 Å, c = 16.43 Å, and $\beta = 122.66°$. There are two dimers per unit cell. The calculated density is 1.635 g/cm^3; the density determined by floatation in bromoform-carbon tetrachloride is 1.623 g/cm^3. Thin single crystals were grown from acetonitrile on quartz substrates. The 5°K single crystal polarized spectra of $[(n\text{-}C_4H_9)_4N]_2[Re_2Cl_8]$ is shown in Figure 32. The assumption that the peak at 694 nm in completely $\pi(z)$ polarized,

Table 23

$M_2X_8^{n-}$ quadruply bonded species

Compound	M-M Å	M-X Å	M_2-X angle degrees	Reference
$K_2Re_2Cl_8 \cdot 2H_2O$	2.241	2.26	101.7	1
		2.31	105.8	
$(pyH)_2Re_2Cl_8$	2.22	2.43		1, 2
$Re_2Cl_6[PEt_3]_2$	2.222	2.294	103.1	
		2.352	116.3	3
$Cs_2Re_2Br_8$	2.228	2.469		
		2.484		4
$(pyH)_2Re_2Br_8$	2.207			5
	2.27			6
$K_4Mo_2Cl_8 \cdot 2H_2O$	2.139	2.44	104.5	
		2.46	105.8	7
$(enH_2)_2Mo_2Cl_8 \cdot 2H_2O$	2.134	2.442	104.6	
		2.460	105.5	8
$(NH_4)_4Mo_2Cl_8 \cdot H_2O \cdot NH_4Cl$	2.150	2.415	103.4	
		2.490	107.3	9

Table 23 (Cont'd)

Related Carboxylate Bridged Species

	M-M Å	M-X Å	M-O Å	M_2-X degrees	M_2-O degrees	
$Re_2[O_2CCH_3]_2Cl_4 \cdot 2H_2O$	2.224	2.30	1.97	104	90	10
$Re_2[O_2C\phi]_2I_4$	2.198	2.621	2.014	110.1	90.3	11
$Re_2[O_2C\phi]_4Cl_2$	2.235		2.00		89.5	
			2.03		90.8	12
$Mo_2[O_2CCH_3]_4$	2.11		2.07			
			2.12			13
$Mo_2[O_2CCF_3]_4$	2.090					14

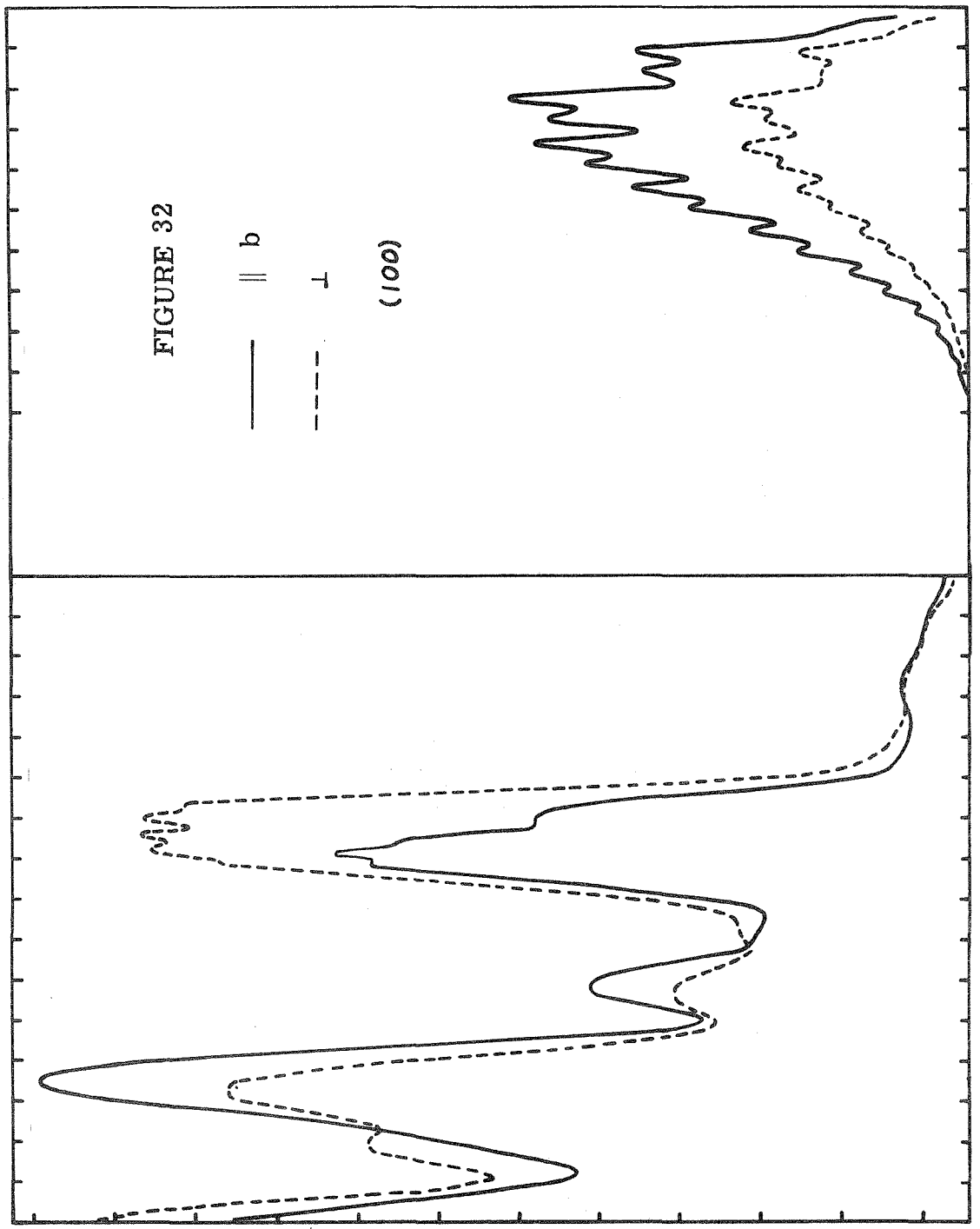
FIGURE 32
∥ b
⊥
(100)
ABSORBANCE
250
300
350
NM
650
700

$$\frac{A_{\parallel}}{A_{\perp}} = 2.203,$$

and the peak at 324 nm is completely σ (x, y) polarized,

$$\frac{A_{\perp}'}{A_{\parallel}'} = 2.199,$$

allows the orientation of the C_4 axis to be calculated from equations 19 and 20. The values $\theta = 34°1'$ and $\phi = 3°19'$ are obtained for the (100) face. This orientation is very similar to that of the (100) face of $Cs_2Re_2Br_8$[4] - $\theta = 35°0'$ and $\phi = 10°4'$. The observed absorptions are

$$A_{\parallel b} = .6871\ A\pi + .3129\ A\sigma \tag{51}$$

$$A_{\perp b} = .3119\ A\pi + .6881\ A\sigma \tag{52}$$

The inverse matrix

$$\begin{bmatrix} A\pi \\ A\sigma \end{bmatrix} = \begin{bmatrix} 1.8340 & -.8340 \\ -.8312 & 1.8312 \end{bmatrix} \begin{bmatrix} A_{\parallel} \\ A_{\perp} \end{bmatrix} \tag{53}$$

was used to resolve the spectra, Figure 33.

$[(n\text{-}C_4H_9)_4N]_2[Re_2Br_8]$ was prepared by treating a methanol solution of the chloride with HBr.[18] The complex was recrystallized from acetonitrile. Crystal could also be obtained from nitromethane. Diamond shaped crystals, apparently ismorphous to the chloride, were dichroic-green parallel to the short axis, orange perpendicular. A few non-dichroic orange yellow faces were observed. The 5°K polarized

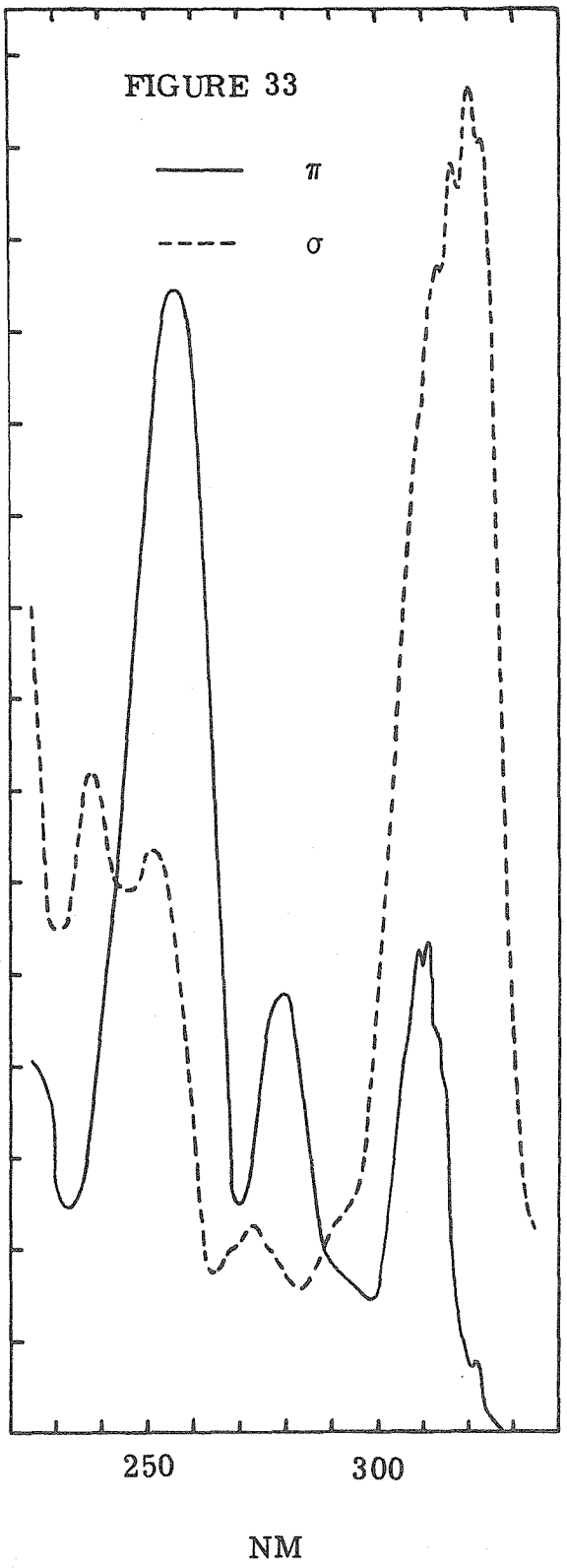
FIGURE 33
π
σ
ABSORBANCE
250
300
NM

spectra are shown in Figure 34. Initial attempts to calculate the orientation of the C_4 axis assuming that the band at 420 nm to be completely σ (x, y) polarized produced values of θ and ϕ which did not reflect the apparent isomorphism with the chloride. Such results suggest that the 420 nm bond contains a vibronic π component. The previously determined $\phi = 3°19'$ value was assumed to be approximately correct. The 713 nm peak had a

$$\frac{A_{\parallel}}{A_{\perp}} = 2.8395$$

ratio. The θ orientation was determined to be $30°44'$.

$$A_{\parallel} = .7381\ A\pi + .2611\ A\sigma \tag{54}$$

$$A_{\perp} = .2602\ A\sigma + .7998\ A\sigma \tag{55}$$

Figure 35 was calculated using the matrix

$$\begin{bmatrix} A\pi \\ A\sigma \end{bmatrix} = \begin{bmatrix} 1.5454 & -.5454 \\ -.5436 & 1.5436 \end{bmatrix} \begin{bmatrix} A_{\parallel} \\ A_{\perp} \end{bmatrix} \tag{56}$$

The compound $Re_2Cl_6[PEt_3]_2$ was prepared by addition of triethylphosphine to a slightly acidified methanol solution of tetrabutylammonium octachlorodirhenate(III).[18, 20] Although a detailed account of the preparation is reported only for the related triphenylphosphine derivative, the crystal structure of $Re_2Cl_6[PEt_3]_2$ is known.[3] The complex is monoclinic, space group P $2_1/n$ with lattice constants a = 7.644 Å, b = 10.985 Å, c = 14,206 Å, $\beta = 96.5°$. There are two molecules per unit cell. The crystals grow as prisms elongated on a.[3]

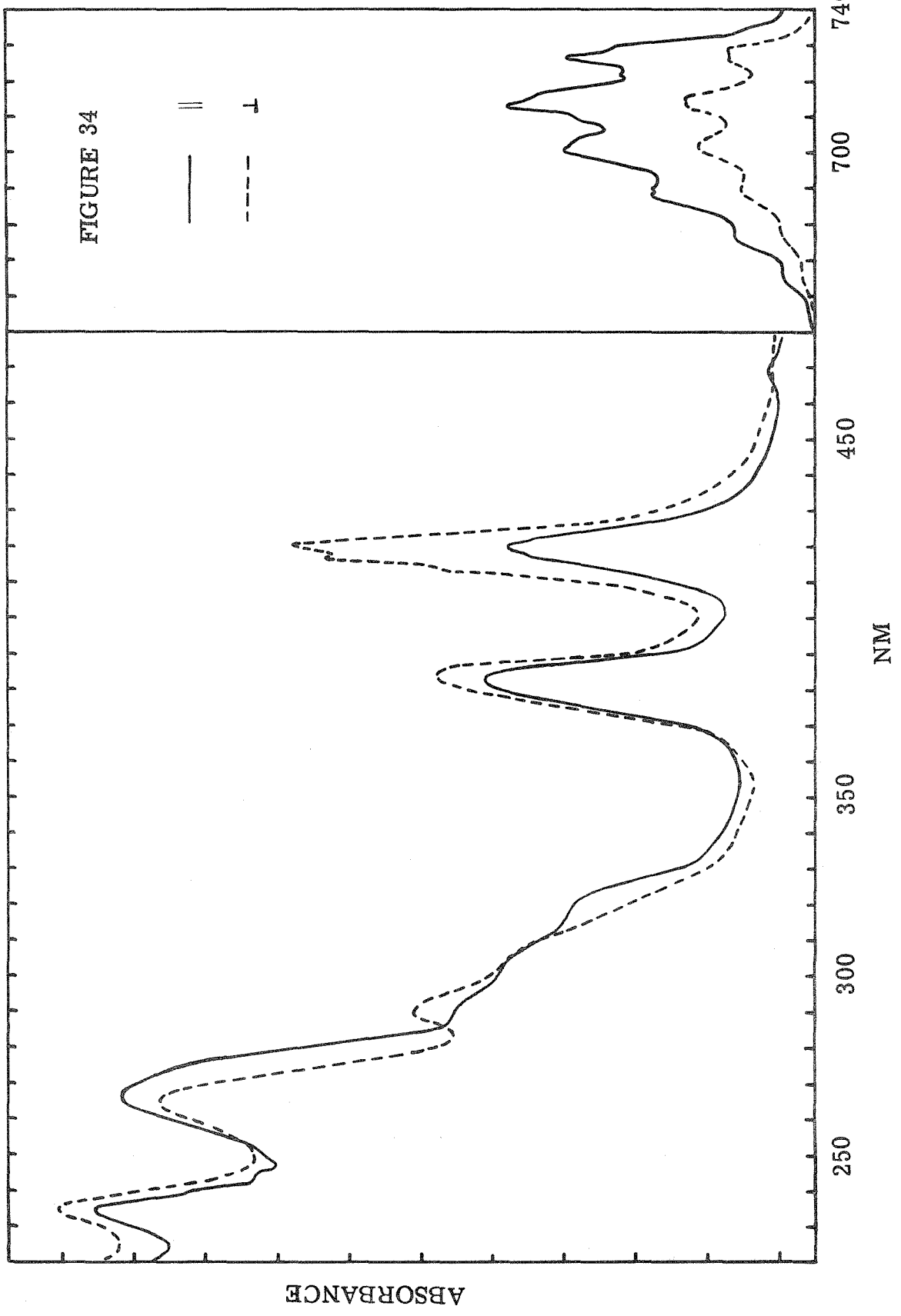
FIGURE 34
∥
⊥
ABSORBANCE
250
300
350
450
700
740
NM

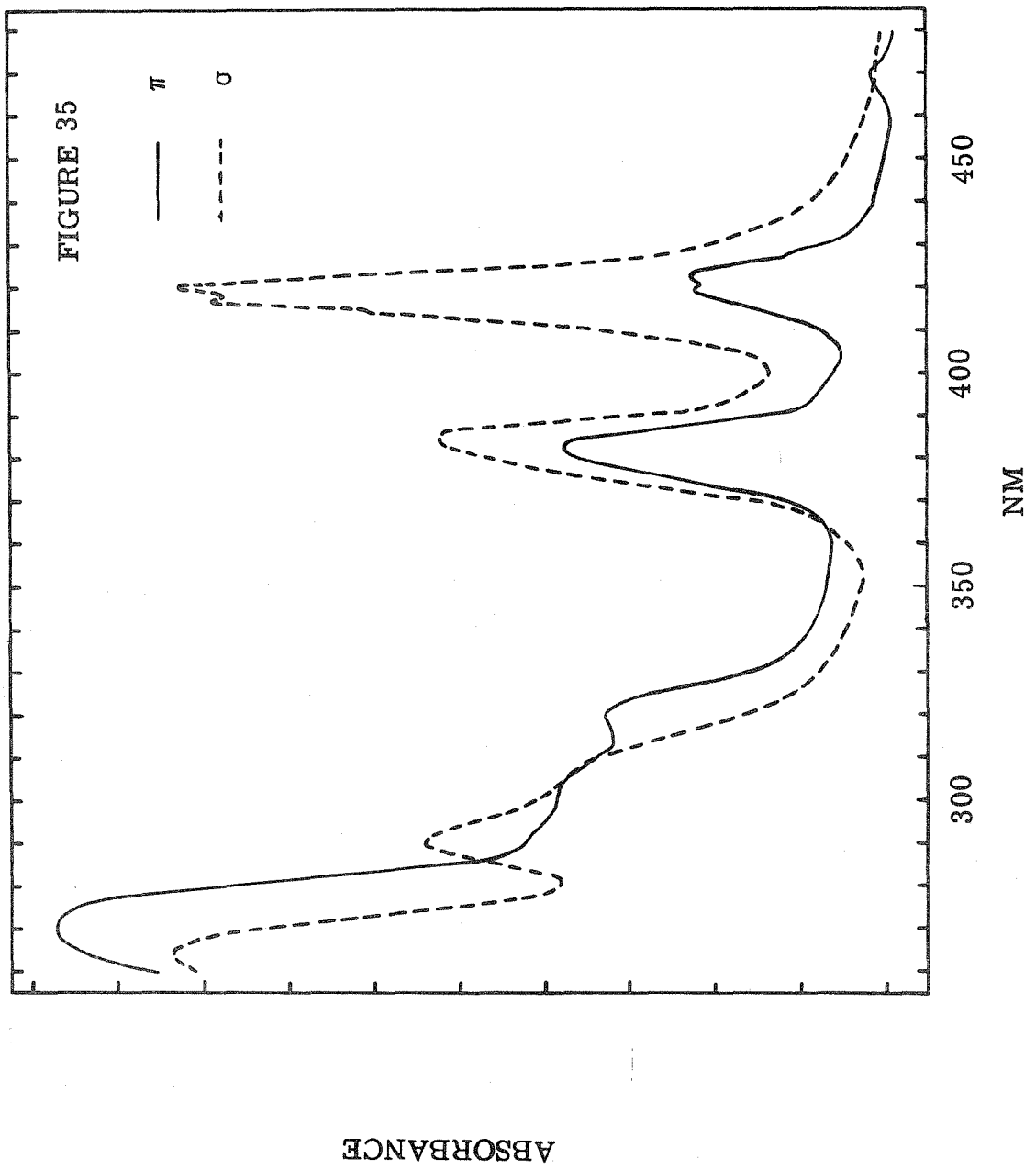
FIGURE 35
π
σ
300
350
400
450
NM
ABSORBANCE

The normal to the well developed face makes an angle of 52.1° with the c* axis, confirming assignment as (011). The crystals were dichroic - blue perpendicular to a, yellow parallel to a. Thin single crystals were grown from chloroform.

The magnetic circular dichroism spectra of the $Re_2X_8^{2-}$ complexes were measured in acetonitrile solution. No A term was observed for either complex in the region of the lowest intense absorption (~ 14000 cm^{-1}). The observed MCD spectra are shown in Figures 36, 37.

The compound $Mo_2(O_2CCH_3)_4$ was prepared by the literature method.[21] $K_4Mo_2Cl_8$ is obtained from the acetate by HCl in hydrochloric acid[22] containing KCl. The substitution of NH_4Cl yields $(NH_4)_5Mo_2Cl_9 \cdot H_2O$.[9] Treatment of a methanol solution with triethylphosphine yields the blue complex $Mo_2Cl_4[PEt_3]_4$.[23] Microcrystals of $K_4Mo_2Cl_8$ were found to be dichroic - purple to pale yellow.

The $^1A_{1g} \rightarrow {}^1A_{2u}$ ($\delta\ b_{2g} \rightarrow \delta^*\ b_{1u}$) transition is both allowed and $\pi(z)$ polarized in D_{4h} symmetry. A Hückel molecular orbital calculation[16] placed the energy of this transition at 19,700 cm^{-1}. The calculation showed the $\delta(b_{2g})$ orbital to be the highest filled MO and the $\delta^*(b_{1u})$ and $\sigma_n(a_{2u})$ orbitals to be the lowest unfilled orbitals. The lowest observed transition, 14,180 cm^{-1} in $Re_2Cl_8^{2-}$ and 13,600 cm^{-1} in $Re_2Br_8^{2-}$, has been assigned by Cotton[16,17] as $^1A_{1g} \rightarrow {}^1B_{1u}$ ($\delta\ b_{2g} \rightarrow \sigma_n\ a_{2u}$), which is laporte-forbidden based on the weak oscillator strength of the band ~.023. However, the $^1A_{1g} \rightarrow {}^1A_{2u}$ ($\delta\ b_{2g} \rightarrow \delta^*\ b_{1u}$) transition will not result in an appreciable change in the dipole

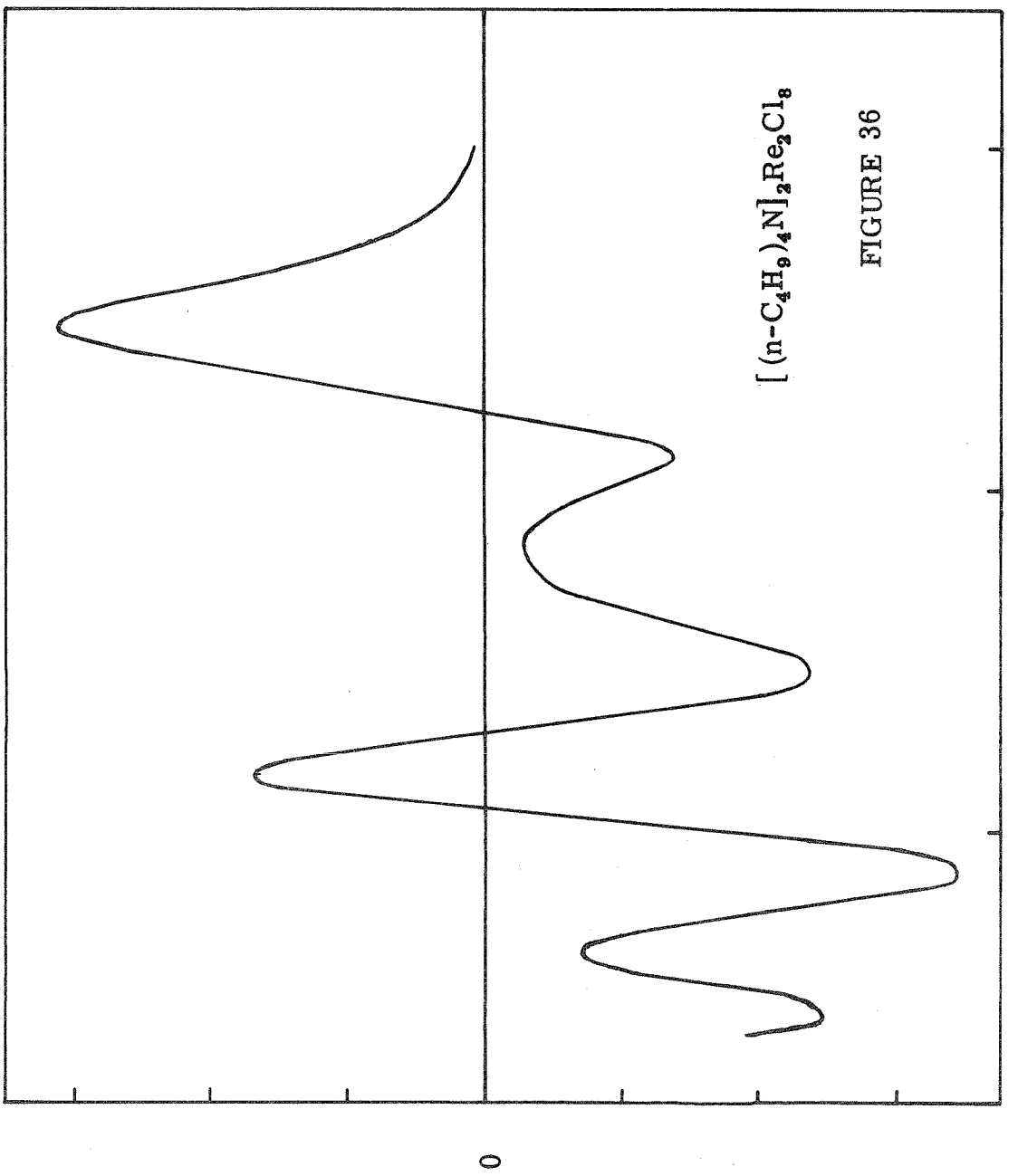

FIGURE 36

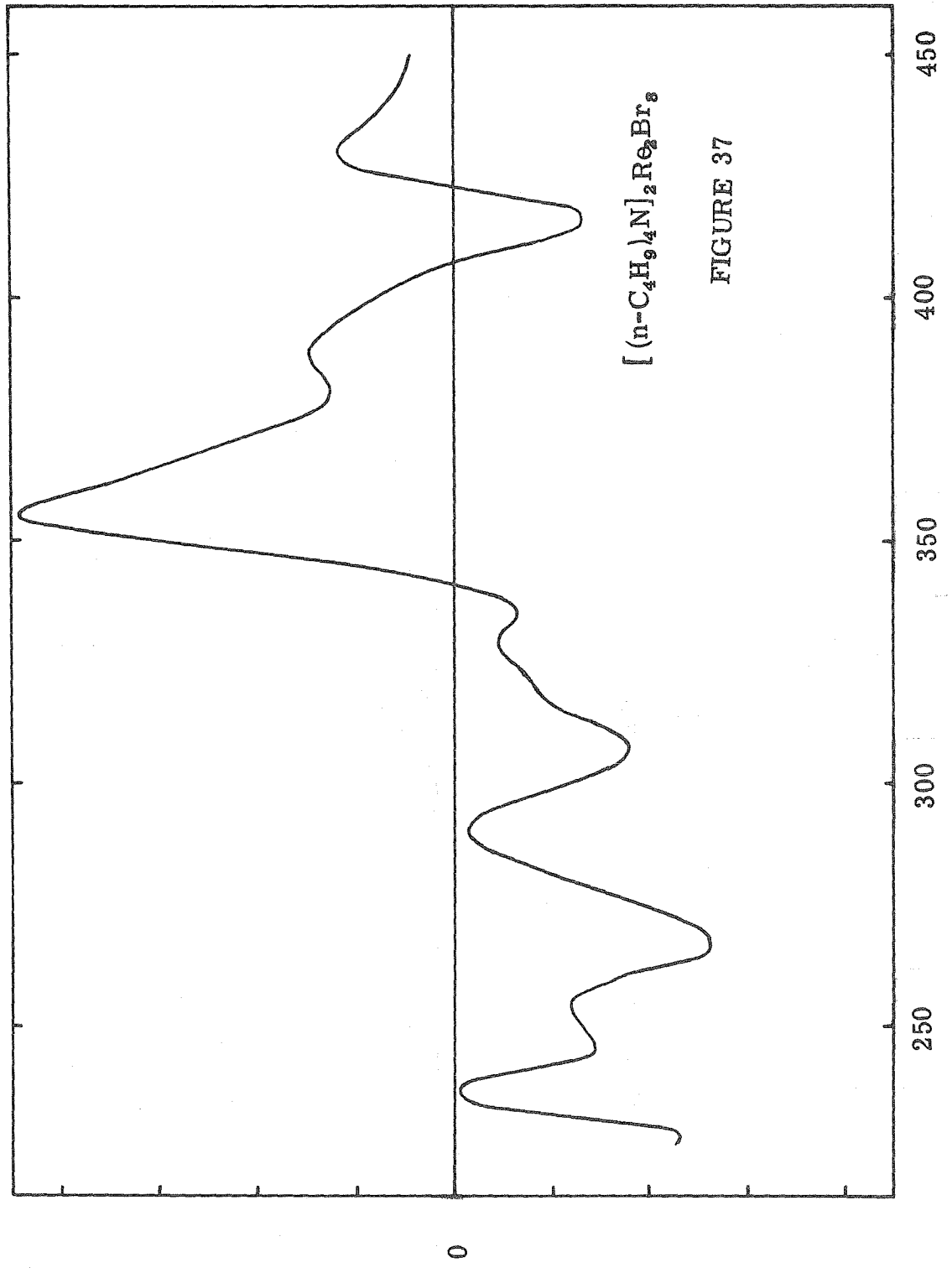

FIGURE 37

moment since both the ground and excited states localize the electron in the same spatial region - the dxy orbitals. The intensity of this allowed transition is not expected to be large.

The most striking characteristic of this band is its allowed temperature dependence: the oscillator strength shows a slight increase at low temperatures. At 77°K a single vibrational progression is observed with a spacing of 254 cm^{-1} for the chloride and 256 cm^{-1} for the bromide. At 5°K the band in $Re_2Cl_8^{2-}$ can be resolved into two progressions of the totally symmetric A_{1g} vibration - Table 24. The progression forming mode (249 cm^{-1}) corresponds to ν_2, the metal-metal stretch.[24] The corresponding band in $Re_2Br_8^{2-}$ is resolved into five progressions at helium temperature - Table 25. In this case the progression forming mode (259 cm^{-1}) corresponds to ν_1, again the metal-metal stretch.[24] The excited state vibrational frequencies are at lower energies than the ground state vibrations.

Analogous bands in $K_4Mo_2Cl_8$ and $Mo_2Cl_4[PEt_3]_4$ show fine structure in the KBr pellet spectra. The spacings observed, 359 cm^{-1} and 336 cm^{-1} respectively agree with the 350 ± 30 cm^{-1} spacing of a similar band observed in $Mo_2(O_2CCH_3)_4$.[25] The raman spectra of the latter compound show a strong absorption at 406 cm^{-1} - corresponding to the A_{1g} metal-metal stretch.[24] This frequency is reduced in the excited state. Raman spectra of $K_4Mo_2Cl_8$ show a strong peak at 350 cm^{-1} which is assigned as the metal-metal stretch.[26]

The bands at 14180 cm^{-1} in $Re_2Cl_8^{2-}$ and 13,600 cm^{-1} in $Re_2Br_8^{2-}$ are responsible for the strong dichroism observed for these

Table 24

Vibrational Progressions of 14183 cm^{-1} Band in $Re_2Cl_8^{2-}$ at 5°K

nm	cm^{-1}		
705.06	14183		
			115
699.41	14298	224	
694.12	14407		245
687.65	14542	247	
682.41	14654		245
676.24	14788	249	
671.00	14903		249
665.06	15036	248	
660.00	15152		246
654.35	15282	250	
649.29	15401		243
644.12	15525	248	
639.00	15649		240
634.29	15766		

ground state

A_{1g} ν_1 ---

ν_2 274

ν_3 115

Table 25

Vibrational Progressions of 13, 597 cm^{-1} Band in $Re_2Br_8^{2-}$ at 5°K

nm	cm^{-1}					
735.47	13597					
730.24	13694		98	168	168	
726.47	13765	253				
722.06	13949		253			
717.00	13847			253	169 x 2	
715.59	13975	255				
713.35	14018		259			
709.00	14104					257
703.94	14206			255		
702.65	14232	256			169	
700.59	14274					
696.35	14361				161	258
692.77	14435			250		
690.12	14490					
688.53	14524					

ground state

A_{1g} ν_1 277

ν_2 184

ν_3 ---

Table 26

Vibrational Progression of 17,897 cm^{-1} Band in $K_4Mo_2Cl_8$ at 5°K

nm	cm^{-1}	Spacing cm^{-1}	
558.76	17897	354	
547.93	18251	356	
537.46	18606	359	
527.28	18965	349	A_{1g} ground state
517.75	19314	349	350 cm^{-1}
508.82	19653	349	
499.94	20002	318	
492.13	20320		

Table 27

Vibrational Progression of 16,322 cm^{-1} Band in $Mo_2Cl_4[PEt_2]_4$ at 5°K

nm	cm^{-1}	Spacing cm^{-1}
612.66	16322	338
600.24	16660	335
588.40	16995	336
576.98	17332	328
566.27	17659	327
555.98	17986	312
546.51	18298	

compounds. Their similar polarization behavior suggests a common assignment. In Figures 32 and 34 this polarization has been correlated to the b crystal axis. The definite absence of an MCD A term in this region rules out an assignment of the band as an xy polarized $^1A_{1g} \rightarrow {}^1E_u$ transition to a degenerate excited state. While the polarization ratios also strongly favor assignment of the band as a z (π) polarized transition, polarization along the metal-metal axis must be clearly proven to substantiate an assignment as $^1A_{1g} \rightarrow {}^1A_{2u}$ $\delta \rightarrow \delta^*$. Proof of this point is based upon symmetry arguments in a related compound of lower symmetry — the C_{2h} species $Re_2Cl_6[PEt_3]_2$.

The compound $Re_2Cl_6[PEt_3]_2$ has been shown by an x-ray crystal structure[3] to have the structure shown in Figure 38.

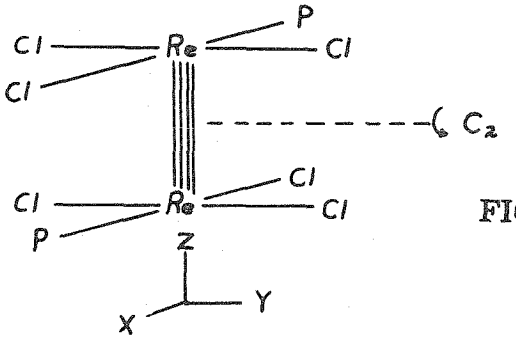

FIGURE 38

The structure retains a center of symmetry. The C_2 axis corresponds to the y axis of the $Re_2Cl_8^{2-}$ parent. The molecular projections in the (011) face are shown in Figure 39. The metal-metal vector is almost exactly perpendicular to the a crystallographic axis; the crystal appears dark blue for light polarized along the metal-metal direction. The C_2(Y) axis is approximately parallel to a. The polarized single crystal spectra are summarized in Table 28. The correlation table for a descent in symmetry from D_{4h} ($Re_2Cl_8^{2-}$) to

FIGURE 39

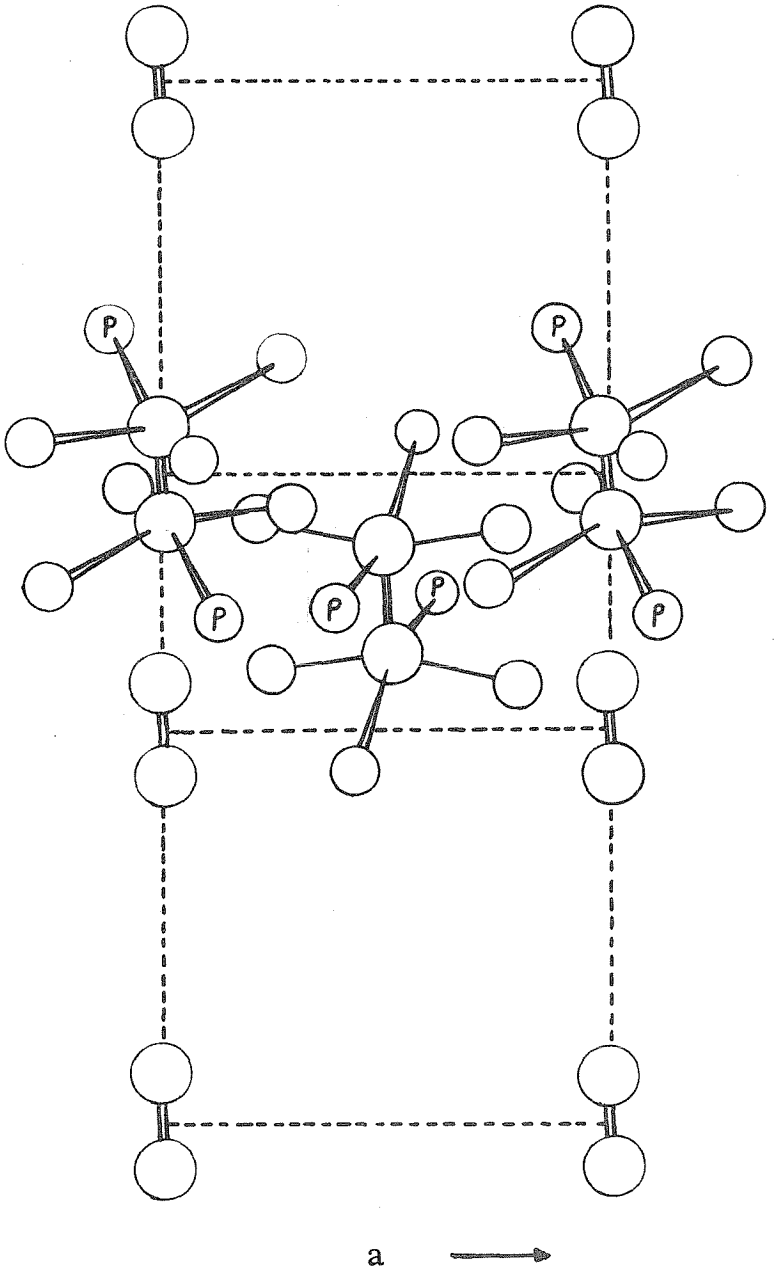

Table 28

$Re_2Cl_6[PEt_3]_2$

H_2CCl_2 Solution		Single Crystal 5°K (011) Face		
nm	cm^{-1}	nm	cm^{-1}	Polarization
717	13950	710	14090	xz(⊥a)
391.5	25550	395	25310	y(‖a)
344.5	29000	345	29000	y(‖a)
272	36770	270	37000	xz(⊥a)

The 710 nm band shows a weak vibrational progression

nm	cm^{-1}	Spacing cm^{-1}
725.4	13785	289
710.5	14074	289
696.2	14363	289
682.5	14652	291
669.2	14943	

$C_{2h}(Re_2Cl_6[PEt_3]_2)$ is given in Table 29.

The $(b_{2g}\ \delta \rightarrow b_{1u}\ \delta^*)\ ^1A_{1g} \rightarrow\ ^1A_{2u}$ transition in D_{4h} becomes $^1A_g \rightarrow\ ^1B_u$ in C_{2h} which is xz polarized. No other transition has the correct polarization! Cotton's assignment of the 14,180 cm^{-1} band as $(b_{2g}\ \delta \rightarrow a_{2u}\ \sigma_n)$ - $^1A_g \rightarrow\ ^1A_u$ (in C_{2h}) - would require Y polarization and a substantial increase in intensity since the band becomes fully allowed in the lower symmetry. Such an assignment is definitely contrary to the experimental data.

The 14180 cm^{-1} transition in $Re_2Cl_8^{2-}$ has been conclusively shown to be the $^1A_{1g} \rightarrow\ ^1A_{2u}$ $(b_{2g}\ \delta \rightarrow b_{1u}\ \delta^*)$ transition. As expected of a feature dependent primarily upon the metal-metal overlap, the position of the band does not shift greatly between the chloride and bromide. Excitation of an electron from the δ bonding orbital into the δ^* antibonding orbital effectively reduces the δ bond order to zero. The lower metal-metal vibrational frequencies observed for this transition in the electronic excited state indicate a weaker force constant is associated with a decrease of the bond order from four to three.

The photochemical behavior of $Re_2Cl_8^{2-}$ also is consistent with assignment of the 14180 cm^{-1} transition as $\delta \rightarrow \delta^*$. No photoreaction occurs upon irradiation into this band.[27] Breaking the δ bond would not labilize any ligands, but only permit rotation about the metal-metal axis. The observation of emission from this band upon excitation with the He-Ne 632.8 nm laser line at 770 nm in $Re_2Cl_8^{2-}$ and

Table 29

D_{4h}	C_{2h}		
A_{1g}	A_g	x	B_u
A_{2g}	B_g	y	A_u
B_{1g}	A_g	z	B_u
B_{2g}	B_g		
E_g	$A_g + B_g$		
A_{1u}	A_u		
A_{2u}	B_u		
B_{1u}	A_u		
B_{2u}	B_u		
E_u	$A_u + B_u$		

796 nm in $Re_2Br_8^{2-}$ [27] shows that there are no lower lying triplet states. Intense emission is also observed from this band in the quadruply bonded molybdenum species.

The assignment of the remaining part of the spectra will be based upon the polarization results and the close correlation of the transition energies and virtual molecular orbitals. The electron repulsion terms are assumed to be constant. Similarly, and more significantly, no spin-orbit allowed triplet states are assigned. The strong metal-metal interaction either relaxes the spin selection rules or the singlets and triplets are not separated due to the absence of electron repulsion terms. Spin orbit coupling will not be considered further.

Polarized spectra reveal two transitions under the band envelope at 30870 cm^{-1} in $Re_2Cl_8^{2-}$. These bands are clearly resolved in the bromide at 23630 cm^{-1} and 26040 cm^{-1}. Both are xy polarized. The MCD A term under the band envelope of $Re_2Cl_8^{2-}$ indicates one of the excited states is degenerate. A similar A term in $Re_2Br_8^{2-}$ is found under the 23,630 cm^{-1} band. A vibrational progression (Table 31) is also found on this band of spacing ~ 200 cm^{-1}, corresponding to a strengthened metal-ligand A_{1g} stretch.[24] A similar progression (Table 30) in the chloride of spacing 386 cm^{-1} also indicates an A_{1g} metal-halogen stretch. The large shift to lower energy in going from the chloride to the bromide suggests that these transitions are best characterized as L → M* charge transfer. Accordingly, the transitions are assigned as $^1A_{1g} \rightarrow {}^1E_u$ ($\pi_L e_g \rightarrow \delta^* b_{1u}$)

Table 30

Vibrational Progression of 30, 873 cm^{-1} Band in $Re_2Cl_8^{2-}$ at 5°K

⊥b (xy polarized)

nm	cm^{-1}	Spacing cm^{-1}	
323.9	30873	386	0 - 0
319.9	31259	386	
316.0	31645	385	
312.2	32030	384	
308.5	32414	372	
305.0	32786		

∥b (z polarized)

nm	cm^{-1}	Spacing cm^{-1}
318.8	31367	348
315.3	31715	346
311.9	32061	346
308.5	32407	347
305.3	32754	346
302.2	33090	

Table 31

Vibrational Progression of 23629 cm^{-1} Band in $Re_2Br_8^{2-}$ at 5°K

⊥b (xy polarized)

nm	cm^{-1}	Spacing cm^{-1}	
423.2	23629	152	0-0
420.5	23781	194	
417.1	23975	191	
413.8	24166	212	
410.2	24378	198	
406.9	24576		

∥b (z polarized)

nm	cm^{-1}	Spacing cm^{-1}
423.2	23629	180
420.0	23809	183
416.8	23992	168
413.9	24160	

and $^1A_{1g} \rightarrow {}^1A_{1g}$ ($\pi_L b_{1u} \rightarrow \delta^* b_{1u}$). Evidence for the latter assignment is based upon the small polarization ratio of the band and upon an MO calculation[16] which shows this bonding ligand orbital to be destabilized.

An alternate assignment of the degenerate xy polarized transition at 30870 cm^{-1} in $Re_2Cl_8^{2-}$ is $^1A_{1g} \rightarrow {}^1E_g$ ($\pi_m e_u \rightarrow \delta^* b_{1u}$), a transition from the π bonding orbital of the metal-metal bond to the δ^* antibonding orbital. This transition in C_{2h} $Re_2Cl_6[PEt_3]_2$ becomes $^1A_g \rightarrow {}^1A_g + {}^1B_g$, neither of which is allowed. The intense feature at 30870 cm^{-1} is absent in the phosphine adduct.

The weak transitions at 27030 cm^{-1} and 28330 cm^{-1} in $Re_2Cl_8^{2-}$ are assigned as $^1A_{1g} \rightarrow {}^1B_{1u}$ ($b_{2g}\ \delta \rightarrow a_{2u}\ \sigma_n$) and $^1A_{1g} \rightarrow {}^1B_{1u}$ ($a_{1g}\ \sigma \rightarrow b_{1u}\ \delta^*$) respectively. Reduction of symmetry to C_{2h} for $Re_2Cl_6[PEt_3]_2$ makes both of these transitions allowed along the C_2 axis - Y allowed. Two intense Y allowed bands are observed at 25310 cm^{-1} and 29000 cm^{-1} in this complex. Irradiation of the $Re_2Cl_8^{2-}$ complex with light $\lambda > 300$ nm breaks the quadruple bond to form the complex $ReCl_4(CH_3CN)_2^-$.[27] This observation is consistent with the proposed assignments; for a $\sigma \rightarrow \delta^*$ transition, the bond order is reduced to 2.5. Weakening the σ bond allows cleavage of the complex.

The most intense feature in the spectra is the allowed z polarized transition $^1A_{1g} \rightarrow {}^1A_{2u}$ ($a_{1g}\ \sigma \rightarrow a_{2u}\ \sigma_n$). This band does not shift greatly from $Re_2Cl_8^{2-}$ to $ReBr_8^{2-}$; the band occurs at 39,215 cm^{-1} and 37,735 cm^{-1} respectively. The complete assignments of the spectra are presented in Tables 32 and 33.

Table 32

$Re_2Cl_8^{2-}$

cm^{-1}	Assignment	Excited State $^1A_{1g} \rightarrow$	Polarization	
			Observed	Predicted
14180	$b_{2g}\ \delta \rightarrow b_{1u}\ \delta^*$	A_{2u}	z	z
27030	$b_{2g}\ \delta \rightarrow a_{2u}, a_{1g}\ \sigma_N$	B_{1u}, B_{2g}	z	
28330	$a_{1g}\ \sigma \rightarrow b_{1u}\ \delta^*$	B_{1u}	z	
30870	$e_g\ \pi_L \rightarrow b_{1u}\ \delta^*$	Eu	xy	xy
31750	$b_{1u}\ \pi_L \rightarrow b_{1u}\ \delta^*$	A_{1g}	xy	
34480	$b_{2g}\ \delta \rightarrow b_{1g}$ (LF)	A_{2g}	xy	
35700	$b_{2g}\ \delta \rightarrow a_{2u}\ \sigma_N$	B_{1u}	z	
36630	$b_{2g}\ \delta \rightarrow b_{2u}$ (LF)	A_{1u}	xy	xy
39050	$a_{1g}\ \sigma \rightarrow a_{2u}\ \sigma_N$	A_{2u}	z	z
39840	$a_{1g}\ \sigma \rightarrow a_{1g}\ \sigma_N$	A_{1g}		
	$b_{2g}\ \delta \rightarrow e_g\ \pi^*_m$	Eg	xy	
42000	$e_g\ \pi_L \rightarrow a_{2u}\ \sigma_N$	Eu	xy	xy

Table 33

$Re_2Br_8^{2-}$

cm^{-1}	Assignment	Excited State $^1A_{1g} \rightarrow$	Polarization	
			Observed	Predicted
13600	$b_{2g}\ \delta \rightarrow b_{1u}\ \delta^*$	A_{2u}	z	z
21275	$a_{1g}\ \sigma \rightarrow b_{1u}\ \delta^*$	B_{1u}	z	
23630	$e_g\ \pi_L \rightarrow b_{1u}\ \delta^*$	E_u	xy	xy
25975	$b_{1u}\ \pi_L \rightarrow b_{1u}\ \delta^*$	A_{1g}	xy	
31250	$b_{2g}\ \delta \rightarrow a_{2u}\ \sigma_N$	B_{1u}	z	
32800	$b_{2g}\ \delta \rightarrow b_{1g}$ (LF)	A_{2g}	xyz	
	$a_{1g}\ \delta \rightarrow a_{1g}\ \sigma_N$	A_{1g}		
34360	$e_g\ \pi_L \rightarrow a_{1g}$	E_g	xy	
38700	$a_{1g}\ \sigma \rightarrow a_{2u}\ \sigma_N$	A_{2u}	z	z

The original objection raised by Cotton et al.[16,17] can be considered at this point. Cotton argued that the 14180 cm^{-1} band in $Re_2X_8^{2-}$ disappears in the eclipsed carboxylate bridged species $Re_2(O_2CR)_4Cl_2$ because this band is a $\delta \rightarrow \sigma_n$ transition. The axially coordinated chlorides utilize the σ_n orbital in bonding; the resultant destabilization of the p_z metal orbital presumably places this transition at much higher energies in $Re_2(O_2CR)_4Cl_2$.

The existence of a quadruple bond in the bridged carboxylate species is an assumption. The complex must have an eclipsed configuration because of the four bidentate carboxylate groups. Although the short metal-metal distance (2.235 Å) is indicative of a quadruple bond, little increase in metal-metal distance (2.29 Å) is shown for a staggered, and thus rigorously triply bonded complex.[28] In those complexes where the σ_n orbital lies above the δ (b_{2g}) orbital, the $\delta \rightarrow \delta^*$ transition is observed. Complexes of this type are $Re_2X_8^{2-}$ (X = Cl, Br), and cis $Re_2(O_2CCH_3)_2Cl_4 \cdot 2H_2O$. Only weak axial bonding can occur because of the steric hindrance of the large halide ligands. For the $Re_2(O_2CR)_4Cl_2$ species the smaller oxygen ligands allow axial coordination. If the σ_n orbital becomes more stable than the δ b_{2g} orbital, it will be occupied preferentially. The $\delta \rightarrow \delta$ transition does not exist because the compound is only triply bonded. This bond is still sufficient to maintain the binuclear unit; the carboxylate species have been shown to be interconvertible with the $Re_2X_8^{2-}$ complexes.[15]

Figure 40

$Re_2X_8^{2-}$

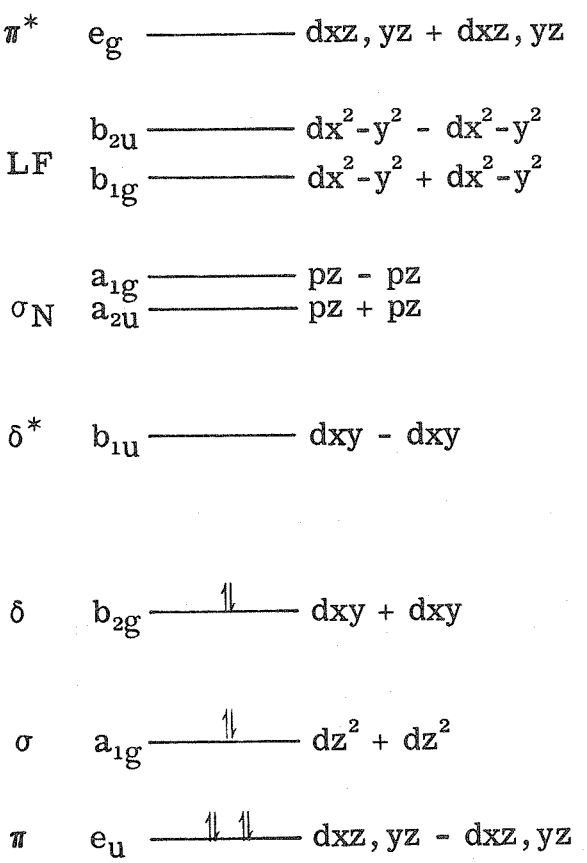

References

1. F. A. Cotton and C. B. Harris, Inorg. Chem., 4, 330 (1965).
2. V. G. Kuznetsov and P. A. Koz'min, Zh Strukt. Khim, 4, 55 (1963).
3. F. A. Cotton and B. M. Foxman, Inorg. Chem., 7, 2135 (1968).
4. F. A. Cotton, B. G. DeBoer, and M. Jeremic, Inorg. Chem., 9, 2143 (1970).
5. P. A. Koz'min, V. G. Kuznetsov, and Z. V. Popova, Zh Strukt. Khim., 6, 651 (1965).
6. V. G. Kuznetsov and P. A. Koz'min, Acta Crystallogr., 16, 41 (1963).
7. J. V. Brencic and F. A. Cotton, Inorg. Chem., 8, 7 (1969).
8. J. V. Brencic and F. A. Cotton, ibid., 8, 2698 (1969).
9. J. V. Brencic and F. A. Cotton, ibid., 9, 346 (1970).
10. P. A. Koz'min, M. O. Surazhskaya, and V. G. Kuznetsov, Zh Strukt. Khim., 11, 313 (1970).
11. F. A. Cotton, Accts. Chem. Res., 2, 240 (1969).
12. M. J. Bennett, W. K. Bratton, F. A. Cotton, and W. R. Robinson, Inorg. Chem., 7, 1570 (1968).
13. D. Lawton and R. Mason, J. Amer. Chem. Soc., 87, 921 (1965).
14. F. A. Cotton and J. G. Norman, J. Coord. Chem., 1, 161 (1972).
15. F. A. Cotton, N. F. Curtis, B. F. Johnson, and W. R. Robinson, Inorg. Chem., 4, 326 (1965).
16. F. A. Cotton and C. B. Harris, ibid., 6, 924 (1967).
17. F. A. Cotton, Inorg. Chem., 4, 334 (1965).
18. F. A. Cotton, N. F. Curtis, and W. R. Robinson, Inorg. Chem., 4, 1696 (1965).

19. R. A. Bailey and J. A. McIntyre, Inorg. Chem., 5, 1940 (1966).

20. M. J. Bennett, F. A. Cotton, B. M. Foxman, and P. F. Stokely, J. Amer. Chem. Soc., 89, 2759 (1967).

21. A. B. Brignole and F. A. Cotton, Inorg. Synth., 13, 87 (1972).

22. J. V. Brencic and F. A. Cotton, Inorg. Chem., 9, 351 (1970).

23. J. San Filippo, Inorg. Chem., 11, 3140 (1972).

24. W. K. Bratton, F. A. Cotton, M. Debeau, and R. A. Walton, J. Coord. Chem., 1, 121 (1971).

25. L. Dubicki and R. L. Martin, Aust. J. Chem., 22, 1571 (1969).

26. A. Ketteringham and C. Oldham, J. Chem. Soc. Dalton, 1067 (1973).

27. G. Goeffrey, private communication.

28. M. J. Bennett, F. A. Cotton, and R. A. Walton, J. Amer. Chem. Soc., 88, 3866 (1966).

CHAPTER 7

Polarized Spectra of $Re_2Cl_9^{2-}$

Spectroscopic studies of the electronic structures of the compounds $[(n\text{-}C_4H_9)_4N]Re_2Cl_9$ and $[(n\text{-}C_4H_9)_4N]_2Re_2Cl_8$ have been presented in Chapters 5 and 6. The goal of such studies has been to develop an understanding of the bonding and electronic structure imposed by metal-metal interactions. Implicit in these studies is the assumption that such knowledge will facilitate an understanding of the bonding in related complexes. Such a compound is $[(n\text{-}C_4H_9)_4N]_2Re_2Cl_9$. Although the structure of the anion is not known, the similarity of the electronic spectra to those of the two end members is striking.[1,2] The existance of a $\delta \rightarrow \delta^*$ transition in a complex of symmetry lower than D_{4h} with only a single δ electron would be important in characterizing the δ bond. Similarly, identification of spectral features related to the mixed-valence nature of the complex would also be highly significant.

The intermediate nature of the $Re_2Cl_9^{2-}$ species between the quadruply bonded $Re_2Cl_8^{2-}$ and the confacial bioctahedral $Re_2Cl_9^{-}$ complexes is clearly demonstrated by their chemical interconvertibility. The complex $[(C_6H_5)_4As]_2Re_2Cl_9$ was first prepared by the reaction of β-$ReCl_4$ with hydrochloric acid in methanol.[1] β-$ReCl_4$ has been shown to possess a polymeric confacial bioctahedral structure in which Re_2Cl_9 units share two terminal chlorides.[3,4] The complex decomposes in acetone or acetonitrile to $[(C_6H_5)_4As]_2Re_2Cl_8$ at room temperature.[1] The action of warm hydrochloric acid also gives the quadruply bonded $Re_2Cl_8^{2-}$ species.[1] The compound can also be converted into the dimeric acetate

$Re_2(O_2CCH_3)_4Cl_2$.[1] The compound $[(n\text{-}C_4H_9)_4N]Re_2Cl_9$ results from the chlorine oxidation of $[(n\text{-}C_4H_9)_4N]_2Re_2Cl_8$. The former has been shown to have a confacial bioctahedral structure.[4] The reduction of the $Re_2Cl_9^-$ species with tin, copper, or mercury in a polar solvent such as acetone produces $[(n\text{-}C_4H_9)_4N]_2Re_2Cl_9$.[2]

The $Re_2Cl_9^{2-}$ anion probably has a structure related to the Re_2Cl_8 structure by addition of an axial chloride.[1] The symmetry of such a species would be reduced from D_{4h} to C_{4V}. An alternate structure similar to $Re_2Cl_9^-$ would have D_{3h} symmetry.[1] A comparison of the available crystallographic data for these compounds is presented in Table 33. The similarity of space group and cell volume between $Re_2Cl_8^{2-}$ and $Re_2Cl_9^{2-}$ indicates that the anions pack in an analogous manner. The effective volume occupied by a tetrabutylammonium group is ~500 Å^3. The volume per $Re_2Cl_8^{2-}$ anion in the cell, 157 Å^3, is exactly that expected for a cube of chlorine atoms 5.33 Å on an edge, 152 Å^3. The volume occupied by the $Re_2Cl_9^{2-}$ anion in its unit cell is only slightly greater, 182 Å^3. The $Re_2Cl_9^-$ anion packs much less efficiently, requiring a volume of 270 Å^3 per anion. The correspondence between $Re_2Cl_8^{2-}$ and $Re_2Cl_9^{2-}$ does not, however, prove that their molecular structures are similar.

In the tetrabutyl ammonium salts, the $Re_2Cl_8^{2-}$ anion sits on an inversion center, and the $Re_2Cl_9^-$ anion is located on a mirror plane. The $Re_2Cl_9^{2-}$ anion occupies a general position. Of the possible structures[1] for $Re_2Cl_9^{2-}$ - C_{4V}, D_{3h} - neither has an inversion center, but both possess mirror planes. This suggests a C_{4V} structure related to $Re_2Cl_8^{2-}$.

The structures of several mixed valence chloride species are known. The d^4, d^5 compound $(NH_4)_3Tc_2Cl_8$ has the D_{4h} eclipsed $Re_2Cl_8^{2-}$

Table 33

Compound	Space Group	Lattice Constants Å	Cell Volume/ 2 Units Å^3	Density g/cm^3 Observed	Density g/cm^3 Calculated
$[(n\text{-}C_4H_9)_4N]_2$ Re_2Cl_8	$P2_1/c$	a = 10.91 b = 15.34 c = 16.43 β = 122.66° z = 2	2314.76	1.623	1.637
$[(n\text{-}C_4H_9)_4N]_2$ Re_2Cl_9	$P2_1/c$	a = 17.22 b = 14.21 c = 19.73 β = 101.50° z = 4	2365.46	1.7	1.652
$[(n\text{-}C_4H_9)_4N]$ Re_2Cl_9	$P2_1/m$	a = 13.62 b = 11.42 c = 10.64 β = 111.36° z = 2	1541.21	1.997 2.03	2.01

structure[5] even though the extra electron occupies the δ^* orbital. The Tc - Tc bond distance is 2.13 Å. The compound Re_2Cl_5 (2,5-dithiahexane)$_2$ also is a d^4, d^5 mixed valence species. The metal-metal bond distance is 2.29 Å and the structure has a staggered configuration[6] and an axial chloride. The compound $(Rb,Cs)_3Mo_2Cl_8$ has a quite different structure. The d^3, d^4 species has a confacial bioctahedral structure in which one bridging chloride is absent.[7] The Mo-Mo distance is 2.38 Å compared to 2.15 Å in the quadruply bonded $Mo_2Cl_8^{4-}$ species. Virtual D_{3h} symmetry is retained. Structural precedants exist for both D_{3h} and C_{4v} mixed valence structures.

The magnetic behavior of the complex $[(n\text{-}C_4H_9)_4N]_2Re_2Cl_9$ is best characterized by a small temperature dependent paramagnetism - μeff = 0.928BM at 301 °K and μeff = 0.55 BM at 87 °K.[4] The corresponding $Re_2Cl_9^-$ complex is antiferromagnetic; the $Re_2Cl_8^{2-}$ complex is diamagnetic. The magnetic behavior indicates the presence of strong metal-metal interactions.

The room temperature and 77 °K infrared spectra of $[(n\text{-}C_4H_9)_4N]_2Re_2Cl_9$ and $[(n\text{-}C_4H_9)_4N]Re_2Cl_9$ have been measured.[8] The infrared spectra are presented in Table 34. Bridging frequencies are at

Table 34

$Re_2Cl_9^-$		$Re_2Cl_9^{2-}$		$Re_2Cl_8^{2-}$[9]
RT cm^{-1}	77 °K cm^{-1}	RT cm^{-1}	77 °K cm^{-1}	RT cm^{-1}
360.7	360.2			
344.4	346.0	332.5	333.8	347
250.3	251.9	326.9	326	335

lower energies than terminal stretches and show a blue shift at low temperatures. The bands at 344 cm^{-1} and 250 cm^{-1} in $Re_2Cl_9^-$ are bridging modes. The bands at 347 cm^{-1} and 335 cm^{-1} in $Re_2Cl_8^{2-}$ are assigned as a_{2u} and e_u modes, respectively.[9] The infrared appears to support a C_{4V} structure. The final criteria for distinguishing between the possible structures is the single crystal spectra. The preparation and crystallization of $[(n\text{-}C_4H_9)_4N]_2Re_2Cl_9$ will be described.

The complex was prepared by adding ~ 1 g of $ReCl_5$ to a solution of 2 ml. H_2O in 60 ml. acetone.[10] The reaction was carried out under nitrogen. To the purple brown solution was added tetrabutyl ammonium chloride in chloroform. The solution changes from green to purple-blue after an hour. The solution was evaporated to a purple oil and water was added to precipitate the purple product. The product was filtered and washed with water, ether, and ethanol. The authentic complex was also prepared by the literature method[2]--reduction of $Re_2Cl_9^-$ with tin.

Thin film crystals were obtained from acetonitrile, dichloromethane and 1,2-dichloroethane. The crystals were dichroic purple-blue to colorless. Spectra were obtained for crystals grown from acetonitrile-dichloroethane mixtures. Several faces were obtained: crystals with polarization ratios at 545 nm of ~ 4/1, 3/1, 2/1 were observed. At room temperature loss of optical quality of the crystals occurred within a half hour; this may be due to either loss of solvent of crystallization or to a phase change. The crystals were stable at low temperatures. The single crystal polarized spectra of $Re_2Cl_9^{2-}$ at 5°K are presented in Figure 41.

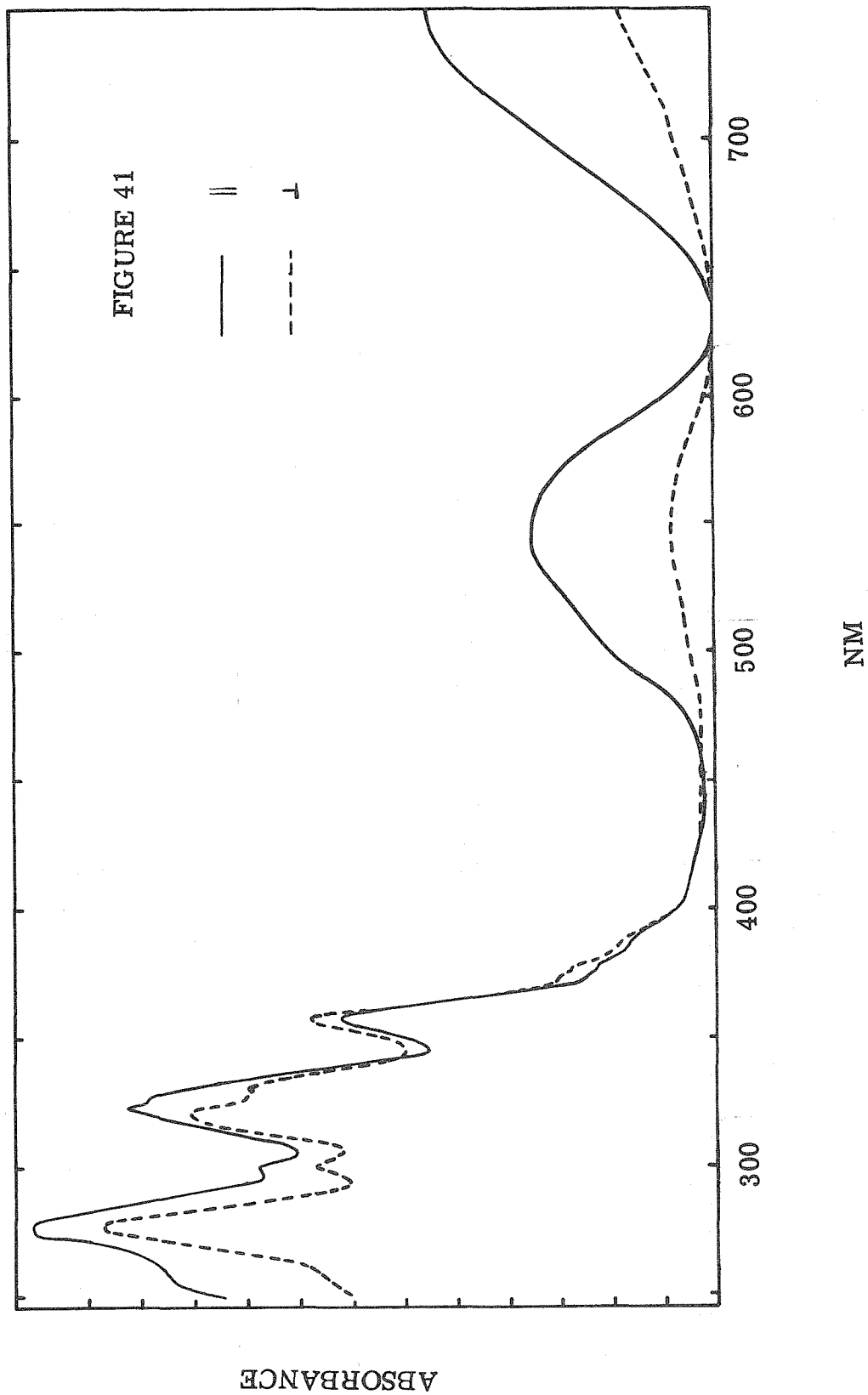
FIGURE 41
||
⊥
ABSORBANCE
300
400
500
600
700
NM

Any attempt to calculate the orientation of the unique molecular axis (either C_3 or C_4) from equations 19 and 20 requires the polarization ratios of two oppositely polarized bands. The π polarized band may be taken as either the 545 nm or 750 nm band. Some difficulty was encountered due to the lack of a well resolved intense σ polarized peak; the π polarized transitions appear to overlap and obscure the σ bands. The bands at 374 and 300 nm were found to have the same polarization ratios when the tails of nearby overlapping bands had been subtracted. The ratio $A\|/A\perp$ was taken as 4.2485 and $A\perp'/A\|'$ as 1.600. The values of $\theta = 48°28'$ and $\phi = 64°33'$ allowed the resolution of the observed spectra as

$$A\| = 0.4397\ A\pi + 0.5603\ A\sigma \tag{57}$$

$$A\perp = 0.1035\ A\pi + 0.8965\ A\sigma \tag{58}$$

The inverse matrix becomes

$$\begin{bmatrix} A\pi \\ A\sigma \end{bmatrix} = \begin{bmatrix} 2.6665 & -1.6665 \\ -0.3078 & 1.3078 \end{bmatrix} \begin{bmatrix} A\| \\ A\perp \end{bmatrix} \tag{59}$$

The π and σ spectra are shown in Figure 42. These calculations assumed the π polarization of the 545 nm feature. The opposite assumption, σ polarization, results in an impossible value of ϕ ($\cos^2\phi > 1$). The polarization ratio along the unique axis (π) must always be greater than that in the perpendicular (σ) direction.

The knowledge that the absorption band at 750 nm (13,330 cm^{-1}) has π (z) polarization is especially significant in differentiating between structures analogous to those of the $Re_2Cl_8^{2-}$ and $Re_2Cl_9^-$ end members.

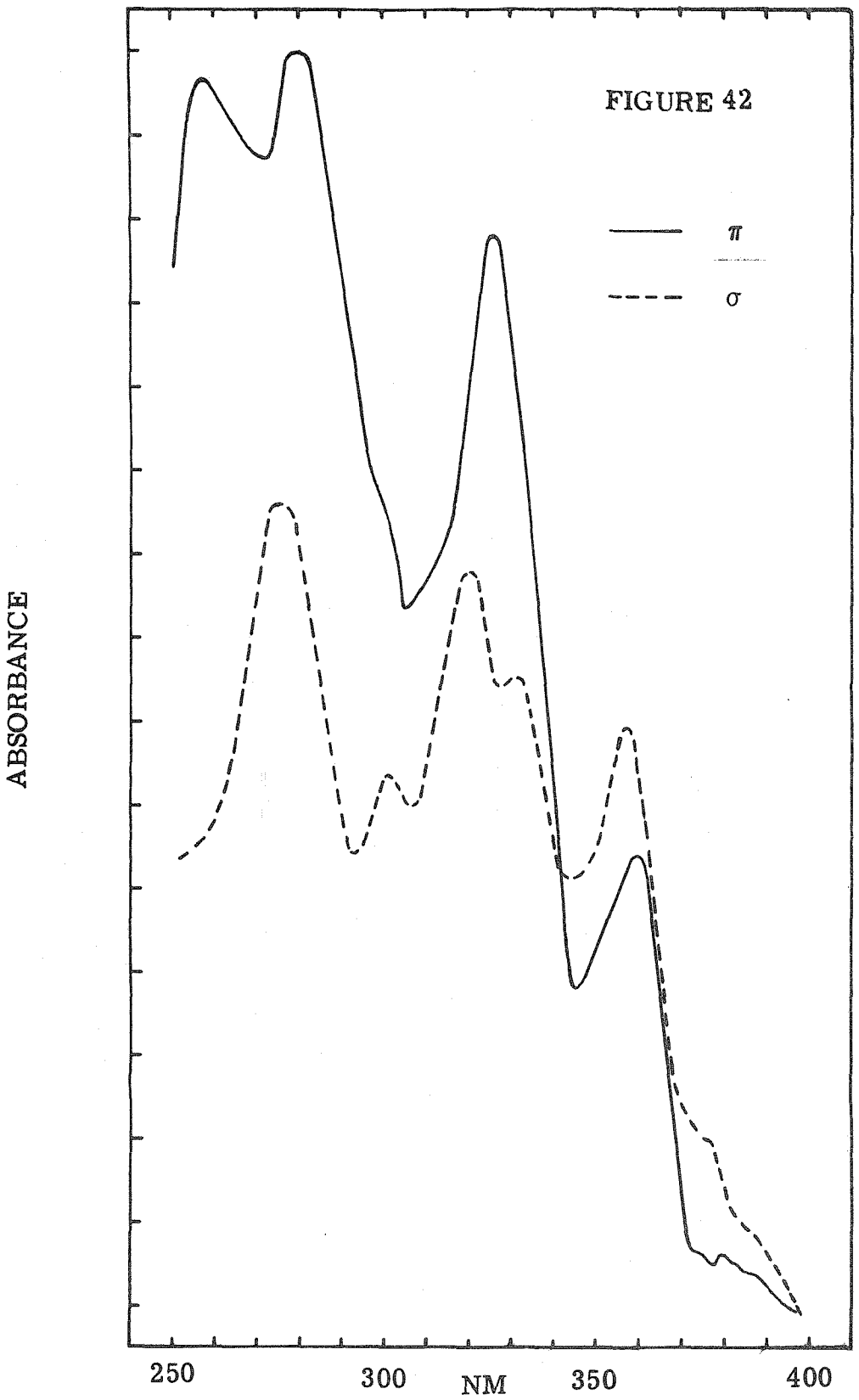
FIGURE 42
π
σ
ABSORBANCE
250
300
NM
350
400

The peak at 680 nm (14, 700 cm^{-1}) in $Re_2Cl_9^-$ has xy polarization and a solution ϵ of 480.[2] In contrast the 705 nm (14, 180 cm^{-1}) band in $Re_2Cl_8^{2-}$ has z polarization and much greater intensity: ϵ is 2622. The reported extinction coefficient for $Re_2Cl_9^{2-}$ is 1380.[2] Both a red shift and a decrease in intensity would be expected for the $\delta \rightarrow \delta^*$ transition because of the reduced metal-metal overlap resulting from axial coordination.

In C_{4V} symmetry, the single unpaired electron in the δ orbital will result in a $^2B_2$ ground state. The correlation between D_{4h} and C_{4V} symmetries is shown in Table 35.

Table 35

D_{4h}	C_{4V}
A_{1g}, A_{2u}	A_1
A_{2g}, A_{1u}	A_2
B_{1g}, B_{2u}	B_1
B_{2g}, B_{1u}	B_2
Eg, Eu	E
x, y $\equiv$ Eu	x, y $\equiv$ E
z $\equiv A_{2u}$	z $\equiv A_1$

The bonding and antibonding combinations of the metal orbitals will belong to the same irreducible representation in C_{4V}. The $^2B_2 \rightarrow {}^2B_2$ ($b_2\delta \rightarrow b_2\delta^*$) transition at 13, 300 cm^{-1} is z allowed. No fine

structure was observed even at 5°K; the band remains broad with the intensity independent of temperature. A second intense z polarized band is observed at 18, 350 cm^{-1}, exactly the energy expected for the L → M charge transfer transition $^2B_2 \rightarrow {}^2B_2$ ($b_2\pi_L \rightarrow b_2\delta$). This transition is not possible in $Re_2Cl_8^{2-}$ where the δ orbital is completely filled. The broad appearance of this band is similar to that of the $\delta \rightarrow \delta^*$ transition and may be due to the in-plane nature of both ground and excited states. The z polarization of this band strongly supports the similar assignment of the b_2 ligand π orbital in the $Re_2Cl_8^{2-}$ MO scheme. The transition $b_2 \rightarrow \delta^*$, again $^2B_2 \rightarrow {}^2B_2$ z polarized, is observed at 30, 900 cm^{-1}. In $Re_2Cl_8^{2-}$ this transition is observed at 31, 300 cm^{-1} in xy polarization. The $b_2 \rightarrow \delta^*$ transition in $Re_2Cl_9^{2-}$ shows vibrational fine structure of frequency ~316 cm^{-1}. Metal chlorine frequencies were observed in this region in the infrared at 332 and 327 cm^{-1}. Vibrational progressions are also observed for this band in $Re_2Cl_8^{2-}$ at 386 cm^{-1} and 358 cm^{-1} (Table 30).

The shoulder at 20, 000 cm^{-1} is especially significant. The transition is assigned as $^2B_2 \rightarrow {}^2A_1$ ($b_2\pi_L \rightarrow a_1\sigma p_z$). The symmetry of this orbital is substantiated by the observation of the z allowed $^2B_2 \rightarrow {}^2B_2$ ($a_1\sigma\, dz^2 \rightarrow a_1\sigma\, p_z$) at 39, 200 cm^{-1}. The transition $^2B_2 \rightarrow {}^2A_1$ ($a_1\sigma\, dz^2 \rightarrow b_2\delta$) is found at 36, 200 cm^{-1}. The σp_z orbital is close in energy, but slightly less stable than the δ orbital for a complex containing one axial chloride. The explanation offered previously for the absence of the $\delta \rightarrow \delta^*$ transition in complexes of $Re_2(O_2CR)_4Cl_2$ was that the σp_z orbital is occupied instead of the δ orbital. For complexes coordinating only a single axial chloride, the δ orbital remains lowest. Solvent coordination in the remaining

vacant axial position could reverse this ordering, breaking the δ bond completely. Rotation to the staggered conformation, the first step in the structural interconversion to a confacial bioctahedron, is then possible (Figure 43).

The proposed assignments for the $Re_2Cl_9^{2-}$ spectra are presented in Table 36. The assignments are internally consistent if the $^2A_1$ states have z polarization and $^2B_1$ states are xy polarized. The latter case requires that the A_2 vibrational mode be ineffective in vibronic coupling. This mode, which corresponds to a twist about the metal-metal axis, was also found to be ineffective in $Re_2Cl_8^{2-}$. The ordering of the molecular orbitals, determined from the electronic state energies, for $Re_2Cl_8^{2-}$ and $Re_2Cl_9^{2-}$ are compared in Figure 44. A number of similarities are apparent: the $b_2\pi$, δ, δ^*, σp_z, and LF orbitals are unchanged in the two complexes. With the exception of the σp_z nonbonding orbital, the other energetically invariant orbitals are all directed along the equatorial ligand direction -x, y. One nonbonding σp_z orbital is unperturbed, while the other is utilized in bonding the axial chloride. The latter is stabilized.

No such correlations of the electronic spectra can be made if the alternate assumption, that the structure of the $Re_2Cl_9^{2-}$ species is related to the confacial bioctahedral $Re_2Cl_9^-$ anion, is adopted. The proposed metal-metal interaction model of $Re_2Cl_9^-$ does not account for the disappearance of the z allowed transition at 385 nm upon the addition of one electron into any unfilled orbital. Similarly a related assignment of the two weak xy polarized bands found at 530 and 680 nm in $Re_2Cl_9^-$ and the two intense z polarized features at 545 and 750 nm in the $Re_2Cl_9^{2-}$

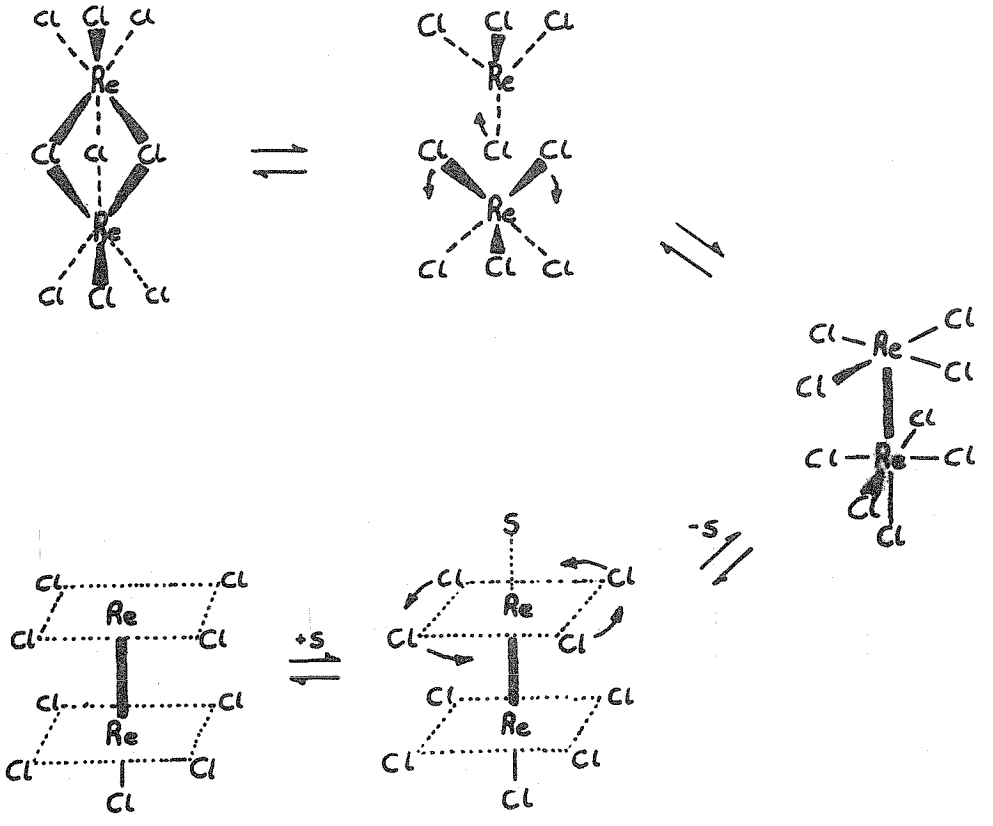

FIGURE 43

Table 36

$Re_2Cl_9^{2-}$

cm^{-1}	Assignment	Excited State $^2B_2 \rightarrow$	Polarization	
			Observed	Predicted
13300	$b_2\ \delta \rightarrow b_2\ \delta^*$	$^2B_2$	z	z
18350	$b_2\ \pi \rightarrow b_2\ \delta$	$^2B_2$	z	z
20000	$b_2\ \pi \rightarrow a_1\ \sigma\ p_z$	$^2A_1$	z	
25650	$b_2\ \delta \rightarrow a_1\ \sigma\ p_z$	$^2A_1$	xyz	
26600	$b_2\ \delta \rightarrow b_1$ LF	$^2B_1$	xy	
27900	$e\ \pi \rightarrow b_2\ \delta$	^2E	xy	xy
30300	$e\ \pi \rightarrow a_1\ \sigma\ p_z$	^2E	xy	xy
30900	$b_2\ \pi \rightarrow b_2\ \delta^*$	$^2B_2$	z	z
33300	$b_2\ \delta \rightarrow b_1$ LF	$^2B_1$	xy	
36200	$a_1\ \sigma \rightarrow b_2\ \delta$	$^2A_1$	z	
	$b_2\ \delta \rightarrow e\ \pi^*$	^2E	xy	xy
39200	$a_1\ \sigma \rightarrow a_1\ \sigma\ p_z$	$^2B_2$	z	z

Figure 44

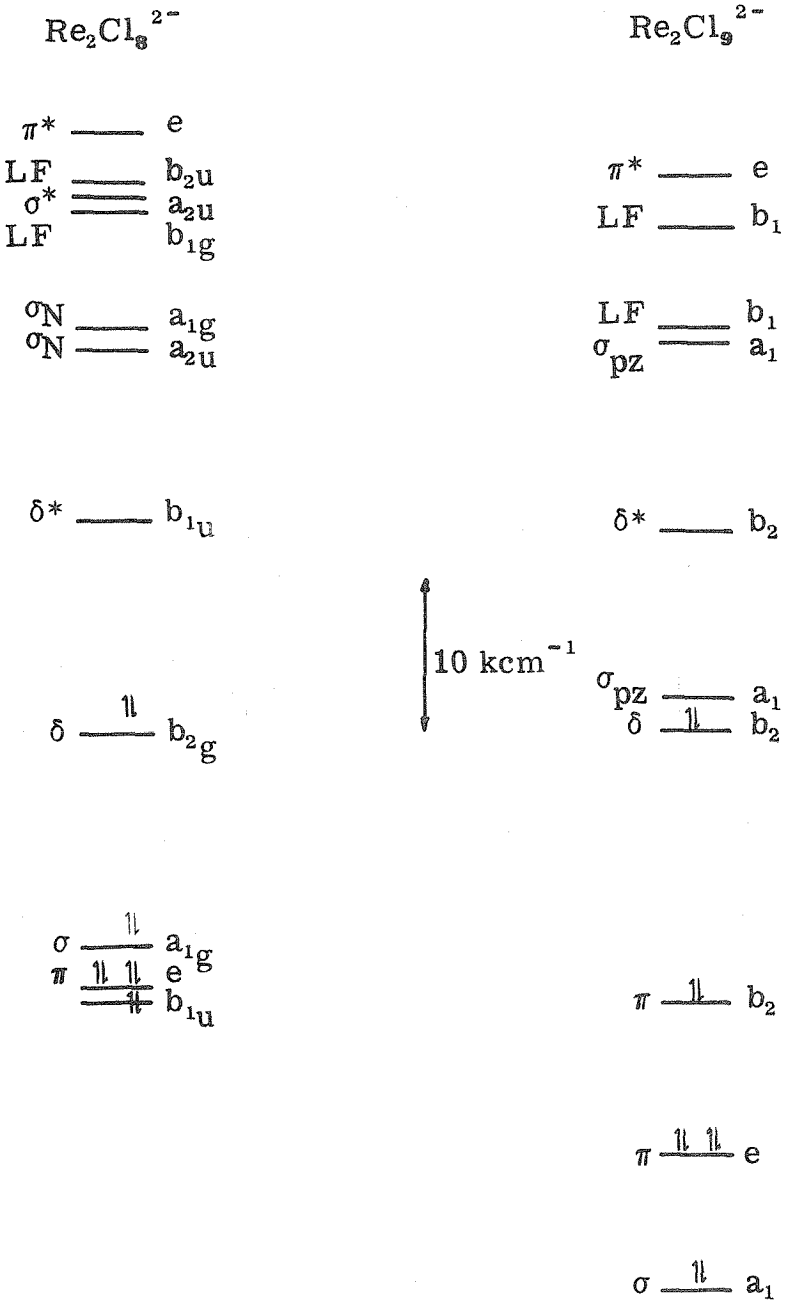
$Re_2Cl_8^{2-}$
π^* e
LF b_{2u}
σ^* a_{2u}
LF b_{1g}
σ_N a_{1g}
σ_N a_{2u}
δ^* b_{1u}
δ b_{2g}
σ a_{1g}
π e
b_{1u}
$Re_2Cl_9^{2-}$
π^* e
LF b_1
LF b_1
σ_{pz} a_1
δ^* b_2
10 kcm^{-1}
σ_{pz} a_1
δ b_2
π b_2
π e
σ a_1

spectra is not possible. The spectral data do not support a confacial bioctahedral structure for $[(n\text{-}C_4H_9)_4N]_2Re_2Cl_9$.

The spectral assignments presented in Table 36 did not require the assumption of either intervalence charge transfer or a delocalized electron phenomena. No evidence exists in the present case for the presence of such phenomena. The spectra can be adequately explained as a C_{4V} derivative of the quadruply bonded $Re_2Cl_8^{2-}$ species.

References

1. F. A. Cotton, W. R. Robinson, and R.A. Walton, Inorg. Chem., 6, 223 (1967).
2. F. Bonati and F. A. Cotton, Inorg. Chem., 6, 1353 (1967).
3. M. J. Bennett, F. A. Cotton, B. M. Foxman, P. F. Stokely, J. Amer. Chem. Soc., 89, 2759 (1967).
4. P. F. Stokely, Ph.D. Thesis, Massachusetts Institute of Technology, (1969).
5. F. A. Cotton and W. K. Bratton, J. Amer. Chem. Soc., 87, 921 (1965).
6. M. J. Bennett, F. A. Cotton, and R. A. Walton, J. Amer. Chem. Soc., 88, 3866 (1966).
7. M. J. Bennett, J. V. Brencic, and F. A. Cotton, Inorg. Chem., 8, 1060 (1969).
8. G. Myers and D. Powers, private communication.
9. W. K. Bratton, F. A. Cotton, M. Debeau, and R. A. Walton, J. Coord. Chem., 1, 121 (1971).
10. E. A. Allen, N. P. Johnson, D. T. Rosevear, and W. Wilkinson, Inorg. Nuc. Chem. Letters, 5, 239 (1969).

Proposition 1

(i) It is proposed that the structure of the $Re_2Cl_9^{2-}$ anion be investigated by x-ray crystallography.

(ii) It is proposed that the complex $Rb_3Mo_2Cl_8$ contains a bridging hydride ligand to account for its unusual structure. Such a complex would be an example of a protonated metal-metal multiple bonded system. Experiments to verify the presence of the hydride and the oxidation state of the metals are proposed.

In the final chapter of this thesis, the spectroscopic study of the complex $[(n\text{-}C_4H_9)_4N]_2Re_2Cl_9$ was presented. The observed polarization data were correlated to a chromophore of C_{4v} structure, consisting of an axial chloride coordinated to the Re_2Cl_8 unit. Unfortunately, the most likely alternative, a confacial bioctahedral D_{3h} structure, cannot be completely disregarded as either a stable or metastable species.

A previous attempt to determine the structure of $[(n\text{-}C_4H_9)_4N]_2Re_2Cl_9$ by x-ray crystallography was a complete failure.[1] Only the space group and lattice constants were obtained. Crystals are reported to be multiple and to decompose slowly in the x-ray beam. The widely varying densities obtained for crystals grown from methyl ethyl ketone-ethyl acetate[1] suggest the presence of solvent of crystallization. Loss of solvent of crystallization at room temperature for crystals grown from acetonitrile-dichloroethane was observed by this worker. Single crystals of optical quality were observed under a polarizing microscope

to form microcrystals within a half hour. Such a "decomposition" was apparently halted at lower temperatures.

This suggests that a low temperature x-ray investigation using liquid nitrogen as a coolant gas might be successful.

Crystals of $[(n\text{-}C_3H_7)_4N]_2Re_2Cl_9$ were prepared by adding tetra-propylammonium instead of tetrabutylammonium to $ReCl_5$ in acetone.[2] Stable purple crystals were obtained. The smaller cation may be more suitable for x-ray crystallographic analysis.

The size of the cation has been shown to effect the amount of metal-metal interaction in confacial bioctahedral complexes $A_3^I M_2Cl_9$.[3] Large cations occupy the equatorial "B" sites, while smaller cations are coordinated along the axial "A" sites -- Figure 1.

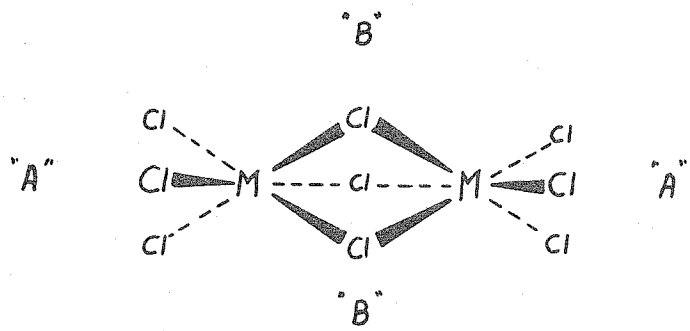

The larger cation in the B site sterically forces the M-Cl-M angle to open, increasing the metal-metal separation. The decrease in metal-metal interaction with larger cations is also shown from magnetic measurements by the magnitude of the exchange integral, -J.[4]

Table 1

Compound	M-M (Å)	<MXM	-J(°K)
$K_3 Mo_2Cl_9$	2.53	61°	800
$Cs_3Mo_2Cl_9$	2.68	64°	605
$(Me_4N)_3Mo_2Cl_9$	3.13	77°	400
$(Et_4N)_3Mo_2Cl_9$	3.43	86°	345

The large tetrabutylammonium cation may decrease the metal-metal interaction to such an extent that structural interconversion between D_{3h} and C_{4v} structures is possible. The choice of a smaller cation should stabilize that structure which allows the greater metal-metal interaction -- the C_{4v} structure.

The large cation in the compound $Rb_3Mo_2Cl_8$ apparently stabilizes a pseudo D_{3h} structure in which one of the bridging chlorides is missing.[5] The metal-metal distance of 2.38 Å is intermediate between the quadruply bonded $Mo_2Cl_8^{4-}$ species (2.134 - 2.050 Å)[6-8] and the bond distances in $Mo_2Cl_9^{3-}$ complexes[9] (see Table 1). The short metal-metal bond has been rationalized as due to the reduced steric repulsion resulting from a missing bridging chloride.[5] That this complex retains D_{3h} symmetry is suspicious.

Both the quadruply bonded and the bridged $Mo_2Cl_8^{N-}$ species are formed from $Mo_2(O_2CCH_3)_4$ by the action of hydrochloric acid.

[10] $Mo_2(O_2CCH_3)_4 + 4HCl + 4KCl \xrightarrow{0°C} K_4 Mo_2Cl_8 + 4CH_3 COOH.$

[5] $Mo_2(O_2CCH_3)_4 + 5HCl + 3RbCl \xrightarrow{60°C} Rb_3Mo_2Cl_8 + 4CH_3COOH + H^+ + e^-.$

The latter reaction seems unreasonable; the following reaction is suggested

$$Mo_2(O_2CCH_3)_4 + 5HCl + 3RbCl \xrightarrow{60\,^\circ C} Rb_3\,H\,Mo_2Cl_8 + 4CH_3COOH.$$

The species $H\,Mo_2Cl_8^{3-}$ is an example of a protonated metal-metal multiple bond. Protonated metal-metal single bonds have recently been shown to exist.[11] The elevated reaction temperature required for formation of this species is due to the endothermic nature of the reaction. The existence of a protonated Mo-Mo multiple bond is consistent with the observed loss of six chlorides per dimer in acid solution.[12]

$$Mo_2Cl_8^{4-} \xrightarrow{H_3O^+} Cl_3Mo\begin{matrix}\diagup\,H\,\diagdown\\ -Cl-\\ \diagdown\,Cl\,\diagup\end{matrix}MoCl_3^{3-} \xrightarrow{\text{aquation}} (H_2O)_N Mo\begin{matrix}\diagup\,H\,\diagdown\\ -Cl-\\ \diagdown\,Cl\,\diagup\end{matrix}Mo\,(H_2O)n^{3+} + 6\,Cl^-$$

Spectral data[12] for this reaction indicate the presence of a species characterized by strong metal-metal interaction: a peak maxima at 512 nm (ϵ = 336). The $Mo_2(H_2O)_N^{4+}$ species has a band maxima at 504 nm (ϵ = 337).[12]

The oxidation state of the $Mo_2Cl_8^{3-}$ species deserves some comment. As originally proposed by Cotton et al.,[5] the complex is a d^3 - d^4 mixed valence species. If instead a proton attacks the quadruply bonded $Mo_2Cl_8^{4-}$ moiety (a d^4 - d^4 system), a "redox isomer" of the type $H\,Mo_2Cl_8^{3-}$ (now a d^3 - d^3 system) results.

The $d^3 - d^3$ $Mo_2Cl_9^{3-}$ species has a bridged confacial bioctahedral structure. The fluxional behavior of the hydrogens in $FeH_2(\phi P(OCH_3)_2)_4$,[13] another redox isomer, may explain why the "vacant" bridging position in $Rb_3Mo_2Cl_8$ was completely disordered.[5]

It is proposed that this compound be re-examined by neutron diffraction to confirm the presence of the bridging hydride. In addition the low temperature infrared (800 - 2000 cm^{-1}) region should be examined for the asymmetric Mo-H-Mo vibration. This vibration should be very weak; nothing was observed at room temperature.[5] The Raman active symmetric mode should be much more intense. Although the complex is paramagnetic,[5] the high field NMR should also be carefully examined. Such a proton would be highly shielded. Finally the oxidation state of the molybdenums should be carefully determined. Ferric-ceric ion titrations have been successfully utilized to determine the oxidation state of related molybdenum species.[12]

References

1. P. F. Stokley, Ph.D. Thesis, Massachusetts Institute of Technology (1969), Appendix A.

2. E. A. Allen, N. P. Johnson, D.T. Rosevear, and W. Wilkinson, Inorg. Nuc. Chem. Letters, 5, 239 (1969).

3. P. W. Smith and A. G. Wedd, J. Chem. Soc. A., 2447 (1970).

4. I. E. Gray and P. W. Smith, Aust. J. Chem., 24, 73 (1971).

5. M. J. Bennett, J.V. Brencic, and F. A. Cotton, Inorg. Chem., 8, 1060 (1969).

6. J. V. Brencic and F. A. Cotton, Inorg. Chem., 8, 7 (1969).

7. J. V. Brencic and F. A. Cotton, Inorg. Chem., 1, 346 (1969).

8. J. V. Brencic and F. A. Cotton, Inorg. Chem., 8, 2698 (1969).

9. I. E. Grey, Ph.D. Thesis, University of Tasmania (1969).

10. J. V. Brencic and F. A. Cotton, Inorg. Chem., 9, 351 (1969).

11. D. C. Harris, Ph.D. Thesis, California Institute of Technology, (1973) and private communication.

12. A. R. Bowen, Ph.D. Thesis, Stanford University (1973).

13. A. E. Schweizer, Ph.D. Thesis, California Institute of Technology, (1974).

Proposition 2

Carbon and Oxygen Isotopic Fractionation Effects in Metal Carbonyls

The development of high precision mass spectrometers in the past two decades has allowed geochemists to measure small variations in isotopic ratios precisely. Detection of differences in equilibrium isotopic composition has important applications in the field of chemistry. It is proposed that subtle differences of structure and bonding within a molecule will produce different isotopic fractionations at any site where exchange or preferential reaction is possible. Knowledge of the isotopic fractionation factors can be correlated to existing ideas of bonding and will help resolve questions of the nature of the transition state.

The isotopic fractionation factor $\alpha_{A\text{-}B}$ is defined as a ratio of the isotopic abundances of A and the isotopic abundances of B. For oxygen

$$\alpha_{A\text{-}B} = \frac{\left(\frac{^{18}O}{^{16}O}\right)_A}{\left(\frac{^{18}O}{^{16}O}\right)_B}$$

Similar α's relate the $^{13}C/^{12}C$ abundance of A and B. Systematic multiplicative and additive errors in the measurement of the absolute isotopic ratios could make α useless for measuring the small effects found naturally. However, these errors can be shown to cancel if the quantity δ is measured[1] instead.

$$\delta = \left[\frac{\left(\frac{^{18}O}{^{16}O}\right)_A - \left(\frac{^{18}O}{^{16}O}\right)_{\text{standard}}}{\left(\frac{^{18}O}{^{16}O}\right)_{\text{standard}}} \right] 1000$$

δ is expressed in parts per mil. Similar expressions apply to B and to the isotopic abundances of other elements. By simple mathematics

$$\alpha_{A-B} = \frac{1 + \frac{\delta_A}{1000}}{1 + \frac{\delta_B}{1000}}$$

The quantity δ may be determined to a precision of $0.1‰$.

The preferential concentration of ^{18}O in silicate minerals with Si-O-Si bonds, $\delta = 10$, over those with Si-O-Al, $\delta = 8$, and Si-O-Fe, $\delta = 6$, has been observed.[2] The metal carbonyls present a simple chemical system in which structurally non-equivalent ligands undergo exchange. It is proposed that isotopic fractionation factors for oxygen and carbon be measured.

The metal carbonyls exchange by reactions of the type

$$M(^{12}CO)_x + {}^{13}CO \rightleftharpoons M(^{12}CO)_{x-1}\,(^{13}CO) + {}^{12}CO \qquad (1)$$

$$M(C^{16}O)_x + C^{18}O \rightleftharpoons M(C^{16}O)_{x-1}\,(C^{18}O) + C^{16}O \qquad (2)$$

Nickel carbonyl, $Ni(CO)_4$, undergoes rapid carbonyl exchange. The isotopic fractionation observed[3]

$$\alpha_1 = 1.020 \quad \alpha_2 = 1.005 \quad \text{at } -10^\circ C$$

$$\alpha_1 = 1.010 \quad \alpha_2 = 1.000 \quad \text{at } +10^\circ C$$

indicate a small ^{18}O enrichment.

Oxygen exchange by attack of water on the species $Re(CO)_6^+$ has been observed.[4] The proposed mechanism[5] involves a formation of a carboxylic acid intermediate.

$$\begin{array}{l} Re(C^{16}O)_6^+ + H_2{}^{18}O \rightleftharpoons (^{16}OC)_5\,Re{-}\overset{\overset{^{16}O}{|}}{C}{-}{}^{18}OH + H^+ \\ \qquad\qquad\qquad\qquad\qquad\qquad\qquad\qquad\qquad\qquad \rightleftharpoons \\ Re(C^{16}O)_5(C^{18}O)^+ + H_2{}^{16}O \rightleftharpoons (^{16}OC)_5\,Re{-}\overset{\overset{^{16}O}{|}}{C}{=}{}^{18}O + H^+ \end{array} \qquad (3)$$

The $Re(CO)_6^+$ species was found to be significantly enriched in ^{18}O by exchange with $H_2{}^{18}O$ within thirty minutes.[4] The oxygen isotopic fractionation has not been studied in detail. A comparison of $\delta^{18}O$ obtained by exchange with water and $\delta^{18}O$ from $C^{18}O$ exchange should provide information of the effect of the metal-carbon bond upon the carbon-oxygen bond.

A study of the carbon and oxygen isotopic fractionation of isoelectronic species $Mn(CO)_6^+$, $Cr(CO)_6$, and $V(CO)_6^-$ would allow correlation of the effect of charge upon carbonyl fractionation.

A more complicated case in which structurally distinct carbonyls exist is found in the metal carbonyl halide system.

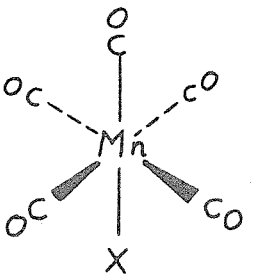

Debate has arisen[6, 7] as to whether or not the structurally non-equivalent axial and equatorial carbonyls exchange at different rates. Early work on the $Mn(CO)_5X$ (X = Cl, Br, I) system with radioactive ^{14}CO was interpreted as indicating that the four equatorial carbonyls exchanged at a faster rate than the carbonyl trans to the halide (axial carbonyl).[8] Infrared studies following ^{13}CO and $C^{18}O$ substitution onto $Mn(CO)_5X$ appear to show no difference in the rate constants for substitution at the two different positions.[6] However, recent work with $Cr(CO)_4L_2$ (L_2 = o-Phenanthroline) (Figure 2) by infrared techniques found that carbonyls trans to L exchanged at a slower rate than those trans to CO.[9]

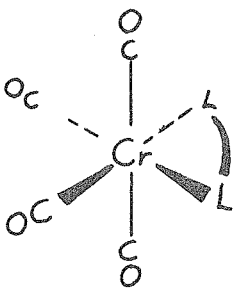

The cleavage of H $Re_3(CO)_{14}$ with ^{13}CO, equation (4),

$$H\,Re(CO)_{14} + {}^{13}CO \xrightarrow{\text{benzene}} H\,Re(CO)_5 + Re_2(CO)_9\,(^{13}CO) \qquad (4)$$

gave ^{13}CO enrichment in an equatorial position.[10] Cleavage with triphenylphosphine yielded the axially substituted product, $Re_2(CO)_9(\phi_3P)$.[11] A mechanism involving rearrangement following cleavage and significant enrichment in the equatorial position may be suggested.

Detailed isotopic fractionation studies for structurally different carbonyls have not been done.

An examination of the mixed metal dimers, such as $(OC)_5Mn - Re(CO)_5$, should be of interest. The effect of the metal as well as the structural factors on fractionation could be examined.

The following simple experiment should provide information about the transition state: the system $Mn(CO)_5X$ is allowed to equilibrate with a carbon monoxide reservoir. The reservoir is removed--the required time is unimportant since the system is in equilibrium. Some of the $Mn(CO)_5X$ is removed from the system and thermally decomposed. The $\delta^{13}C$ and $\delta^{18}O$ are determined for the CO liberated. The remaining compound is reacted with a non π bonding ligand, which replaces only two equatorial carbonyls.[12]

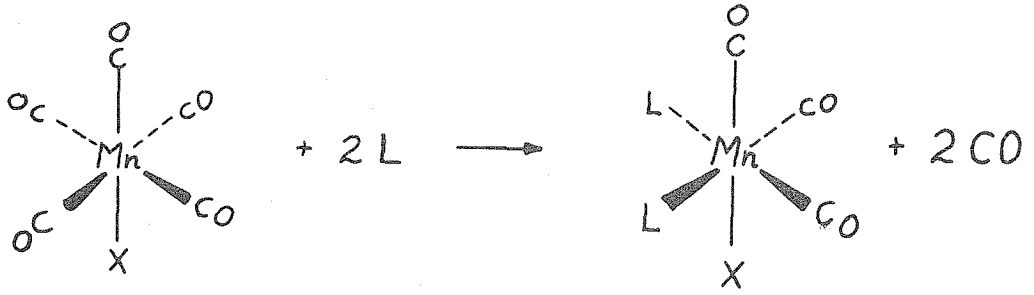

δ values are obtained for both the $Mn(CO)_3L_2X$ and CO. If δ is the same for the species $Mn(CO)_5X$ and both $Mn(CO)_3L_2X$ and CO then a transition state in which all carbonyls are equivalent is proved. Otherwise, the mass balance equation

$$\delta_{system} = 1/5\ \delta \text{ axial} + 4/5\ \delta \text{ equatorial}$$

will allow computation of δ axial and δ equatorial for the non-equivalent carbonyls.

$$\delta_{system} = \delta\ Mn(CO)_5X$$

$$\delta_{equatorial} = \delta\ CO$$

$$\delta_{axial} = 3\ \delta\ Mn(CO)_3L_2X - 2\ \delta_{CO}$$

References

1. S. Epstein, in Research in Geochemistry, ed. by P. Abelson, John Wiley & Sons, New York, N.Y., (1959).
2. H. Taylor and S. Epstein, Bull. Geol. Soc. Am., 73, 675 (1962).
3. E. Monse and W. Spindel, J. Chem. Soc., 37, 2393 (1962).
4. E. Muettertics, Inorg. Chem., 4, 1841 (1965).
5. T. Kruck and M. Novak, Chem. Bur., 97, 1695 (1964).
6. B. Johnson, J. Lewis, J. Miller, B. Robinson, P. Robinson, and A. Wojeicki, J. Chem. Soc. A, 522 (1968).
7. T. Brown, Inorg. Chem., 7, 2673 (1968).
8. A. Wojeicki and F. Basolo, J. Amer. Chem. Soc., 83, 525, (1961).
9. M. Dokyia, R. D. Johnson and F. Basolo, Inorg. Chem., 9, 997 (1970).
10. R. W. Harrill and H. D. Kaesz, Inorg. Nuc. Chem. Letters, 2, 69 (1966).
11. R. W. Harrill, Ph.D. Thesis, UCLA (1967).
12. F. A. Cotton and G. Wilkinson, Advanced Inorganic Chemistry, Interscience, New York, N.Y., p. 743 (1966).

Proposition 3

The existence of a δ metal-metal bond was originally proposed by Cotton[1] to explain the eclipsed structure[2] and observed diamagnetism[3] of the $Re_2X_8^{2-}$ species. The δ bond has been characterized spectroscopically in Chapter 6 of this thesis by the $\delta \rightarrow \delta^*$ transition. This transition was observed at 14180 cm^{-1} in $Re_2Cl_8^{2-}$, 13600 cm^{-1} in $Re_2Br_8^{2-}$, 17,900 cm^{-1} in $Mo_2Cl_8^{4-}$ and 16320 in $Mo_2Cl_4[PEt_3]_4$. The position of this band depends only upon the metal-metal overlap of the dxy orbitals. Presumably the red shift observed between the chloride and bromide is the result of increased metal-ligand π bonding in the latter.[4] Such π bonding weakens the metal-metal π bond; the resulting increase in the metal-metal bond distance decreases the δ orbital overlap. The smaller metal-metal bond distance in the $Mo_2Cl_8^{4-}$ complex, 2.139 Å,[5] compared to that in $Re_2Cl_8^{2-}$, 2.241 Å,[2] is reflected in the positions of the $\delta \rightarrow \delta^*$ transition. There is a definite blue shift as the metal-metal bond distance decreases and the δ orbital overlap increases.

It is proposed that the $d^4 - d^4$ complex $Li_4Cr_2(CH_3)_8 \cdot THF$ be examined by low temperature single crystal polarized spectroscopy. The $Cr_2(CH_3)_8^{4-}$ unit has both structural[6] and magnetic properties consistent with the presence of a δ bond. The Cr-Cr distance is 1.980 Å (Cr-Cr in the metal is 2.54 Å). Since π bonding is not possible for methyl groups, the position of the $\delta \rightarrow \delta^*$ transition should be due to the metal-metal overlap alone. This band would be expected at even higher energies than the quadruply bonded molybdenum compound

because of the shorter Cr-Cr bond distance. Assignment of a $\delta \rightarrow \delta^*$ transition for the $Cr_2(CH_3)_8^{4-}$ anion is important to determine the potential strength of such a bond in a first row transition element. The observation of vibrational fine structure would be most interesting.

The compound can be prepared as yellow crystals by the reaction[7]

$$2\ CrCl_2 + 8\ LiCH_3 \xrightarrow{THF} Li_4Cr_2(CH_3)_8 \cdot THF + 4\ LiCl$$

The tetragonal crystals are stable in inert atmosphere at low temperatures - to prevent loss of the solvent of crystallization.[6] Neither of these requirements presents any real experimental difficulties to the type of liquid helium temperature polarization study described in this thesis.

It is possible that such an investigation would not reveal any transitions with the correct π polarization. The electron configuration in such a case would best be described as $(\sigma)^2(\pi)^4(\sigma_N)^2$. A similar bonding scheme has been proposed in Chapter 6 for the carboxylate bridged rhenium species $Re_2(O_2CR)_4Cl_2$.

The x-ray structure of the complex $Re_2(O_2C\phi)_4Cl_2 \cdot 2HCCl_3$[8] has been determined. The Re-Re bond distance, 2.235 Å, is only slightly different than that in the $Re_2Cl_8^{2-}$ anion, 2.241 Å. The chemical interconvertibility of these two species has been cited as evidence for a quadruple bond in the carboxylate bridged compound.[3] These complexes may be prepared by the reaction[4]

$$Re_2X_8^{2-} + 4\ CH_3COOH \rightleftharpoons Re_2(O_2CCH_3)_4X_2 + 4\ HX + 2X^-$$

$$Re_2(O_2CCH_3)_4X_2 + R\ COOH \rightleftharpoons Re_2(O_2CR)_4X_2 + CH_3COOH$$

The absorption spectra of these complexes in acetonitrile solution have been reported.[4] The larger R (alkyl) substituents are more soluble in organic solvents. A polarized single crystal study of these complexes would also be appropriate. Although these complexes do not contain any intense absorption features in the visible, the complex cis $Re_2(O_2CCH_3)_2Cl_4 \cdot 2H_2O$[9, 10] has an intense absorption at 15,900 cm^{-1}. Single crystals grown from acetonitrile-acetic acid or from nitromethane are intensely dichroic-blue to colorless. Preliminary 77 °K spectra show vibrational fine structure and splitting on this band. The Re-Re distance of 2.224 Å[10] indicates a quadruple bond. The observation of a $\delta \rightarrow \delta^*$ type transition is in agreement with this hypothesis.

The apparent splitting of this band is highly significant. The σ_N orbital was postulated to lie below the δ orbital in the completely carboxylate-substituted complex. A detailed investigation of this system should provide useful information on the ordering of orbitals for a complex with weakly bound axial (H_2O) ligands.

A spectroscopic study of the complex trans- $Re_2(O_2C\phi)_2I_4$, which contains no axial ligands and has a Re-Re distance of 2.198 Å,[11] would also be interesting. The effect of trans versus cis carboxylate substitution upon the $\delta \rightarrow \delta^*$ transition could be determined.

The complex $Rh(O_2CCH_3)_4(H_2O)_2$ has the copper acetate structure with a Rh-Rh distance of 2.45 Å[12] (Rh-Rh in the metal is 2.69 Å). The bonding in this d^7 - d^7 system has alternately been described as a single bond $[(\sigma)^2(\pi)^4(\delta)^2(\delta^*)^2(\pi^*)^4]$[13] and as a triple bond $[(\sigma)^2(\pi)^4(\delta)^2(\sigma_N)^2(\sigma_N')^2(\delta^*)^2]$.[14] The latter explanation accounts for the large metal-metal separation in terms of repulsion between the filled δ and δ* orbitals. The bidentate bridging ligands force the retention of the eclipsed configuration. MO calculations are cited as support for both bonding schemes.[13,14] The ordering obtained by Dubicki and Martin[13] is unusual because the π bonding orbital is more stable than the σ bonding orbital. This ordering scheme was also suggested in Chapter 6 of this thesis to explain the polarized spectra of $Re_2Cl_8^{2-}$. The MO calculation by Cotton et al.,[14] is experimentally better supported with respect to the stabilization of the σ_N orbitals. Strong evidence exists in the compound $Ru_2(O_2CC_3H_7)_4Cl$ (d^5-d^6) for the proximity of the δ* and σ_N orbitals; there are three unpaired electrons.[14] The ruthenium centers are crystallographically[14] equivalent despite the non-integral valence.

The absorption spectra of the complexes $Rh(O_2CC_3)_4X_2$ are especially interesting. The visible spectra contain two absorption peaks at ~ 600 and 450 nm.[13] The lower energy absorption is very sensitive to the position in the spectrochemical series of the axial ligands;[15] the higher energy transition is not. The metal-metal separation of a related complex with axial ligands, $Mo_2(O_2CCF_3)_4py_2$, has been shown to be significantly longer (.039 Å)[16] than the metal-

metal bond distance in the unsubstituted complex, 2.090 Å.[17]
The compounds are prepared by the reaction[15]

$$2\ Rh(OH)_3 \cdot H_2O + 4\ CH_3\ COOH \rightarrow Rh_2\ (O_2CCH_3)_4 + 6H_2O$$

$$Rh_2(O_2CCH_3)_4 + 2X\ (neat) \rightarrow Rh(O_2CCH_3)_4X_2$$

$$X = H_2O,\ THF,\ CH_3CN,\ py,\ NH_4,\ NO$$

All the substituted rhodium (II) acetate complexes are soluble and stable in polar organic solvents. Thin film single crystals should be readily obtainable. Single crystal polarization studies of the position, intensity, and polarization of the absorption bands for a wide variety of ligands could be obtained. The question of whether the bonding in $Rh(O_2CCH_3)_4X_2$ is better described as a single or triple bond could also be resolved from such a study.

References

1. F. A. Cotton, Inorganic Chem., 4, 334 (1965).
2. F. A. Cotton and C. B. Harris, ibid., 4, 330 (1965).
3. F. A. Cotton, N. F. Curtis, B. F. G. Johnson, and W. R. Robinson, ibid., 4, 326 (1965).
4. F. A. Cotton, C. Oldham, and W. R. Robinson, ibid., 5, 1798 (1966).
5. J. V. Brencic and F. A. Cotton, ibid., 8, 7 (1969).
6. J. Krausse, G. Marx and G. Schödl, J. Organometallic Chem., 21, 159 (1970).
7. E. Kurras and J. Otto, ibid., 4, 114 (1965).
8. M. J. Bennett, W. K. Bratton, F. A. Cotton, and W. R. Robinson, Inorg. Chem., 7, 1570 (1968).
9. F. A. Cotton, C. Oldman, and R. A. Walton, Inorg. Chem., 6, 214 (1967).
10. P. A. Koz'min, M. D. Surazhskaya, and V. G. Kuznetsov, Zhur. Strukt. Khim., 11, 313 (1970).
11. F. A. Cotton, Accts Chem. Res., 2, 240 (1969).
12. M. A. Porai-Koshits and A. S. Antsyshkima, Dokl. Akad. Nauk. SSSR., 140, 1102 (1962).
13. L. Dubicki and R. L. Martin, Inorg. Chem., 9, 673 (1970).
14. M. J. Bennett, K. G. Caulton, and F. A. Cotton, Inorg. Chem., 8, 1 (1969).
15. S. A. Johnson, H. R. Hunt, and H. M. Neumann, ibid., 2, 960 (1963).

16. F. A. Cotton and J. G. Norman, J. Amer. Chem. Soc., 94, 5697 (1972).

17. F. A. Cotton and J. G. Norman, J. Coord. Chem., 1, 161 (1972).

Proposition 4

Photochemistry of Metal Cluster Compounds

Recent investigations of the solution photochemistry of the quadruply bonded Re(III) species $Re_2Cl_8^{2-}$ have shown that the multiple metal-metal bond may be cleaved photochemically. Presumably attack by the acetonitrile solvent at the vacant axial positions of the dimeric complex preceeds the homolytic bond cleavage.

$$Re_2Cl_8^{2-} + 4\ CH_3CH \overset{h\nu}{\rightharpoonup} 2\ ReCl_4(CH_3CN)_2^- \qquad (1)$$

$$ReCl_4(CH_3CN)_2^- + CH_3CN \overset{h\nu'}{\rightharpoonup} ReCl_3(CH_3CN)_3 + Cl^- \qquad (2)$$

Single metal-metal bonds may be photochemically cleaved[2] by a reaction such as

$$Re_2(CO)_{10} \overset{h\nu}{\rightharpoonup} 2\ Re(CO)_5. \qquad (3)$$

It is proposed that the photochemistry of metal cluster compounds be examined. The species $Re_3^{III}Cl_9$ and $Mo_6^{II}Cl_8^{4+}$, shown in Figures 1 and 2, are representative of cluster structures. Both may be considered as linked square planar d^4 units. In the former complex each metal center forms two double metal-metal bonds; each metal in the latter has four single metal-metal bonds. A study of metal-metal bond cleavage in systems containing multiple single or double bonds may provide a synthetic route to presently unknown metal cluster structures.

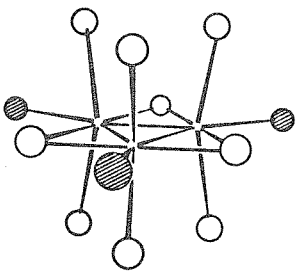

The structure of $Re_3X_9L_3$ molecules. The small circles represent rhenium atoms; the hatched circles represent L groups; the large open circles represent the X groups.

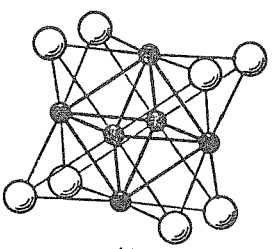

The key structural unit, $M_6X_8^{4+}$, found in all metal-atom cluster compounds of Mo^{II} and W^{II}.

The complex $Re_3Cl_{12}^{3-}$ has D_{3h} symmetry. There are three structurally distinct types of chloride ligands: three bridging, six out-of-plane terminal, and three in-plane terminal.[3-5] The Re-Re distance is 2.477 Å, indicating a bond order of two.[6] The metal-chloride bond distances are 2.39 Å, bridging; 2.359, terminal, out-of-plane; and 2.52 Å, terminal, in-plane. The long bond distance for the latter position is consistent with the observed lability of the three in-plane terminal chlorides. Exchange rates of the in-plane terminal chlorides were found to be much greater than the out-of-plane terminal chlorides; the bridging groups were inert.[7] Larger cations apparently favor formation of partially substituted $Re_3Cl_{11}^{2-}$ and $Re_3Cl_{10}^{-}$ species.[7]

In acetonitrile Re_3Cl_9 is soluble to give $Re_3Cl_9(CH_3CN)_3$ where the solvent molecules are coordinated in terminal in-plane positions (the axial coordination position of the square planar unit). A large number of similar species have been prepared by the addition of ligand to Re_3Cl_9 in solution,[8] i.e., $Re_3Cl_9(py)_3$ and $Re_3Cl_9(\phi_3P)_3$. Analogous bromide species are also known.[9,10] The absorption spectra of these species - $Re_3X_{12}^{3-}$, $Re_3X_{11}^{2-}$, $Re_3X_{10}^{-}$ and $Re_3X_9L_3$ - are all known. The visible spectra consist of two bands at ~ 13,000 cm^{-1} (ϵ = 750) and 19,000 cm^{-1} (ϵ = 2000).[8] The similarity between the individual chloride and bromide spectra suggests the metal-metal nature of the transitions. Possibly these may be related to the type of MO diagram proposed by Cotton et al.[6] The lower energy transition depends upon the nature of the in-plane terminal substituent.[8]

Presumably irradiation into the lowest band will cause dissociation of the most labile groups. Irradiation into the higher energy bands may do one of several things: allow substitution at the terminal out-of-plane positions, break one of the bridging halogen bonds, or cleave the metal-metal bond. It may be possible to synthesize mixed halogen cluster complexes by photochemical substitution. Cleavage of a bridging halogen bond or a metal-metal bond may produce a linear trimer. Since it is known that fusion of Re_3Cl_9 with Et_4NCl will produce $Re_2Cl_8^{2-}$,[11] a novel, direct photosynthetic route to related metal-metal bonded species may be discovered.

The cluster complexes $Mo_6Cl_8^{4+}$ and $W_6Cl_8^{4+}$ consist of a cube of chlorides with a metal ion in each face.[12] The Mo-Mo distance of 2.62 Å is indicative of a single metal-metal bond. In the complex the twenty-four bonding electrons are accomodated in the five bonding molecular orbitals.[6] Since there are twelve bonding contacts (an octahedron has twelve edges) the bond order is one. The empty positions on the faces of the cube can be utilized in weak bonding, i.e., the complexes $[Mo_6Cl_8]Cl_6^{2-}$[13] and $[Mo_6Br_6]Br_4(H_2O)_2$.[14] These facial groups are labile,[15,16] while the other eight halogens are exchanged only by a slow dissociative mechanism.

It is specifically proposed that the solution photochemistry of these species be investigated. Photochemical substitution of one or more of the triply bridging chlorides by Br^- or SCN^- may provide a facile synthetic route to presently unknown mixed ligand molybdenum

clusters. The degree of substitution and the structural configuration adopted would be especially interesting.

It is also possible that photochemical cleavage of single metal-metal bonds may substantially reduce the stability of the $Mo_6X_8^{4+}$ cluster, allowing structural reorganization. Cleavage fragments may include presently unknown $Mo_3X_N^{6-N+}$ or $Mo_4X_N^{8-N+}$ clusters. A comparison of the structures of such species with the rhenium(III) species should further elucidate the relative effects of charge and metal-metal bonding upon the cluster configuration adopted. Since the $Mo_6X_8^{4+}$ species has not been successfully oxidized, the new clusters would be expected to retain the original Mo(II) oxidation state.

References

1. G. Geoffroy, unpublished data.

2. M. S. Wrighton, Ph.D. Thesis, California Institute of Technology (1972).

3. W.T. Robinson, J. E. Fergusson, and B. P. Penfold, Proc. Chem. Soc., 116 (1963).

4. J. A. Bertrand, F. A. Cotton, and W. A. Dollase, J. Amer. Chem. Soc., 85, 1349 (1963).

5. J. A. Bertrand, F. A. Cotton, and W. A. Dollase, Inorg. Chem., 2, 1166 (1963).

6. F. A. Cotton and T. E. Haas, Inorg. Chem., 3, 10 (1969).

7. B. H. Robinson and J. E. Fergusson, J. Chem. Soc., 5683 (1964).

8. F. A. Cotton, S. J. Lippard and J. T. Mayve, Inorg. Chem., 4, 508 (1965).

9. F. A. Cotton and R. A. Walton, Inorg. Chem., 5, 1802 (1966).

10. J. E. Fergusson and B. H. Robinson, Proc. Chem. Soc., 189, (1964).

11. R. A. Bailey and J. A. McIntyre, Inorg. Chem., 5, 1940 (1966).

12. H. Schäfer, Z. Anorg. Chem., 353, 281 (1967).

13. P. A. Vaughan, Proc. Nat. Acad. Sci., U.S., 36, 461 (1950).

14. L. G. Guggenberger and A. W. Sleight, Inorg. Chem., 8, 2041 (1969).

15. J. C. Sheldon, Nature, 184, 1210 (1959).

16. J. C. Sheldon, J. Chem. Soc., 3106 (1960).

Proposition 5

Ion Cyclotron Resonance Photochemistry of Transition Metal Complexes

The photochemistry of transition metal complexes in solution has been extensively investigated.[1] The wavelength dependence of photochemical cleavage and substitution reactions has not been thoroughly pursued. In general, only small effects are observed since in solution radiationless deactivation to either the lowest excited electronic state or to an excited vibrational state of the electronic ground state invariably precedes photochemical reaction.[2] Photoreaction in the gas phase, where the frequency of collisional deactivation is substantially reduced, may demonstrate significantly greater wavelength dependence. It is proposed that the photochemistry of transition metal complexes be investigated by ion cyclotron resonance spectroscopy and that these results be compared to similar solution studies.

The photochemistry of several organic species have been investigated by ICR techniques.[3-6] The standard ICR cell[7] is modified such that light propagates along the ion drift direction. Double resonance techniques allow the identification of the reactant species.[3] The relative abundance of the product ion may be determined as a function of the irradiation wavelength.[3-4] Unlike solution photochemistry where the electronic absorptions of the product species may significantly reduce the incident exciting light

intensity as the reaction proceeds, a steady state is rapidly obtained in the ICR cell. The low pressure within the cell (~ 10^{-5} torr) requires an intense light source to insure a sufficient photon capture rate for the ion during its resonance time within the cell (<1 sec). The availability of commercial tunable visible-ultraviolet dye lasers makes this possible.[8]

A recent investigation of the complex $Fe(CO)_5$[9] has demonstrated the feasibility of using ICR to probe the chemistry of transition metal ions. The limiting factors in such an investigation are an upper mass limit of 500 a.m.u. and a sufficient volatility. The latter criterion is satisfied for those complexes which may be sublimed at temperatures attainable in a heated inlet port. Metal carbonyl and nitrosyl complexes are obvious choices. The solution photochemistry of such complexes have been studied.[10] The photodissociation mechanism operable in the absence of solvent coordination effects would be most interesting. Reactions of the following types could be easily detected:

$$M(CO)_N \overset{+}{L} \xrightarrow{h\nu} M(CO)_N^{+} + L \qquad (1)$$

$$M(CO)_N \overset{+}{L} \xrightarrow{h\nu'} M(CO)_{N-1} \overset{+}{L} + CO \qquad (2)$$

Although both positive and negative ions are formed, the former greatly predominate.

The dissociative photochemistry of the complexes $V(CO)_6^-$ and $Mn(CO)_5^+$ could be compared to both the neutral carbonyl and

and the isoelectronic $Cr(CO)_6$ and $W(CO)_6$ species. The ion photochemistry of the isoelectronic compounds $Mn(CO)_5X$ (X = Cl, Br, I) and $M(CO)_5NR_3$ (M = Cr, Mo) species could also be compared. The volatile complexes (cp) $M(CO)_3H$ (M = Cr, Mo, W)[11] will form the $(cp)M(CO)_3H^+$ ion. The photochemistry of $(cp)Mo(CO)_2I$ has been studied[12] in solution.

Presumably it is possible to find complexes suitable for examination by ICR which contain weaker field ligands. For such cases the ligand field transitions will be sufficiently well separated to provide a direct test of the Wrighton-Gray[2] rules of photodissociation.

Reference

1. V. Balzani and V. Carassiti, "Photochemistry of Coordination Compounds," Academic Press, New York, N.Y. (1970).

2. M. S. Wrighton, Ph.D. Thesis, California Institute of Technology (1972) and references cited therein.

3. J. M. Kramer and R. C. Dunbar, J. Amer. Chem. Soc., 94, 4346 (1972).

4. R. C. Dunbar, ibid., 93, 4354 (1971).

5. R. C. Dunbar, ibid., 95, 472 (1973).

6. B. Freiser, private communication.

7. D. Holtz, J. L. Beauchamp and J. R. Eyler, ibid., 92, 7045 (1970).

8. For example a 250 nm - 750 nm dye laser with .2 nm bandwidth is available from the Molectron Corporation, Sunnyvale, California, 100 w power RMS.

9. M. S. Foster and J. L. Beauchamp, J. Amer. Chem. Soc., 93, 4924 (1971).

10. E. Koerner von Gustorf and F. W. Grevels, Fort. Chem. Forsch., 13, 366 (1969).

11. E. O. Fischer, Inorg. Synth., 7, 136 (1963).

12. R. J. Haines, R. S. Nyholm, and M. H. B. Stiddard, J. Chem. Soc. A., 94, (1967).

Appendix A

Unpaired Electrons	Spin Function	
	O'	D_4'
0	Γ_1	Γ_1
1	Γ_6	Γ_6
2	Γ_4	$\Gamma_2 + \Gamma_5$
3	Γ_8	$\Gamma_6 + \Gamma_7$
4	$\Gamma_3 + \Gamma_5$	$\Gamma_1 + \Gamma_3 + \Gamma_4 + \Gamma_5$
5	$\Gamma_7 + \Gamma_8$	$\Gamma_6 + \Gamma_7 + \Gamma_7$

The notation used is consistent with the tables found on page 51 of Introduction to Ligand Field Theory by C. J. Ballhausen, McGraw-Hill Co., New York, N.Y. (1962).

The equations

$$\chi(\phi) = \frac{\sin(s + \frac{1}{2})\phi}{\sin \phi/2}$$

and

$$\chi(\phi) = \chi(\phi + 2\pi) \text{ for } s \text{ integral}$$

$$\chi(\phi) = -\chi(\phi + 2\pi) \text{ for } s \text{ half integral}$$

were used to compute the representations.

Appendix B

Polarized Spectra of $Ni(TAA)_2$

As part of a detailed investigation of bis(monothioacetylacetonato) metal(II) complexes,[1] the polarized single crystal spectra of $Ni(TAA)_2$ were measured at 5°K between 750 and 400 nm. The compound crystallizes in the orthorhombic space group P_{bca}, with eight molecules per unit cell and lattice constants a = 13.301 Å, b = 16.418 Å, c = 11.468 Å. The observed density, 1.52 g/cm^3, is in agreement with the calculated density of 1.533 g/cm^3. The coordinates of the nickel and sulfur atoms are given in Table 1.

Table 1

	x	y	z
Ni	1.0071	.7104	1.1261
S(1)	.0574	.1787	.2054
S(2)	.1793	.1531	-.0003

The least-squares plane for the entire molecule was found to be

$$.8005x - .0624y + .5961z - 1.786 = 0 \qquad \text{(C-1)}$$

Molecular coordinate axes were chosen such that z is normal to the least-squares plane and y, the C_2 axis of the cis structure, bisects the S-Ni-S angle. A stereoscopic view of the orientation of the $Ni(TAA)_2$ molecules within the unit cell is shown in Figure 1. The direction cosines for the Y axis are

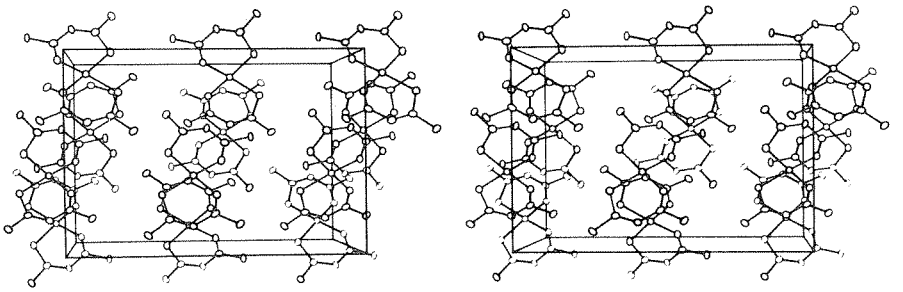

Figure 1

$[(\pm .1375, \pm .9872, \pm .0841), (\pm .1375, \pm .9871, \mp .0814), (\pm .1375,$

$\mp .9871, \pm .0814), (\mp .1375, \pm .9871, \pm .0814)]$.

Thin crystals were grown on quartz substrates by slow evaporation of acetone solutions; crystals were found to be the (010) face. For this face the extinction polarization directions are constrained by symmetry to lie parallel to the a and c axes. The latter direction coincided to the long axis of the crystal flakes. Absorbances along [100] and [001] are characterized by

$$A_c = .3553\ Az + .6381\ Ax + .0066\ Ay \qquad \text{(C-2)}$$

$$A_a = .6408\ Az + .3403\ Ax + .0189\ Ay \qquad \text{(C-3)}$$

Since neither direction contains a significant y component, the spectra were resolved into $\pi(z)$ and $\sigma(x)$ by the inverse matrix

$$\begin{bmatrix} A\pi \\ A\sigma \end{bmatrix} = \begin{bmatrix} -1.2581 & 2.2581 \\ 2.2445 & -1.2445 \end{bmatrix} \begin{bmatrix} Ac \\ Aa \end{bmatrix} \qquad \text{(C-4)}$$

The measured spectra is shown in Figure 2. Figures 3 and 4 present the π and σ resolved spectra.

The thickness of the crystal shown in the right side of Figure 2 and in Figure 3 was determined to be 34 μ thick by direct measurement with both a micrometer and with a microscope. The thickness of the thinner section, shown on the left side of Figure 2 and in Figure 4, displayed interference fringes. The thickness was found to be 3.64 - 3.68 μ. The refractive indices are Na = 1.755

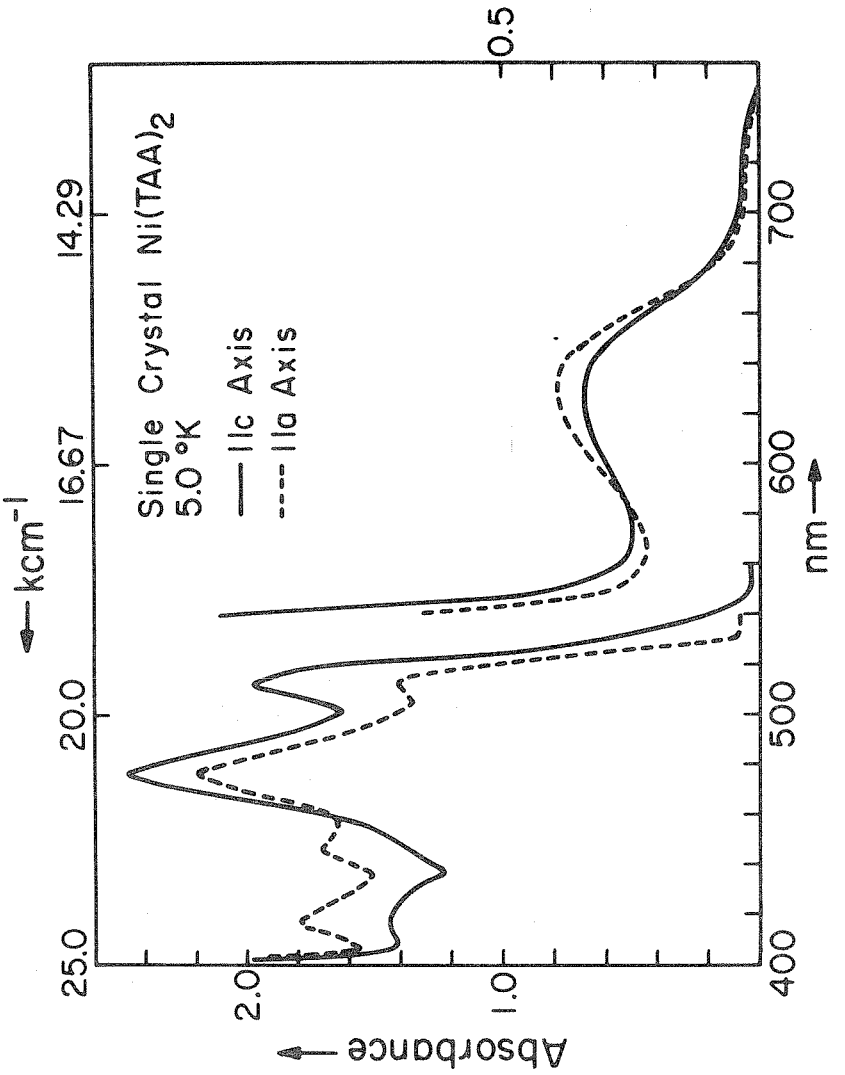
Single Crystal Ni(TAA)2
5.0 °K
IIc Axis
IIa Axis
kcm-1
25.0
20.0
16.67
14.29
nm
400
500
600
700
Absorbance
2.0
1.0
0.5

Figure 2

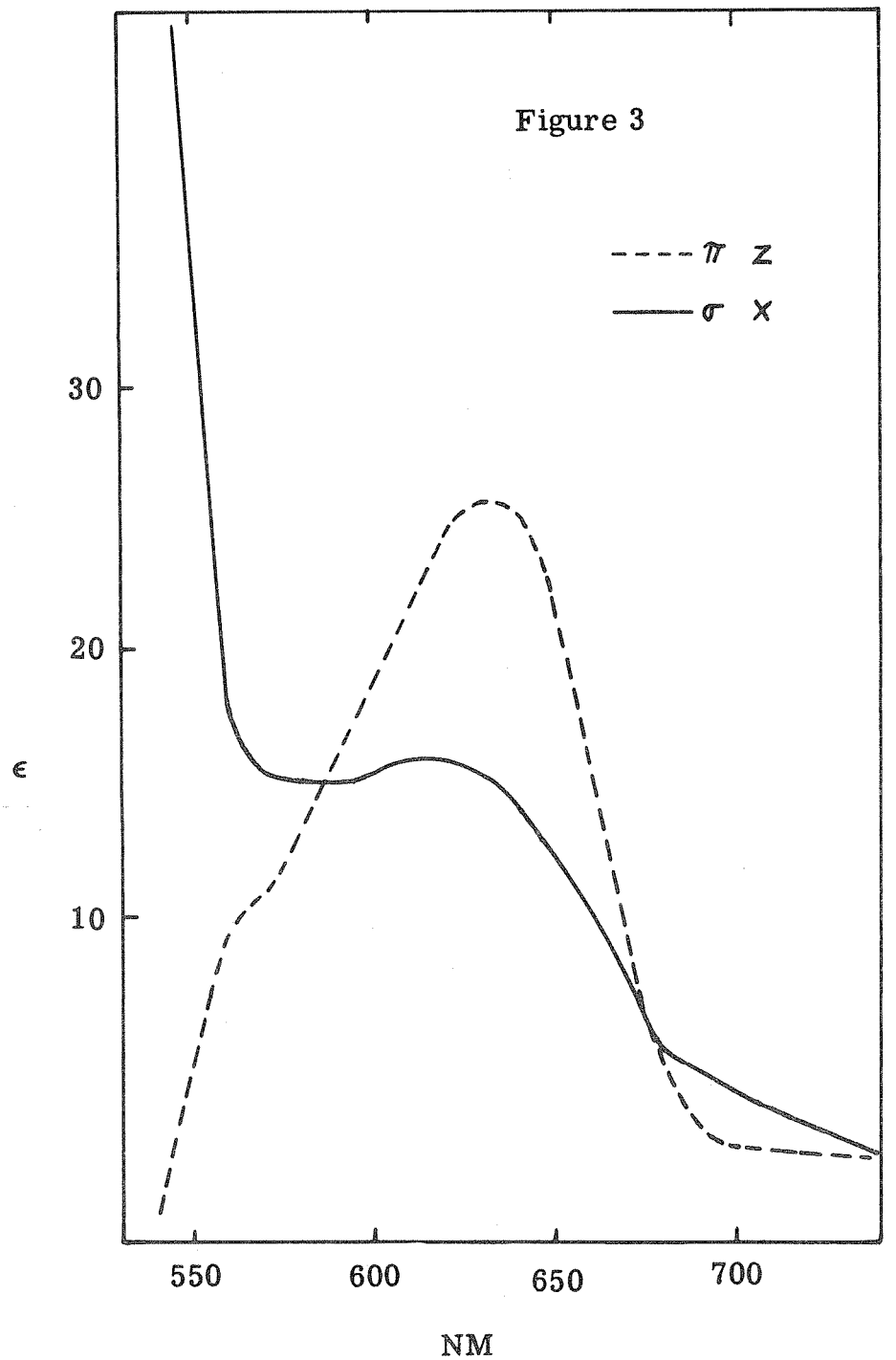
Figure 3
π z
σ x
30
20
10
ε
550
600
650
700
NM

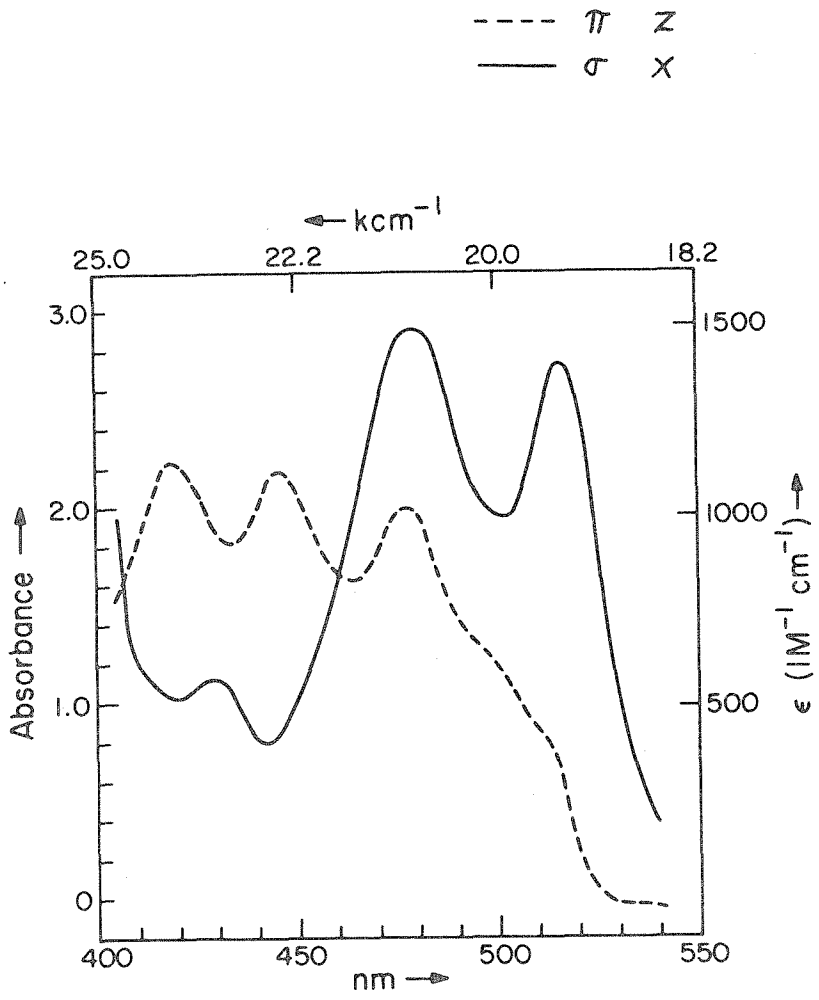
---- π z
—— σ x
kcm⁻¹
25.0
22.2
20.0
18.2
3.0
2.0
1.0
0
Absorbance
1500
1000
500
ε (1M⁻¹ cm⁻¹)
400
450
500
550
nm

Figure 4

and Nc = 1.842, the former was determined by immersion in diiodomethane.

The $Ni(TAA)_2$ molecule possesses approximate C_{2v} symmetry. The transformation properties for the d orbitals and low lying π^* levels are given in Table 2.

Table 2

dxz	A_2	x	B_1
dyz	B_2	y	A_1
dxy	B_1	z	B_2
dx^2-y^2	A_1		
dz^2	A_1	S = 0	A_1
π^*	B_2	S = 1	$A_2 + B_1 + B_2$

The ground state for the d^8 planar complex is $^1A_1$.

The intensity of the broad band centered at 630 nm, Figure 3, suggests that one or more of the spin-allowed d-d transitions are involved. As the calculated π component of this band is clearly dominant, the principle contribution to the intensity is from the z allowed $^1A_1 \rightarrow {}^1B_2$ (a_2 dxz $\rightarrow$ b_1 dxy). The $^1A_1 \rightarrow {}^1A_2$ (b_2 dyz $\rightarrow$ b_1 dxy) transition, which is allowed only through vibronic coupling, is assigned as the shoulder at 560 nm. The chloroform solution spectra of some monothio-β-diketonates, $Ni(R'CSCHCOR'')_2$, where $R' = \phi$, $R'' = OEt$, and $R' = CH_2$, $R'' = OCH_3$, exhibit a low intensity band at 495-500 nm in addition to the 675 nm band.[2] The presence of x polarized d-d bands, $^1A_1 \rightarrow {}^1B_1$ (a_1 dz^2 or dx^2-y^2 $\rightarrow$ b_1 dxy), within the

Table 3

Crystal			Methanol Solution		
nm	cm^{-1}	Polarization	nm	cm^{-1}	ϵ
630	15870	z	641	15,600	77
513	19490	x	495	20,200	1390
477	20960	x			
447	22370	z	438	22,830	3490
428	23360	x			
418	23920	z	383	26,110	4760

band envelope of the 513 nm band is reasonable. The high intensity of this transition is due to intensity stealing from the adjacent x polarized charge transfer band at 477 nm. Additionally the presence of a spin forbidden $^1A_1 \rightarrow {}^3A_2$ (B_1) (dyz $\rightarrow$ dxy) component cannot be eliminated.

The unoriented film spectra of the more intense features reveal a band at ~ 447 nm which is absent for the crystal spectra of the (010) face. This peak must be assigned as the Y-allowed $^1A_1 \rightarrow {}^1A_1$ (b_2 dyz $\rightarrow$ b_2 π^*) metal to ligand charge transfer transition. The intense x(σ) allowed feature at 477 nm is the $^1A_1 \rightarrow {}^1B_1$ (a_2 dxz $\rightarrow$ b_2 π^*). It is reasonable to assume that the lowest available π^* molecular orbital of $Ni(TAA)_2$ will be of b_2 symmetry; the sulfur 3pπ orbitals overlap and derive stabilization from the empty metal 4 pz orbital. The lowest π^* orbital in $Ni(CN)_4^{2-}$ was shown to be of this type.[3]

The two z(π) polarized bands at 418 and 447 nm in Figure are assigned as $^1A_1 \rightarrow {}^1B_2$ (a_1 dz^2, dx^2-y^2 $\rightarrow$ b_2 π^*). The weak band at 447 nm in the σ(x) spectra may be a residual x component of the unobserved $^1A_1 \rightarrow {}^1A_1$ (dyz $\rightarrow$ dxy) band.

The assignments presented here are consistent with a d orbital ordering $dz^2 < dx^2\text{-}y^2 < dyz < dxz \ll dxy < b_2\ \pi^*$ which differs from the ordering proposed for bis(diethyldithiophosphato) nickel(II)[4] and bis (diethyldithiocarbamato) nickel(II)[5] by the destabilization of the dxz, dyz orbitals in the present case.

References

1. O. Siiman, D. Titus, C. Cowman, J. Fresco, and H. B. Gray, submitted for publication.

2. S. H. H. Chaston and S. E. Livingstone, Aust. J. Chem., 20, 1079 (1967).

3. C. Cowman, C. J. Ballhausen, and H. B. Gray, submitted for publication

4. J. D. Lebedda and R. A. Palmer, Inorg. Chem., 11, 484 (1972).

5. R. Dingle, Inorg. Chem., 10, 1141 (1971).